RESEARCH REPORT H-68-1

AN EXPERIMENTAL STUDY OF BREAKING-WAVE PRESSURES

by

W. J. Garcia, J.

September 1968

Sponsored by

Office, Chief of Engineers
U. S. Army

Conducted by

U. S. Army Engineer Waterways Experiment Station
CORPS OF ENGINEERS
Vicksburg, Mississippi

RESEARCH REPORT H-68-1

AN EXPERIMENTAL STUDY OF BREAKING-WAVE PRESSURES

by

W. J. Garcia, Jr.

September 1968

Sponsored by

Office, Chief of Engineers
U. S. Army

Conducted by

U. S. Army Engineer Waterways Experiment Station
CORPS OF ENGINEERS
Vicksburg, Mississippi

THE CONTENTS OF THIS REPORT ARE NOT TO BE USED FOR ADVERTISING, PUBLICATION, OR PROMOTIONAL PURPOSES. CITATION OF TRADE NAMES DOES NOT CONSTITUTE AN OFFICIAL ENDORSEMENT OR APPROVAL OF THE USE OF SUCH COMMERCIAL PRODUCTS.

FOREWORD

Authority for the U. S. Army Engineer Waterways Experiment Station to conduct Engineering Study No. 813, "Wave Force on Breakwaters," was contained in letters from the Office, Chief of Engineers, dated 1 December 1947 and 14 September 1948; however, the tests reported herein, which were the first tests conducted in connection with ES 813, were not begun until 27 June 1963 because of a shortage of personnel. The investigation was accomplished in the Hydraulics Division of the Waterways Experiment Station during the period June 1963 to September 1964. The tests were performed by CPT William J. Garcia, Jr., under the supervision of Mr. R. Y. Hudson, Chief of the Water Waves Branch, and Mr. E. P. Fortson, Jr., Chief of the Hydraulics Division. This report was prepared by CPT Garcia.

Successive Directors of the Waterways Experiment Station during the conduct of this study and the preparation and publication of this report were COL Alex G. Sutton, Jr., CE; COL John R. Oswalt, Jr., CE; and COL Levi A. Brown, CE. Technical Director was Mr. J. B. Tiffany.

CONTENTS

NOTATION

a = one-half wave height

b = distance above bottom of wall

$b_{p_{max}}$ = elevation of the point of maximum pressure above bottom of wall

c = wave celerity

d = water depth

d_B = water depth in which wave will break

d_w = water depth at wall

D = thickness of layer of air trapped between the face of the breaking wave and the wall

E = total energy of wave

E_K = kinetic energy of wave

E_o = total energy of wave in deep water

E_p = potential energy of wave

F = energy flux

F_{avg} = average energy flux of wave per wave period

g = acceleration of gravity

H = wave height

H_B = wave height at breaking

H_o = wave height in deep water

I = shock impulse

k = constant of proportionality

K length of water column in Bagnold's equation for maximum shock pressure

L = wavelength

L_o = wavelength in deep water

$m = 2\pi/L$

n = an unknown exponent

p = shock pressure

p_{max} = maximum shock pressure

p_2 = secondary pressure

t = time coordinate

t_p = total duration of pressure

T = wave period

v = velocity of water upon striking wall

x = horizontal coordinate

y = vertical coordinate or vertical distance

y_B = elevation of crest of breaking wave above bottom of wall

z = beach slope

η = elevation of water surface above the still-water level

ρ = mass density of water

$\sigma = 2\pi/T$

ϕ = velocity potential

CONVERSION FACTORS, BRITISH TO METRIC UNITS OF MEASUREMENT

British units of measurement used in this report can be converted to metric units as follows:

Multiply	By	To Obtain
inches	2.54	centimeters
feet	0.3048	meters
pounds	0.45359237	kilograms
pounds per square inch	0.070307	kilograms per square centimeter
pounds per square foot	4.88243	kilograms per square meter
pounds per cubic foot	16.0185	kilograms per cubic meter
Fahrenheit degrees	5/9	Celsius or Kelvin degrees*

* To obtain Celsius (C) temperature readings from Fahrenheit (F) readings, use the following formula: $C = (5/9)(F - 32)$. To obtain Kelvin (K) readings, use: $K = (5/9)(F - 32) + 273.16$.

SUMMARY

Tests were conducted to gain more information concerning the shock pressures created by water waves breaking against vertical barriers. These wave pressures were studied using small-scale oscillatory waves in a flume fitted with a beach slope and test wall. The variation of pressure with both time and position on the wall was determined for several wave heights, wave periods, water depths, and beach slopes.

Great scatter in the magnitude of the shock pressure was observed for each of the wave conditions tested. This variation in the value of the shock pressure is believed to be caused by slight variations in the shape of the incident breaking wave. Therefore, many tests were made using the same wave conditions in order to more accurately determine the magnitude of the shock pressure.

The variation of pressure with time was found to be similar to that reported by previous investigators. The pressure-time variation can be divided into two parts; namely, initial shock pressure which occurs as the wave strikes the wall and a secondary pressure which is associated with the runup. The shock pressure is characterized by a very intense pressure peak of short duration and is followed by the much less intense but longer duration secondary pressure.

The maximum shock pressure that occurred for each wave condition was localized over a small region of the test wall between the still-water level at the wall and the elevation of the crest of the wave striking the wall. Above the region of maximum shock pressure, the magnitude of pressure decreases to zero. Below the region of maximum pressure, the shock pressure also decreases but to a value of approximately one-tenth the magnitude of the shock pressure and it then remains fairly constant to the bottom of the test wall. This type of distribution of shock pressures on the wall was observed for all tests.

Upon analysis of the maximum shock pressures observed for each of the wave conditions tested, it was found that the shock pressure increased with both wave height and wavelength. It was found through dimensional analysis that pressure is proportional to the cube root of the wave energy. Upon comparison of the data collected in this experimental program with the above relation between pressure and wave energy, only fair conformity was noted due to the small range of test data. Therefore, the range of data was expanded by the inclusion of the shock pressure data of other

investigators from both model and prototype studies. Very good agreement was noted over this larger range of data.

As opposed to the shock pressure, little scatter was noted in the magnitude of the secondary pressure. It was also noted that the secondary pressure varies regularly along the wall from a maximum at the bottom to zero at the point of maximum runup. This regular distribution is expected since the secondary pressure is caused by the runup of the wave rather than its impact on the wall. The secondary pressure was compared with the pressure caused by the same size wave forming a clapotis on the wall. The clapotis pressure was almost identical with the observed pressure.

The characteristics of the wave at the point of breaking were also studied in order to make a comparison between waves breaking on an unobstructed beach and on a beach obstructed by a wall. Although it might be expected that a barrier on the beach would have a great effect on the breaking waves, the data showed the effect to be negligible. The depth of water in which the wave would break on an unobstructed beach is slightly greater than the depth of water at the wall which would cause the same wave to break and produce maximum shock pressures. The wave height at breaking for both the obstructed and the unobstructed beach was found to be the same.

AN EXPERIMENTAL STUDY OF BREAKING-WAVE PRESSURES

PART I: INTRODUCTION

1. This report is concerned with the pressure caused by a wave breaking against a plane vertical wall. Observations of such waves breaking against vertical walls have shown that they cause a much greater pressure on the wall than waves that strike the wall without breaking. There is a great deal of theoretical and experimental knowledge concerning nonbreaking waves and the pressures caused by them. However, relatively little is known about breaking waves or the pressure caused by such waves. The methods now available to predict breaking-wave pressure are inadequate. Therefore, this study was conducted to gain more information concerning breaking-wave pressures and to aid in the further development of a sound method of predicting breaking-wave pressure. Consequently, this study deals primarily with the effects of a wave breaking against a vertical wall, rather than the causes of the pressure or the mechanics of breaking waves.

2. The pressure caused by a wave striking a vertical wall without breaking has been the object of several theoretical and experimental investigations. It has been found that the pressure caused by a nonbreaking wave is approximately equal to the hydrostatic pressure due to the water on the wall at any instant of time. A breaking wave, on the other hand, does not cause such a regular and predictable pressure. Depending upon where the wave breaks in relation to the position of the wall, the maximum pressure may vary from a value approximately equal to that caused by a nonbreaking wave to an extremely high shock pressure. Under the proper conditions the pressure on the wall rises very rapidly as the face of the breaker strikes the wall and then falls very rapidly. Following this initial pressure spike, called the shock pressure, the pressure increases slowly to a second maximum which occurs at the time of maximum runup. This second maximum is called the secondary pressure. Under certain conditions the magnitude of the shock pressure may be as much as 50 times the

secondary pressure. The initial shock pressure was the main object of investigation during this study.

3. From the standpoint of the designer, any procedure that might be developed for predicting the pressure due to breaking waves should include only those variables which are readily obtainable in the prototype situation. Both at sea and at the site of the proposed structure, the wave height, wavelength, and wave period can be determined. In addition, measurements of the bottom slope and water depth at the site of the proposed structure are obtainable. In light of the above limitations, any usable procedure may incorporate these variables, but may not make use of variables which cannot be measured in nature. Thus, in the analysis of the data herein, wave characteristics which could be measured in the prototype were related to the pressure which occurred.

4. Ten series of tests were made in which the wave period was varied from 1.49 sec to 1.94 sec and the wave height was varied from 1.11 in.* to 3.29 in. In order to obtain some information on the effect of the shape of the bottom in front of the wall, beach slopes of 1/25 and 1/10 were tested. A regular train of oscillatory waves was used. Although a spectrum of waves is found at sea, it is believed that a regular train of waves adequately represents the individual waves of a spectrum. Since this experimental program covered only a small range of wave conditions, the data obtained were supplemented by the laboratory data of other investigators and the limited quantity of prototype data available.

5. The laboratory equipment consisted of a wave flume with a flap-type wave generator, a beach slope, and a test wall. Wave gages were used to measure wave height, period, and celerity. A pressure transducer was mounted in the test wall to measure the pressure caused by the wave breaking on the wall. The pressure was recorded at different positions on the wall in order to determine pressure distribution.

6. At the start of the experimental program it became apparent that the conditions necessary to cause maximum shock pressure were very critical. Consequently, much variation in the magnitude of the shock pressure

* A table of factors for converting British units of measurement to metric units is presented on page xi.

was observed for seemingly identical wave conditions. This great variation in the shock pressure was also observed by other investigators. Considering only the highest shock pressure for each point on the wall, the most intense pressure was observed to occur in an area on the wall between the still-water level and the crest of the breaking wave. Above and below this area the pressure decreased considerably. The maximum pressure occurring on the wall for each of the wave conditions was found to be a function of the deepwater wave height and the deepwater wavelength. Upon empirical analysis of the data from this study and the data of other investigators, the maximum shock pressure was found to be directly proportional to the one-third power of the deepwater wave energy. The wave energy is a function of the wave height and wavelength. The distribution of the initial shock pressure on the wall was also found to be a function of the wave characteristics. The secondary pressure was found to be very nearly equal to the pressure caused by the clapotis, or nonbreaking wave.

7. The effect of the wall on the breaking characteristics of the wave was also observed. The breaking characteristics of the waves causing maximum shock pressure on the wall were compared with the theoretical and experimental breaking-wave data for the case of an unobstructed beach. It was found that the wall had little effect on the breaking characteristics of the waves. Regardless of whether or not the vertical wall was present, the waves tended to have the same height at breaking and tended to break in the same depth of water.

8. Although this study was not intended to provide all the answers to questions concerning the pressure caused by breaking waves, it is hoped that the results of this study will aid in the future design of coastal structures by providing a more rational approach to the prediction of breaking-wave pressures, and be a stepping stone for further research on the action of breaking waves on coastal structures.

PART II: HISTORICAL BACKGROUND

9. The problems and phenomena involved in the action of water waves have attracted mathematicians, scientists, and engineers alike. Many of the early mathematicians such as Stokes, Airy, and Gerstner developed mathematical theories which could be used in the analysis of waves. The engineers then took the mathematical theories and applied them to actual wave problems and to the design of coastal structures.

10. A regular train of waves with relatively small wave height can be treated quite adequately with mathematical theory. However, when waves reach shallow water and approach the breaking point, the existing mathematical theory is inadequate. It has been said that the breaking wave is one of the most complex phenomena known to man.

11. The mathematical theories are the foundations upon which the engineers developed design procedures for coastal structures. In cases where the waves do not break, accurate methods have been developed for the prediction of the pressure caused by waves striking vertical-face structures such as breakwaters, jetties, and seawalls. One of the most famous theories for the prediction of nonbreaking-wave or clapotis pressures was developed by George Sainflou[1] in 1928. This theory is based on the orbital motion of the water particles of the waves. The pressure is a function of the velocity with which the water particles in motion strike the barrier. Sainflou's theory is very widely used, and since the time it was developed there have been many modifications made to it and similar theories have been developed by other engineers and mathematicians.

12. The forces caused by waves which break against vertical-wall structures are greater than the force caused by nonbreaking waves, and the object of several investigations in the past has been a better understanding of this phenomenon. Some of these investigations were precipitated by the more impressive breakwater failures which occurred throughout the world. However, due to the complexity of the phenomenon of breaking waves, no fully satisfactory theories or methods of design have as yet been developed.

13. One of the earliest investigators of the problem of waves breaking against vertical walls was D. D. Gaillard[2] of the U. S. Army Corps of Engineers, whose work was published in 1904. Gaillard made a number of measurements on seawalls and breakwaters situated on the Great Lakes using spring dynamometers and flexible-diaphragm dynamometers. In addition to his own measurements, Gaillard also tabulated some of the wave-pressure measurements of other investigators. He assumed that the pressure produced by a wave breaking against a vertical wall was analogous to the pressure on the face of a plate held normal to a stream of water. In the comparisons made in Gaillard's work, the pressure caused by a wave breaking against a wall was very close to the pressure calculated by considering the wave to be a stream of water. Gaillard himself said that the dynamometers used were not sensitive to any shock pressure which might have occurred. However, he considered the shock pressure to be insignificant in that it had little, if any, effect on the structure. It is believed that the pressure measured by Gaillard was the secondary pressure, which occurs after the instant of shock pressure and is of a much lesser magnitude.

14. In 1920 an investigation similar to Gaillard's was carried out in Japan by Isamu Hiroi.[3] Hiroi also made prototype pressure measurements and it appears that he used more sensitive measuring apparatus because he recorded pressures which seem to be in the range of shock pressures. Hiroi also attempted to measure the energy of waves by means of a pendulum apparatus which he called a wave motor, but no attempt was made to relate the pressures caused by breaking waves to the wave characteristics.

15. Gaillard and Hiroi were among the first to measure the pressure caused by breaking waves, but due to their lack of refined equipment they were unable to measure the shock pressures caused by breaking waves. They did, on the other hand, recognize that breaking waves do more damage than nonbreaking waves when they strike a wall. As a result of this observation, they led others to study the problem more closely with more sophisticated equipment. In the succeeding paragraphs the more significant studies of the pressures caused by breaking waves will be discussed.

The Pioneer Breaking-Wave Pressure Studies

16. By far the greatest number of experiments on the effects of breaking waves on vertical walls have been conducted in the laboratory. The laboratory investigation is much easier to conduct and gives a great amount of information since most variables can be controlled. The experiments conducted on prototype structures tell what is actually happening without resorting to extrapolation of the laboratory data. However, prototype experiments are infinitely more difficult to conduct since one must rely on nature to provide the proper conditions.

17. The first laboratory investigation of breaking waves was conducted by Jean Larras[4] in France in 1937. In addition to investigating the nature of the pressure created on a vertical wall by a breaking wave, he also investigated the characteristics and mechanism for breaking waves on a beach with no barrier. The aim of his investigation on breaking waves without a barrier was to confirm the theories of breaking waves with regard to the depth of water at breaking and to the wave height at breaking. Larras also investigated the effect of bottom roughness on the breaking characteristics of the wave and the energy expended by the breaking wave. The results of the laboratory experiments were compared with results of the prototype investigations conducted by Gaillard and others. Larras concluded that very little scale effect was evident in the breaking of waves on a beach with no barrier present.

18. In measuring the pressure of breaking waves, Larras used sensing equipment which was sensitive enough to record high-frequency fluctuations of pressure. He discovered that the pressure rose very rapidly and then dropped rapidly as the wave first hit the wall. After this initial spike there was a longer duration pressure of lesser intensity. Larras concluded that the development of the pressure was strictly a hydrodynamic phenomenon. However, no attempt was made to develop any relations from which the pressure might be predicted and no numerical data were presented.

19. He did, however, investigate the effect of lowering the top of the wall to the still-water level. In comparison of the results of the tests conducted with the high wall at which no overtopping occurred and

with the wall lowered to the still-water level, he found that the shock pressure was almost completely eliminated in the latter case.

20. In addition to the testing program, Larras also developed a mathematical theory to predict the breaking characteristics of a wave on a beach with no barrier.

21. At the same time that Larras was conducting his experiments in the laboratory, three other investigators--A. de Rouville, P. Besson, and P. Pétry[5]--were conducting breaking-wave pressure experiments on actual concrete breakwaters on the coasts of France and Algeria. Although the face of these breakwaters had a slight batter, they can be considered to be vertical for the purposes of this discussion. De Rouville, Besson, and Pétry measured the pressures due to the waves breaking against the breakwaters with piezoelectric pressure cells. These pressure cells were mounted in fixed locations in the face of the breakwater. The results of their experiments were very significant since their data showed the same type pressure pulse as that which was measured in the laboratory by Larras. These three men made the first measurements of the high shock pressures as they actually occur in nature. For one particular wave which had a height of 8.2 ft at breaking, they recorded a shock pressure of 98 psi. The shock pressure is more than 50 times the hydrostatic pressure of the wave on the wall. A very detailed report was made of their findings, including some photographs of the pressure-time records. Their study is the only prototype investigation which has contributed any significant data concerning the shock pressures due to breaking waves.

22. Having been inspired by the findings of de Rouville, Besson, and Pétry, Ralph A. Bagnold[6] of England conducted laboratory experiments in 1938. The purpose of Bagnold's experiments was to aid in discovering the nature of breaking waves. The laboratory tests were conducted in a flume of such dimensions that solitary waves with a height of 10 in. could be generated in 18 in. of water. The waves were generated with a paddle-type generator. The wave generator was timed so that the forward stroke coincided with the reflection of the crest of the wave returning from the test wall; thus, a series of solitary waves was generated in the flume as opposed to a train of oscillatory waves. Bagnold used a sloping

beach to cause the waves to break at the wall.

23. His pressure measuring equipment consisted of a quartz piezoelectric pressure gage fitted in a T-slot in the test wall in such a manner as to enable the cell to be moved to various positions up and down the wall. The pressure was recorded by photographing the oscilloscope trace. However, there was no way of triggering the camera automatically, and as a result Bagnold made no photographs of the trace of any shock pressure pulse.

24. From his observation of the waves breaking against the wall, Bagnold theorized that the short-duration shock pressure was caused by the compression of a thin layer of air which was trapped between the face of the breaking wave and the wall. This thin layer of air was assumed to be compressed at such a rapid rate that it caused a pressure of very high intensity but of short duration on the wall. However, if the layer of air is thicker, it decreases the pressure since it gives a cushioning effect to the face of the breaking wave.

25. Rather than attempt to draw conclusions from the maximum pressure alone, Bagnold analyzed the phenomena with regard to the impulse transferred to the wall by the wave hitting it. This approach was taken since the impulse is only a function of the pressure variation observed and not of the thin layer of air which he visualized.

26. Bagnold assumed that the wave striking the wall was analogous to a solid plunger compressing air. This plunger had a unit cross-sectional area and an undetermined length. The density of the plunger was assumed to be equal to the density of water. In order to cause the impulse on the wall it was further assumed that this plunger moves at the same velocity as the wave front striking the wall. The shock impulse transferred to the wall by the breaking was equated to the momentum of the above-mentioned fictitious mass of fluid or plunger. Thus, the length dimension of the mass of fluid could be easily calculated from the measurable quantities. This length is approximately one-fifth of the wave height.

27. Bagnold compared this theory with the results of the prototype tests conducted by de Rouville, Besson, and Pétry at Dieppe in 1935 and

1937. In some instances there was close agreement. However, in about half of the results tabulated by Bagnold there is little agreement between the observed impulse and the momentum of the fictitious column of fluid. It is difficult to say whether or not there is a definite correlation since only seven values were tabulated by Bagnold, and many other factors enter into the prototype measurements.

28. Having arrived at a method of calculating the length of the water column involved in the shock pressure, Bagnold considered the rate at which this column compresses a layer of air and the maximum pressure produced when the water column comes to rest. In order to accomplish this, he let the water-column plunger compress a layer of air of given thickness with an initial pressure equal to the atmospheric pressure. It is assumed that the layer of air is compressed adiabatically. From a number of theoretical pressure-time curves which were computed by graphical integration, Bagnold then gave the peak pressure to be

$$p_{max} = \frac{2.7\rho U^2 K}{D}$$

which produces results within ± 10 percent in any consistent units. In the above equation p_{max} is the maximum pressure, ρ is the mass density of the water, U is the velocity with which the wave strikes the wall, K is the length of the column of water and is assumed to be equal to one-fifth of the wave height, and D is the thickness of the entrapped layer of air.

29. Bagnold went on to say that in a vacuum, true water-hammer pressures could occur. However, since under atmospheric conditions some air will always be trapped, no direct impact between the water and the wall can occur.

30. In comparing the values of the shock pressure he observed with the data obtained by de Rouville, Besson, and Pétry, and applying the normal model laws for pressure, Bagnold noted that the laboratory pressures were comparatively much higher than the prototype values. Bagnold hypothesized that this was due to the irregularities in the surface of the sea which were not present in the laboratory and also due to the additional

cushioning created by the presence of foam and froth in the sea water which was also absent in the laboratory.

Minikin's Equation

31. In 1946 R. R. Minikin,[7,8] also in England, combined results of Bagnold with his own experiences and set forth an equation for the maximum shock pressure that can be expected. This equation gives the maximum shock pressure in terms of wavelength, wave height, and water depth. It is used widely today and has the following form:

$$p_{max} = 101\rho g(d_w + d)\frac{d_w}{d}\frac{H}{L}$$

This equation is not dimensionally homogeneous. In the English system, p_{max} is the maximum shock pressure in pounds per square foot, ρg is the specific weight of the water in pounds per cubic foot, d_w is the depth of water at the toe of the wall in feet, d is the water depth in deeper water in feet, and H and L are the wave height and wavelength, respectively, both in feet. The equation was developed originally for a composite type of breakwater, in which case d_w would be the depth of water at the toe of the vertical wall and d would be the depth of the water at the toe of the rubble-mound foundation.

32. The maximum pressure is assumed to act at the still-water level. The pressure at other points on the wall is given by the equation

$$p = p_{max}\left(1 - \frac{2y}{H}\right)^2$$

where p is the pressure at a point y distance above or below the still-water level, p_{max} is the maximum shock pressure, and H is the wave height. The hydrostatic pressure due to runup is added to the shock pressure. The hydrostatic pressure is assumed to be zero at a point $H/2$ above the still-water level. Although Minikin's equation has been modified and tempered by personal experience of engineers who have used it, it is one of the most widely used equations for pressure due to breaking waves.

Further Experiments with Breaking-Wave Pressures

33. Primarily because of the work of Bagnold and the theory that he presented, many recent studies have been made and different equations have been proposed. The first of these later studies was conducted by Douglas F. Denny.[9] Denny's study was primarily a continuation of Bagnold's work, but he approached the problem in a different manner and made no attempt to either verify or disprove Bagnold's hypothesis. Denny used essentially the same facility as Bagnold except that he replaced the sloping beach with a berm. He stated that this change was made because the length and height of a berm were easier to change than a slope and thus the breaking of the wave could be more easily controlled. The recording equipment used by Denny was also different from that used by Bagnold. Denny used a magnetic induction device to measure and record pressure. To check the maximum pressure which had occurred he used a gage which recorded only the maximum pressure. In addition to pressure, Denny also measured the impulse transferred to the wall by a breaking wave. The impulse was measured by the deflection of a heavy wall suspended on knife edges and springs.

34. The procedure Denny used in analyzing his results differed from the methods of the previous investigators in that he used a statistical approach. Many measurements of pressure were taken for a given wave condition. The frequency of occurrence was then plotted versus the ratio of shock pressure to wave height. A similar distribution of shock impulse was made. The plots shown in Denny's paper indicate that the most frequently occurring pressure varied from approximately one-fourth to one-third of the maximum pressure which he recorded. He went on to say that both the maximum pressure and the most frequently occurring pressure appear to be directly proportional to wave height. However, the variation of pressure with wave height was the only relation presented. The range of wave height used by Denny (7 in. to 15 in.) provides too limited a range to afford reliable extrapolation to prototype size waves. The system Denny used to generate the waves was the same as that used by Bagnold. The periods of the oscillatory waves were synchronized with the

natural period of the wave tank. Tests were also conducted using solitary waves.

35. The conclusions concerning the duration and intensity of the shock pressure were similar to those of Bagnold. Denny found that the intensity of the shock pressure was inversely proportional to its duration, and the area of the pressure-time curve of the shock pressure or shock impulse tends toward a maximum which is a fraction of the total momentum of the wave before breaking.

36. Further laboratory experimentation on the pressure caused by breaking waves was reported in 1953 by Culbertson W. Ross.[10,11] The research conducted by Ross was done at the U. S. Army Corps of Engineers Beach Erosion Board (now the Coastal Engineering Research Center). The paper by Ross[10] is of particular value since it is one of the very few in which the data are presented in detail.

37. The apparatus used in Ross' experiments consisted of a steel wall in which either one or two pressure cells could be mounted. When two cells were used, they were mounted 9 in. apart horizontally. Provision was made to enable the pressure gages to be raised or lowered to various positions on the wall. The sensing elements of the pressure cells consisted of a stack of four thin disks of tourmaline crystal. Ross varied the wave height, wave period, water depth, and beach slope. The range of wave period reported was from 3.5 to 5.0 sec, the wave height varied from 3.5 to 7.5 in., and the still-water depth varied from 10.7 to 14.2 in. The beach slopes used in these tests were 0.078, 0.094, 0.144, and 0.176. The height of the pressure cell varied within a range of approximately 4 in. along the wall.

38. In addition to the pressure, Ross also measured the pressure-time integral of the shock pressure. He found that this integral was essentially constant regardless of the magnitude of the shock pressure, thus supporting Bagnold's findings. Upon comparison of the measured value of the shock impulse with the total momentum of the wave, it was found that the measured shock impulse was usually less than 10 percent of the total momentum of a corresponding solitary wave. It was mentioned that the data obtained were insufficient to draw any relation between the

pressure and wave characteristics. However, an approximately linear relation was indicated between shock pressure and wave height.

39. Another recent and noteworthy investigation of the shock pressure due to breaking waves was conducted by Shoshichiro Nagai[12] in Japan. Extensive measurements of the pressures due to waves breaking on composite-type breakwaters were made during his investigation. His tests involved the observation of the effects of both solitary and oscillatory waves. However, no comparison between the pressures due to solitary waves and oscillatory waves was reported.

40. Nagai tested a variety of different breakwaters and wave conditions. The slope in front of the vertical-wall structure varied from 1/2 to 1/10. The effect of a berm in front of the wall at the top of the slope was also studied. The wave height tested by Nagai ranged between 2.4 and 8.7 in. The wave period of the oscillatory waves varied from 1.2 to 2.0 sec.

41. High-speed motion pictures were taken of the waves at impact and related to the pressure measurements. From these motion pictures it was determined that the fast-rising impact pressure occurs as the wave strikes the wall, a minimum pressure occurs just after the time of maximum runup (and momentum reversal), and the second maximum occurs as the water is falling back down the wall. Thus, it was assumed that the impulse transferred to the wall is equal to the area under the first peak of the pressure-time curve. The area under the second peak of the pressure-time curve is assumed to be equal to the momentum gained by the retrogressive wave. It was found that in most cases the ratio of impulse to momentum change was less than one.

42. The pressure distribution on the wall was found to have two general shapes. The first had its maximum at or near the still-water level and decreased parabolically to zero at points equidistant above and below the maximum. This distribution was the same as that proposed by Minikin. The second type of pressure distribution had its maximum at the bottom of the wall and also decreased parabolically to zero.

43. Nagai determined that the maximum shock pressure was a function of water depth at the wall, d_w ; water depth in the horizontal bottom

portion of the channel, d ; and the wave steepness in the horizontal bottom portion of the channel, H/L . In terms of these variables, the upper limiting value of the maximum pressures p_{max} was expressed in grams per square centimeter as follows:

$$p_{max} = 300 \left(0.051 + \frac{d_w^2}{d} \frac{H}{L}\right)^{1/3}$$

44. Nagai proposed that this relation for the maximum shock pressure be applied to prototype structures using the Froudian model relations. Upon comparison with the maximum pressure measurements of de Rouville, Besson, and Pétry, there is favorable agreement with Nagai's formula in most cases. However, in a few of the cases the value measured in the prototype was almost twice as great as that predicted by Nagai's equation.

45. Nagai concluded that the very high shock pressure occurs only for a small range of wave conditions. Thus, the probability of its occurrence is small. He also concluded that this probability increases as the slope in front of the vertical wall becomes flatter.

46. In 1958 Lennart Rundgren[13] reported on research conducted in Sweden on both breaking and nonbreaking waves. He went into great detail in the case of nonbreaking waves, but the presentation concerning breaking waves was less extensive. Using different wave conditions and a beach slope of 1/9.4, and varying the water depth, he investigated the character of the breaking-wave pressures and the conditions under which they occur. Rundgren compared the breaking-wave parameters which he observed for waves breaking on vertical wall with those predicted by Munk's solitary-wave theory.[18] He concluded that the wall had an effect on the breaking characteristics of the wave. The depth of water necessary at the wall to cause high shock pressure was significantly less than that in which the wave would break on an unobstructed beach slope. The breaking depth on the unobstructed beach slope was that depth predicted by Munk's theory.[18] Rundgren made simultaneous pressure measurements at six different elevations on the test wall and found that the peak pressures did not quite occur simultaneously. The peak pressure first occurred at the lowest point and then successively occurred at higher points up the wall.

The rate at which the pressure peak moved up the wall varied from test to test.

47. Rundgren compared his test results with those of other investigators and concluded that the following relation between shock pressure and wave steepness was applicable:

$$\frac{p_{max}}{\rho g H_o} = c_1 \ln (H_o/L_o) + c_2$$

where p_{max} is the maximum shock pressure, ρg is the specific weight of the water, H_o and L_o are the deepwater wave height and wavelength, respectively, and c_1 and c_2 are two undetermined constants.

48. Rundgren stated that in his pressure measurements some error is probably involved due to the close proximity of the natural frequency of the pressure cells used and the frequency of the shock pressure. However, in spite of this error, he also concluded that his tests and those of others point to an approximately linear relation between shock pressure and wave height.

49. Also in 1958 two Japanese investigators, Taizo Hayashi and Masataro Hattori,[14] reported the results of their laboratory studies on breaking-wave pressure on a vertical wall. The main concern of Hayashi and Hattori was not the initial shock pressure, but the longer duration secondary pressure following the shock pressure. They assumed that the secondary pressure was directly proportional to the velocity head of the water striking the test wall. The aim of the investigation was to determine the constant of proportionality. A preliminary theoretical investigation was made starting from the existing theory of the dynamic pressure caused by a jet striking a plate. It was thus determined that the pressure was proportional to the velocity in the following manner:

$$\frac{p_2}{\rho g} = \frac{2U^2}{g}$$

where p_2 is the pressure caused on the wall by the wave, excluding the initial shock pressure; ρg is the specific weight of the water; U is the

velocity of the water at impact on the wall; and g is the acceleration of gravity.

50. The testing program consisted of making five simultaneous pressure measurements at different elevations on the vertical test wall. A solitary wave was used in order to eliminate the effects of the previous waves in a train of oscillatory waves. Beach slopes of 0.044, 0.069, and 0.088 were used in addition to various water depths and wave dimensions. The velocity of the water at impact was determined from motion pictures of the breaking wave. No firm conclusions were drawn concerning either the secondary pressure or the initial shock pressure, but Hayashi and Hattori did publish their data in tabular form. A few of their shock pressure measurements are included in the graphs presented later herein.

Studies of the Total Force due to Breaking Waves

51. There have been many studies of the pressure caused by breaking waves, but relatively few concerned the total force of breaking waves. The two most noteworthy studies of the total force due to breaking waves were conducted in 1954 by John H. Carr[15] and in 1961 by J. J. Leendertse.[16]

52. Both Carr and Leendertse used the same type of equipment. A three-component force balance was used to measure the force and momentum of a breaking wave. In Carr's experiments the still-water depth was fixed at 2 ft; however, the water depth at the toe of the wall was adjustable so that the waves could be made to break directly on the structure. The beach slopes used in this study were 1/3, 1/10, and 1/30. The wave conditions were also varied. The effect of inclining the barrier to an angle of 30 deg shoreward from vertical was studied along with the vertical barrier.

53. Carr presented a number of dimensionless plots of force, moment, and impulse versus deepwater wave steepness for different conditions. Utilizing these plots, Carr concluded that the forces obtained were in excess of the forces calculated by the Minikin method. He also found that inclining the barrier 30 deg shoreward from the vertical tends to halve the forces which would occur on a vertical barrier.

54. In addition to force measurements, Carr also made some pressure

measurements using a barium titanate piezoelectric pressure cell. The results of these tests were not reported; however, it was stated that the measurements were similar to those reported by other investigators. Stroboscopic photography was employed to gain more information concerning the kinematics of breaking waves, but no data from the photographs were presented.

55. The impulse measurements by Carr showed that the impulse of the short-duration transient force does not exceed about 10 percent of the total impulse of the force on the wall from the time of wave contact to the time of momentum reversal. Carr assumed that momentum reversal occurred at the second maximum of the force-time curve. This point was determined by analogy from the essentially sinusoidal force-time curve due to a clapotis. In the case of the clapotis, the maximum force occurs when the flow has been brought to rest, or at the instant of momentum reversal.

56. Leendertse's study was similar to Carr's; however, he considered only a beach slope of 1/10. The waves used by Leendertse varied in height from 0.2 to 0.6 ft. Leendertse's data were presented in a manner similar to the way in which Carr presented his data. There is close agreement between the results of the two studies. Leendertse went one step further and presented a method of analyzing breakwaters for the effects of breaking waves. The method of analysis was based on the results of his study.

Summary of Historical Background

57. The present study was based largely on investigations conducted by previous authors. Both their data and their methods of analysis were used as a basis for comparison with the results obtained from this experimental program. In the preceding sections of this Part short summaries of some of the more significant investigations were presented in order to familiarize the reader with what has been done and to point out some of the accomplishments and shortcomings of these investigations. A wealth of information has been gathered concerning the pressure due to waves breaking on vertical-wall structures, but for the most part much of it has never been put together. By using the results and some of the data of

others who have studied the problem, it is believed that a more comprehensive study could be made.

PART III: EXPERIMENTAL EQUIPMENT AND PROCEDURE

58. This Part describes the experimental portion of this study in general terms. A detailed discussion of the experimental equipment and procedure along with a discussion of the accuracy of the equipment is presented in Appendix A.

59. The experimental portion of this study was conducted in a wave flume approximately 1 ft wide (fig. 1). The waves were caused to break on

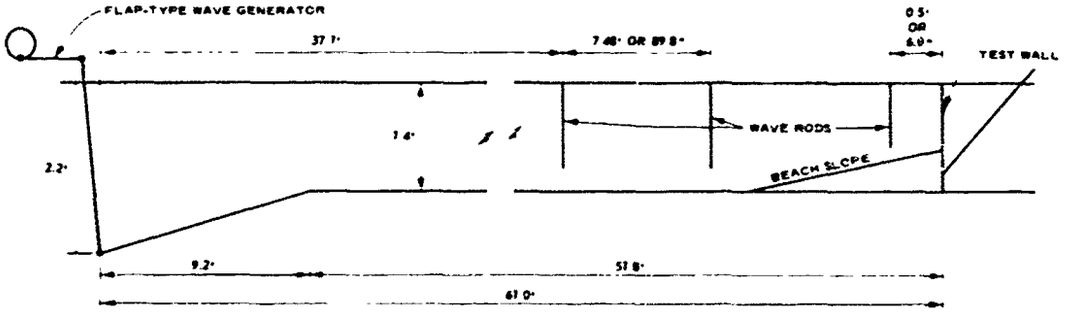

Fig. 1. Diagram of wave flume

the vertical test wall by the use of a beach slope fitted in front of the wall. The test wall was constructed of aluminum plate and fitted with a pressure transducer. Photographs of the front and back of the test wall are shown in fig. 2.

60. The variation of pressure with time was recorded by an oscillograph capable of accurately recording the high-frequency pressure variations. The pressure cell was movable in the vertical direction on the test wall so that pressure could be measured at various locations. No arrangement was made for more than one pressure cell; thus, no simultaneous pressure measurements at different points on the wall were obtained. However, based on the work of other investigators, it was assumed that the shock pressure acts on all points on the wall at the same time.

61. The wave heights were recorded at three locations in the flume using resistance-type wave height gages. Two gages were placed in the portion of the flume with the horizontal bottom. The third gage was placed close to the test wall to measure the wave height at breaking. The wave

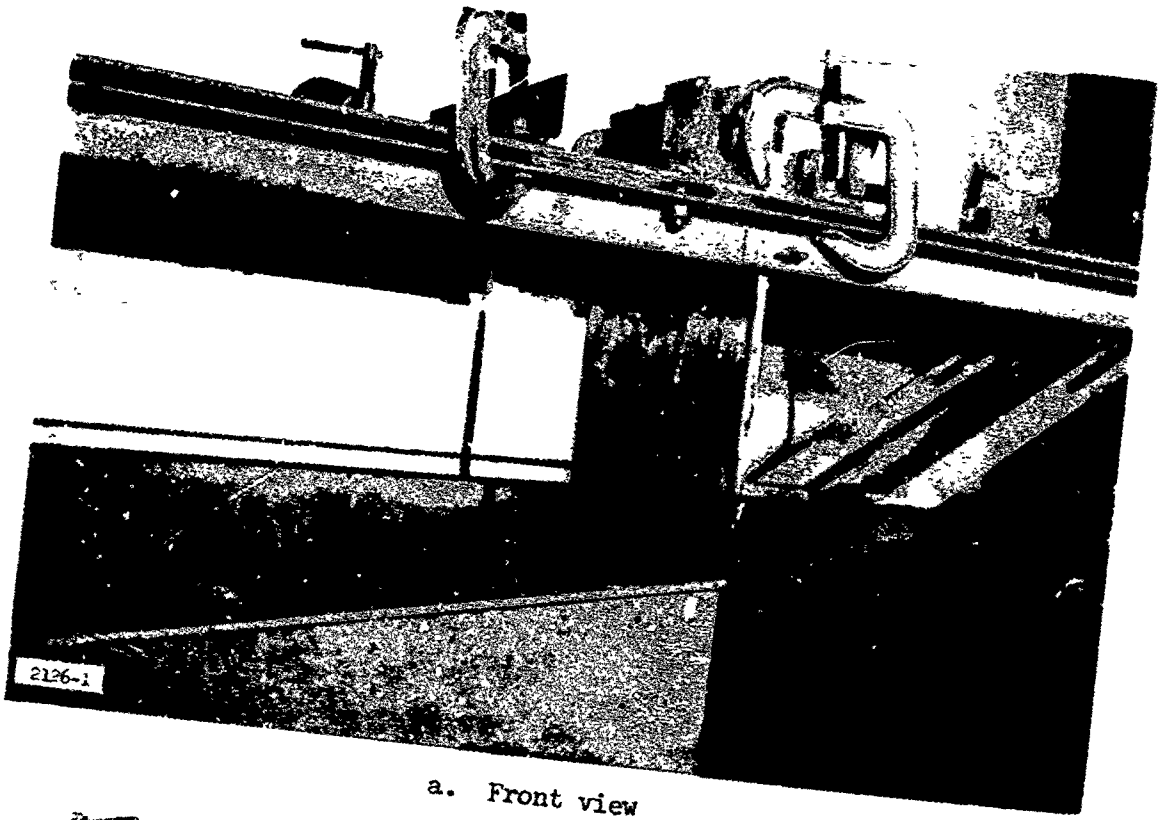

a. Front view

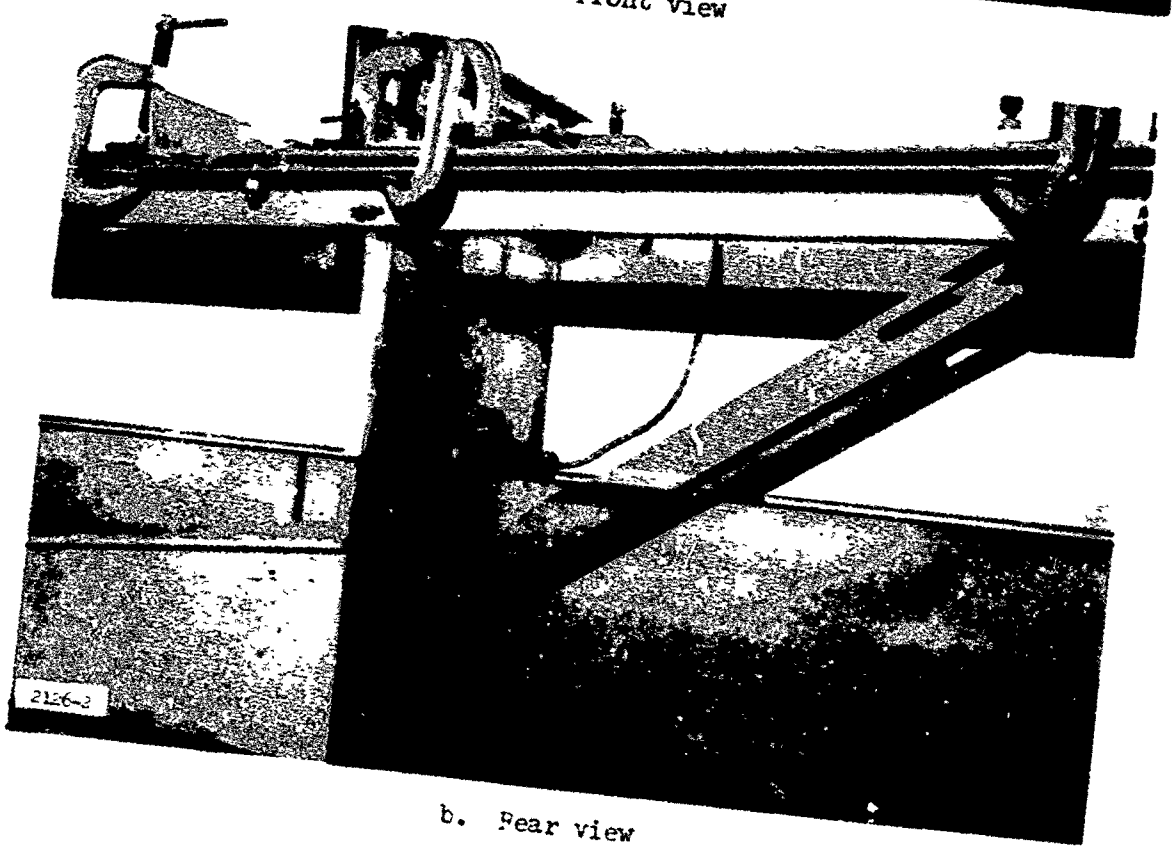

b. Rear view

Fig. 2. Test wall

heights were recorded on an oscillograph.

62. The sizes of the waves used in this study were dictated by the size of the flume and the capabilities of the wave generator. Due to the limited depth of the flume, the maximum wave height in the flume was approximately 3-1/2 in. Although there was no lower limit or minimum wave height, the smallest practical wave height was about 1 in. The longest period which the wave generator was capable of producing was 2 sec. The wave generator was capable of producing waves of very short period (less than 1 sec); however, for periods below about 1-1/2 sec the uniformity of the waves within a train became difficult to control. The water depth was determined by the height and period of the waves used since the water depth at the wall could only be changed by changing the water depth in the flume. The height of the beach slope above the flume bottom at the test wall was fixed. Two different beach slopes were used. One beach had a slope of 1/25 and was used for the first seven series of tests. The other beach had a slope of 1/10 and was used for the remaining three series of tests.

63. The actual wave dimensions used were chosen in order to give a representative spread of the effects of wave height, period, and steepness. A summary of the data, including wave dimensions, is given in table 1.

64. It was immediately apparent that there would be much scatter of the shock pressure values. Therefore, in order to increase the probability of recording the highest pressure which might be expected, many tests with identical conditions were conducted. The variations in the shock pressure measurements are discussed in detail in Part IV.

PART IV: DISCUSSION AND ANALYSIS OF THE DATA

A Detailed Discussion of the Data of One Test Series

65. The experimental program consisted of ten series of tests, each series involving different wave and flume characteristics. During each test run of a series, the wave characteristics were kept constant and the position of the pressure cell on the test wall was varied. In order to facilitate the presentation of the data, the discussion will begin with the single test run, and will then continue with a discussion of the data for a group of identical test runs. The discussion will then continue with a close examination of the first test series. Then all of the test series will be combined and compared with the first test series. It is believed that this type of presentation of the data will help the reader follow the testing program more easily, and enable him to see how each test fits into the whole program.

66. An experimental test series was begun by setting a water depth, beach slope, and wave period. The wave height was varied so as to obtain maximum shock pressure on the test wall due to the impact of one of the first four breaking waves, preferably the first or second breaking wave. The pressure was measured at a point near the still-water surface. The choice of this point was based on the findings of previous investigators. Once the wave causing the highest shock pressure was found, it was assumed that this wave would cause the highest pressures on all points along the wall. This means that a wave of a different height but of the same period and in the same water depth, etc., will not cause a shock pressure at any point in the wall which is higher than the pressure at that same point caused by the wave causing maximum shock pressure.

67. The work of previous investigators has shown that the distribution of the shock pressure is not regular along the wall in the vertical direction. Therefore, one of the aims of this investigation was to determine the shape of the distribution of the shock pressure on the wall. To accomplish this aim, the pressure cell was moved in 0.25-in. increments up and down the test wall. Since only one pressure cell was used, it was

assumed that the shock pressure acts simultaneously at all points on the wall. This assumption is not exactly true as has been found by Rundgren; however, for practical purposes it is believed to be a valid assumption.

68. To aid in the discussion of the variations and patterns of the test data from any one test series, test series 1 will be used. Let us begin the discussion with the results of any one single test run, which consisted of measuring the wave characteristics and the pressure caused by the first four consecutive waves which break against the test wall. Due to the energy used in putting the water in motion, since the waves were started in still water, the first few waves generated by the wave machine did not break on the test wall. These waves were reflected, forming clapotis-type action on the test wall. The number of nonbreaking waves preceding the train of breaking waves was found to be dependent on the characteristics of the wave and the flume. These characteristics include the wave period and height, the water depth, the beach slope, and the water depth at the toe of the test wall.

69. The first four breaking waves appeared to the eye to be quite uniform in their characteristics. They all seemed to break at the same point and sent spray as high as 5 ft in the air as they struck the wall. After the fourth breaking wave, the water in the vicinity of the test wall became very disturbed due to splash and reflections of the previous waves.

70. For test series 1, the still-water depth in the uniform-depth portion of the flume was 10.50 in., while the still-water depth at the test wall (which was located on top of the beach slope) was 3.18 in. The slope of the flume bottom (the beach slope) in front of the test wall was 1/25. The average wave conditions for test series 1 were as follows: wave period, 1.93 sec; wave height in uniform-depth portion of flume, 2.30 in.; wavelength in uniform-depth portion of flume, 114.2 in.; wave height at breaking (6.0 in. from face of test wall), 3.15 in. The deepwater wave height and wavelength were calculated by use of the first-order approximation of oscillatory-wave theory as described in Appendix B. The deepwater wave height was 2.21 in., and the deepwater wavelength was 229.1 in.

71. The pressure-time diagram for any point on the test wall was found to be similar to the diagram shown in fig. 3. The pressure rises

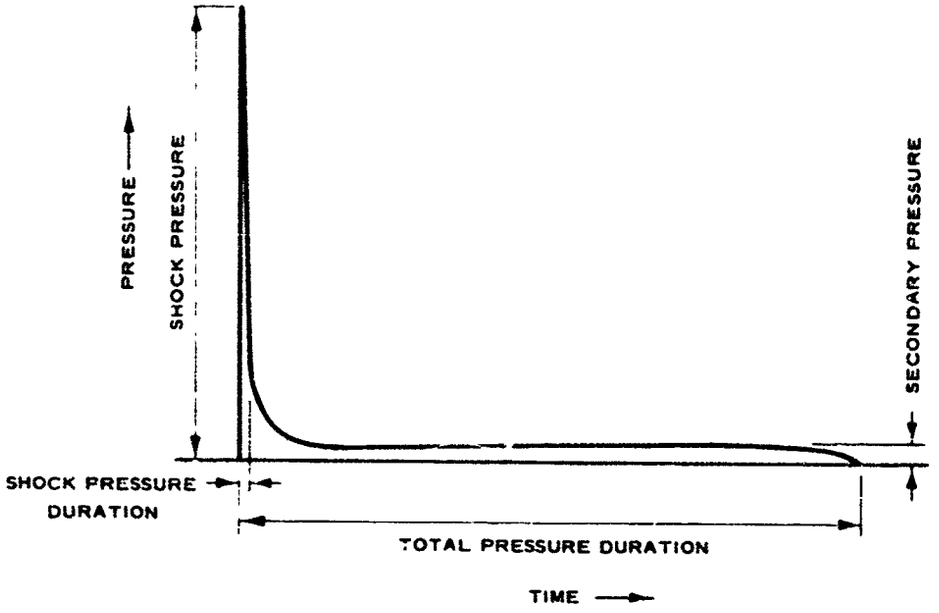

Fig. 3. Typical pressure-time curve

very rapidly to a maximum as the face of the wave strikes the wall and then falls quickly. This initial spike in the pressure-time curve is called the shock pressure, and its duration can be measured in milliseconds. Following the initial spike of the pressure-time curve, there is a second rise in pressure and finally the pressure returns to zero as the wave recedes. The value of the second maximum of the pressure-time diagram is called the secondary pressure and has a much longer duration than the shock pressure. The duration of the secondary pressure from the end of the shock pressure to the final return to zero of the pressure at the still-water level is approximately two-tenths of the wave period. In fig. 3, showing a sketch of a typical pressure-time curve, the various elements have been labeled. Fig. 4 shows a sequence of eight motion-picture frames which show the action of the wave on the wall that causes this type of pressure pulse. These motion pictures were taken at a film speed of 64 frames per second.

72. Within any single test run the magnitude of the shock pressure varied considerably while the magnitude of the secondary pressure remained approximately the same for each of the four waves. To illustrate this, the following are the values of the shock pressure and the average value of

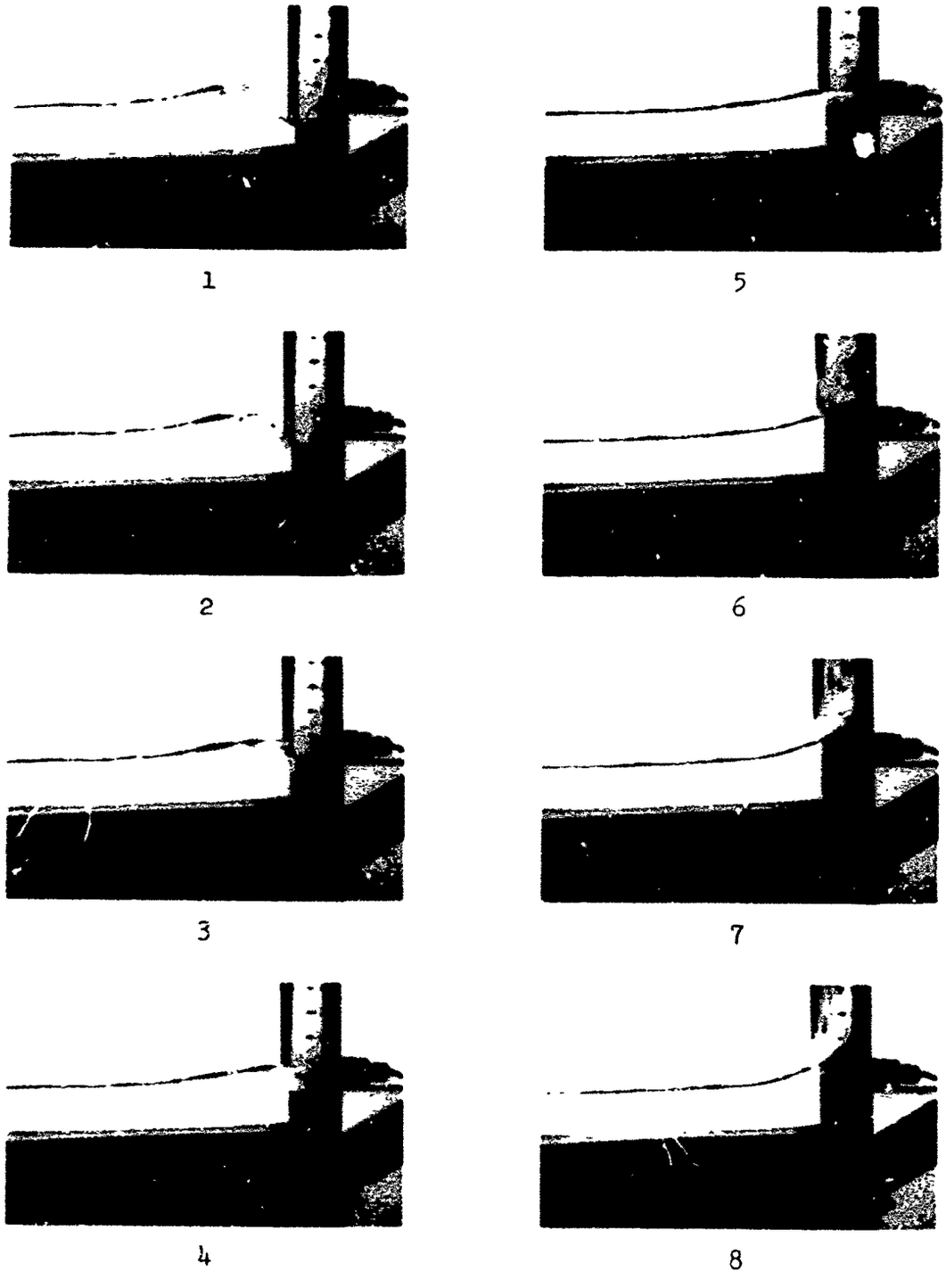

Fig. 4. Sequence of photographs showing wave breaking on test wall

the secondary pressure for the test run of test series 1 in which the highest shock pressure was recorded. The average secondary pressure was 0.10 psi while the shock pressures caused by each of the first four breaking waves were 1.08, 4.08, 2.15, and 1.20 psi, respectively. These measurements were taken at a point 3.75 in. above the foot of the test wall or approximately 1/2 in. above the still-water level.

73. The variation in the magnitude of the shock pressure is evident in these values. They are typical of the spread of most of the shock pressure measurements for any single test, especially in the zone of maximum pressure. Above and below the zone of maximum pressure where the value of the shock pressure decreased considerably, there was much less variation in the magnitude of the shock pressure.

74. In addition to variation of the shock pressure caused by each of the waves in any single test run, there was also considerable variation in the shock pressure from test to test for any given point on the test wall. Due to this variation, numerous measurements were made at each point on the test wall. For example, there were ten test runs made with the pressure cell located 3.75 in. above the bottom of the test wall for test series 1. The values of the shock pressure caused by the first four breaking waves for these ten tests are shown below.

	Shock Pressure, p.i, for the Successive Breaking Waves Indicated			
Test No.	First	Second	Third	Fourth
1	1.18	0.70	0.91	No record
2	1.10	1.71	0.76	0.71
3	1.12	2.47	0.40	0.36
4	1.08	4.08	2.15	1.20
5	1.36	1.81	0.46	0.85
6	1.08	2.51	0.72	0.55
7	1.03	2.06	0.92	0.82
8	1.58	0.80	0.79	0.83
9	1.37	1.58	0.54	0.48
10	1.40	0.71	0.61	0.60

75. Here again the variation from test to test is representative of all of the data of all the tests for any point on the wall. It was also observed that there was less variation in the shock pressure from test to test in the regions on the test wall where the magnitude of the shock

pressure was much less. As mentioned previously, the greatest variations in the magnitude of the shock pressure occurred in the area of maximum pressure. The secondary pressure did not exhibit great scatter as in the case of the shock pressure.

76. Careful examination of the preceding tabulation reveals that there is less variation in the value of the shock pressure between tests for any given wave than between waves for any given test. In other words, there were more generally consistent results between the pressures recorded for a given wave for all the tests than between the four waves of a single test. From the tabulation it can also be seen that the pressures due to the first and second breaking waves of each train were generally higher than the pressures due to the third and fourth waves. Similar results were observed on all the tests. This observation leads one to the conclusion that each of the waves in the train was significantly different even though they looked the same, and there was greater similarity between the wave trains produced in each test than between the waves in any one train.

77. The variation in the data of each of the test series can be more easily seen when presented graphically. In order to illustrate the variation in pressure between the successive waves of a train the arithmetic mean of the shock pressure for each wave of the train was plotted. Fig. 5 shows the results of these computations for test series 1. In this figure are four plots of the mean shock pressure. The numbers 1, 2, 3, and 4 on the curves refer to the number of the breaking wave. It can be seen that there is great variation between each of the successive waves of the train in the area from 3 to 5 in. above the bottom of the wall. This is the region of maximum pressures, the area where greatest variation was always noted. Below 3 in. and above 5 in. the curves tend to merge together. In the area above and below the area of maximum pressures there was great consistency both between each of the waves from test to test and between the successive waves of a single test.

78. Similar results were also noted in the other test series in which waves of different characteristics were tested. The mean shock pressures for each of the waves in the train were also plotted for the

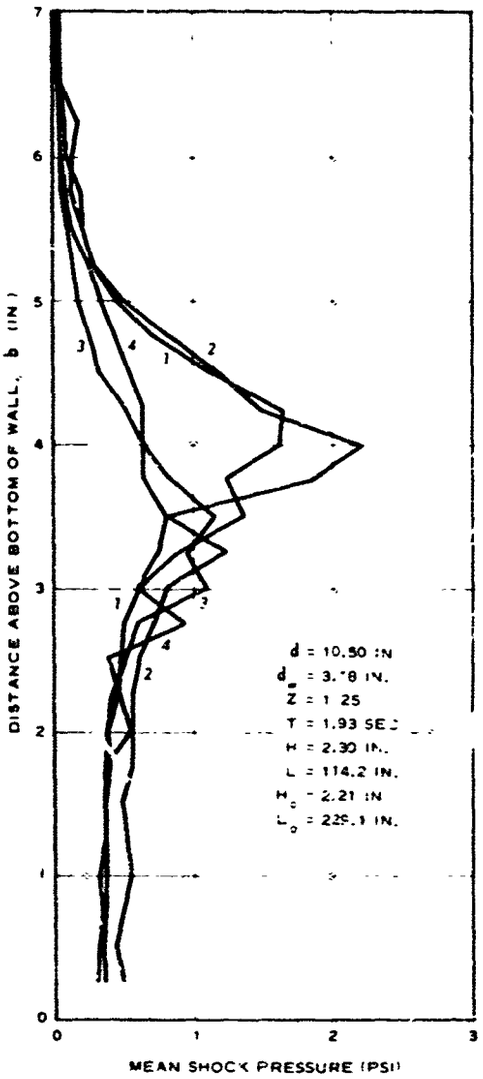

Fig. 5. Variation of mean shock pressure for each of the first four breaking waves; test series 1

other series. These plots are shown in figs. 6 through 14. The notation on these plots is the same as that for fig. 5.

79. A detailed examination of the variation in the secondary pressure was not conducted since the secondary pressure showed little variation. The little variation in the secondary pressure fell within the limits of accuracy of the pressure cell. It was therefore concluded that the secondary pressure is not greatly affected by small changes in wave shape and probably can be accurately predicted. A more detailed discussion of the secondary pressure is presented in paragraphs 111-116.

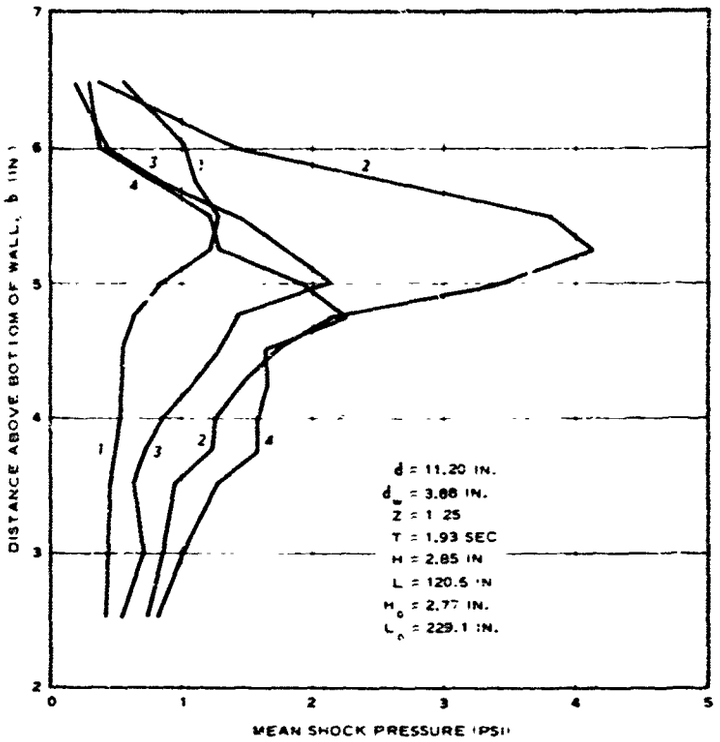

Fig. 6. Variation of mean shock pressure for each of the first four breaking waves; test series 2

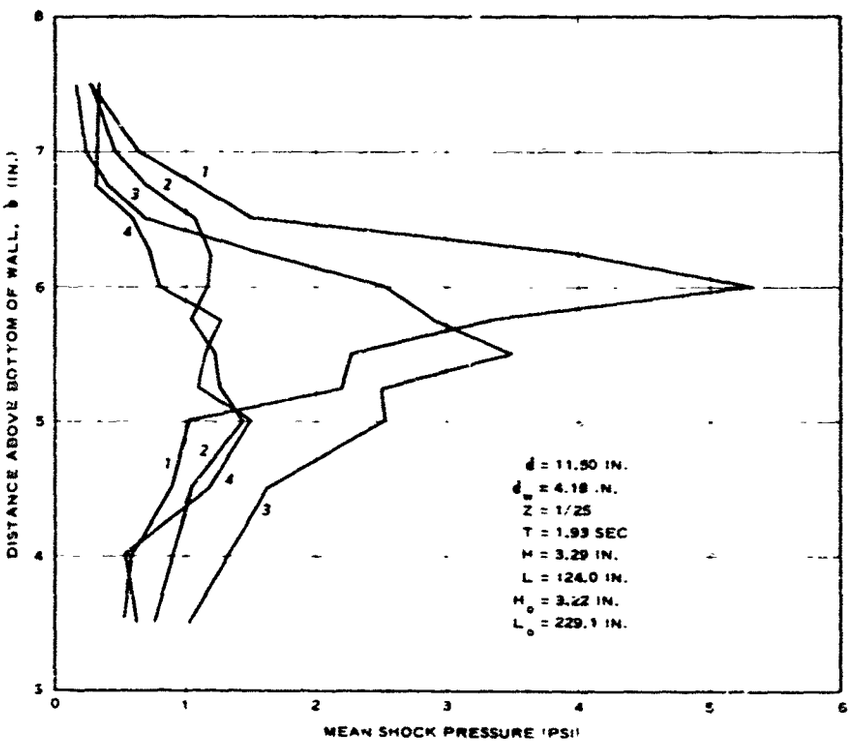

Fig. 7 Variation of mean shock pressure for each of the first four breaking waves; test series 3

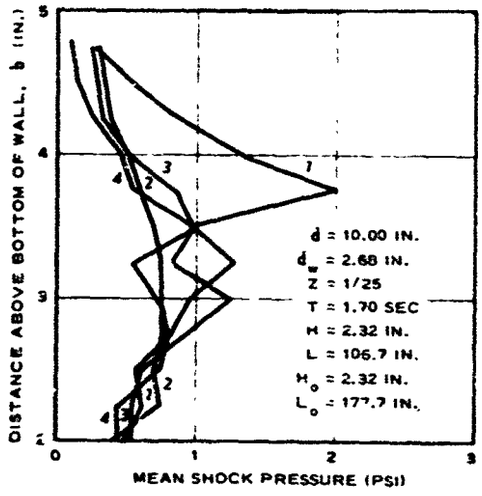

Fig. 8. Variation of mean shock pressure for each of the first four breaking waves; test series 4

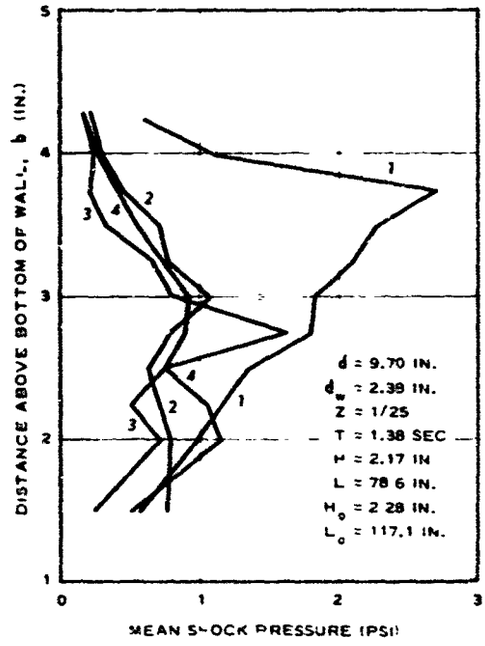

Fig. 9. Variation of mean shock pressure for each of the first four breaking waves; test series 5

Fig. 10. Variation of mean shock pressure for each of the first four breaking waves; test series 6

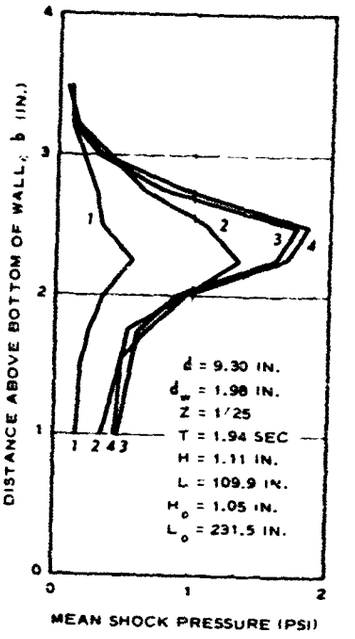

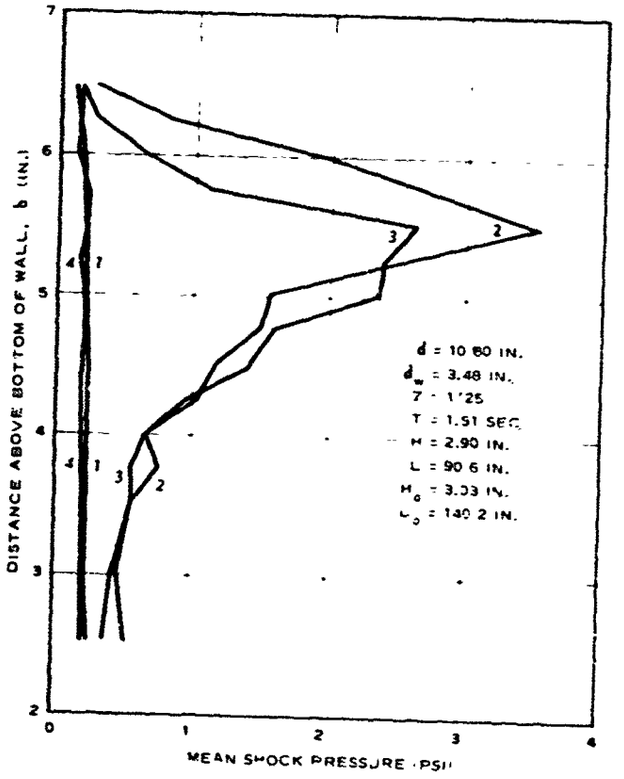

Fig. 11. Variation of mean shock pressure for each of the first four breaking waves; test series 7

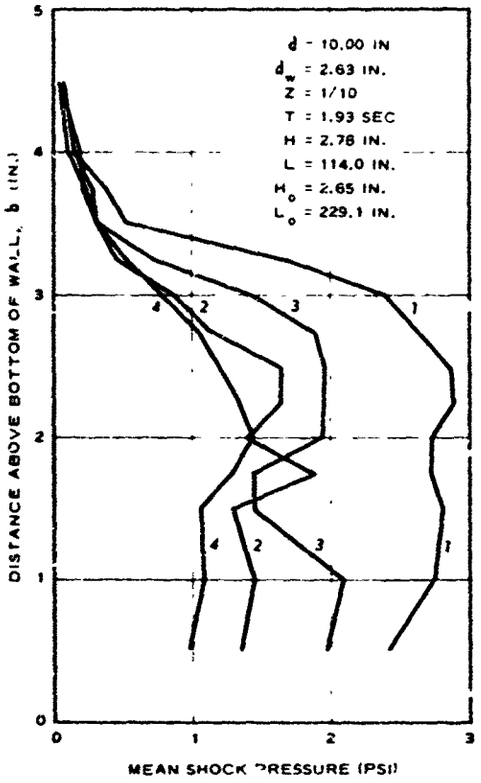

Fig. 12. Variation of mean shock pressure for each of the first four breaking waves; test series 8

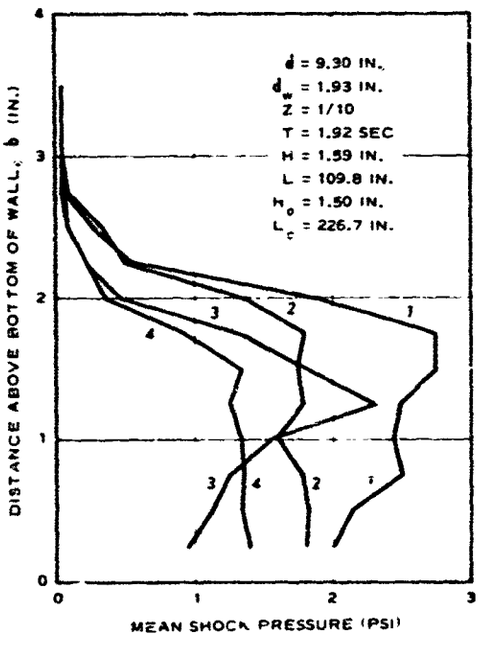

Fig. 13. Variation of mean shock pressure for each of the first four breaking waves; test series 9

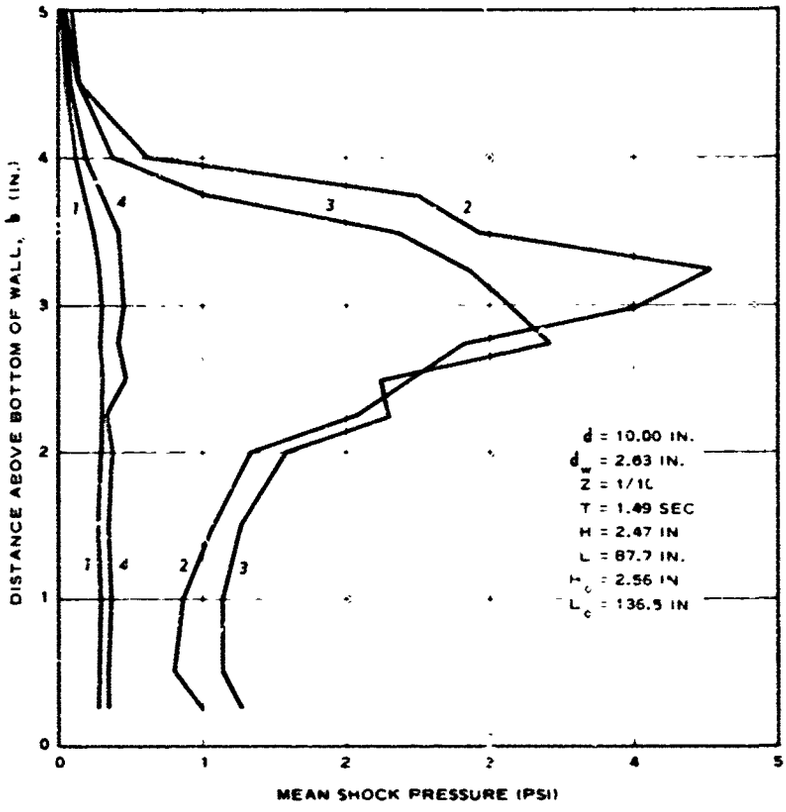

Fig. 14. Variation of mean shock pressure for each of the first four breaking waves; test series 10

80. In test series 1, pressure measurements were taken at 0.25-in. increments vertically along the wall. The lowest position of the center of the pressure cell was 0.25 in. above the bottom, with the edge of the 0.50-in.-diam sensing element of the pressure cell at the bottom of the test wall. The uppermost measurement was made 7 in. above the bottom of the test wall. At approximately this point, both the shock pressure and the secondary pressure became too small to measure. The pressure distribution thus observed was similar to that observed by earlier investigators. The maximum pressure occurred near the still-water level, in this case at a small distance above the still-water level. Above this point of maximum pressure, the shock pressure decreased approximately parabolically to zero. Below the point of maximum shock pressure, the shock pressure decreased to a lesser value and then was fairly uniform to the base of the wall. The general shape of the pressure distribution was similar to the distribution of the mean shock pressure shown in fig. 5. However,

when the maximum pressures observed were plotted, the cusp at the point of maximum pressure became more pronounced. In considering the maximum pressures on the test wall, the maximum pressure observed at a point on the wall was noted regardless of which wave in the train caused it. Thus, the resulting distribution curves of maximum shock pressure represent the maximum of all shock pressures recorded. In this particular test series the higher shock pressure generally was caused by the second breaking wave of the train.

81. This particular method of plotting maximum pressure was chosen due to the great variation in their magnitudes. The aim of the test series was to measure the maximum pressures caused by a wave of given characteristics. It soon became evident that huge numbers of tests would have to be conducted to arrive at an absolute maximum pressure or even a maximum pressure which could be computed statistically. Therefore, in order to come as close to the goal as possible and yet keep the experimental program within the limitations of time and facilities, a relatively small amount of data was taken for each wave condition. Although the data of one test series in themselves do not provide any absolutes, when they are combined with the data of the other test series, and the corresponding data of other investigators, useful results and general trends can be developed.

82. The complete shock pressure data from test series 1 are presented in table 2. The left-hand column of the table gives the elevation of the pressure measurement measured in inches above the bottom of the wall. The pressure data shown are the values of shock pressure measured in pounds per square inch above atmospheric pressure, for the first through the fourth breaking waves of the train. Tables 3 through 11 show the data from the other nine test series. Similar results were observed in these tests.

83. The maximum shock pressures observed in test series 1 were plotted (solid curve, fig. 15). It can be seen that the higher shock pressure occurs in the area in which the face of the breaking wave strikes the wall. The elevations of the crest and the trough of the breaking wave are also shown in the figure. The breaker crest and trough elevations were

measured at a point 6 in. from the face of the wall. However, these elevations are very close to those of the crest, as the wave strikes the wall, and the maximum drawdown. It is impossible to measure the breaking-wave height accurately at a point close to the wall due to the runup of the wave and the splash. Also shown in fig. 15 is the still-water level. It was observed that, although the higher shock pressures occurred between the crest and the trough of the breaking wave, a shock pressure developed below the point of maximum drawdown as low as the bottom elevation of the wall.

84. The pressures observed in this experimental program were compared with corresponding pressures predicted by Minikin's equations.[7,8] Minikin's equations were used as a basis of comparison since they are widely used in the United States for the prediction of shock pressures on vertical walls due to breaking waves. Minikin's equation for maximum shock pressure is given in paragraph 31. The maximum pressure is assumed to act at the still-water level. The equation for the pressure at other points on the test wall is also given by Minikin (see paragraph 32). Computations were made for the waves used in test series 1, and they are plotted in fig. 15 together with the observed data. For this one test series, the pressures predicted by Minikin's method compare favorably with the observed shock pressures. The main differences lie in the assumption that the maximum pressure acts at the still-water level and the assumption that there is no shock pressure developed below $H/2$ below the still-water level. The other two curves in fig. 15 are discussed in subsequent paragraphs.

A Comparison of the Results of All Test Series

85. It is believed that the results of the first test series have been discussed in sufficient detail to relate those data to the data obtained in the succeeding test series. The results of all of the test series will be related to each other in an attempt to determine common factors and trends. The data will be discussed first relating the observations, then applying these observations to what is already known or

hypothesized about the shock pressures caused by breaking waves.

86. In order to more easily compare the results of each of the test series, separate plots of the maximum shock pressure distribution for each test series were made. These plots are similar to fig. 15, and are shown in figs. 16 through 24. As in fig. 15, the shock pressure predicted by Minikin's method is also presented on each of the latter figures in order to facilitate comparison for each wave condition.

87. In order to gain some knowledge of the effect of the slope of the beach in front of the barrier, the beach slope in the last three series of tests was changed from 1/25 to 1/10. Test series 1 through 7, which were conducted with the 1/25 beach slope, will be discussed first. In general, the results of test series 2 through 7 were similar to those of test series 1. The shape of the pressure distribution and the location and magnitude of the maximum pressure were similar to those obtained in the first series of tests. The pressure distribution for each of the series was similar in shape with the maximum pressure occurring above the still-water level and near the elevation of the crest of the breaking wave. In general, the larger waves, both in height and wavelength, tended to produce higher pressures at all points on the test wall. The one marked exception to the similarity of the test data was test series 5. This series was conducted using a relatively short-period wave (1.38 sec) and a great deal of disturbance was noted at the wall due to reflections and splash. The shock pressure distribution for this test series bore little similarity to those of the other series. However, upon examination of fig. 9 for the variation of the mean shock pressure for test series 5, it can be seen that the mean shock pressure for the first breaking wave did conform to the distribution found in the other tests.

88. Since considerable similarity was noted in the distribution of maximum shock pressures on the wall for each of the series of tests thus far discussed, an expression for this common shape was sought. The parabolic distribution proposed by Minikin quite closely approximates the actual distribution of maximum shock pressures. The data from this investigation indicate that the distribution of pressures on the wall is determined by the characteristics of the waves at breaking. The wave height

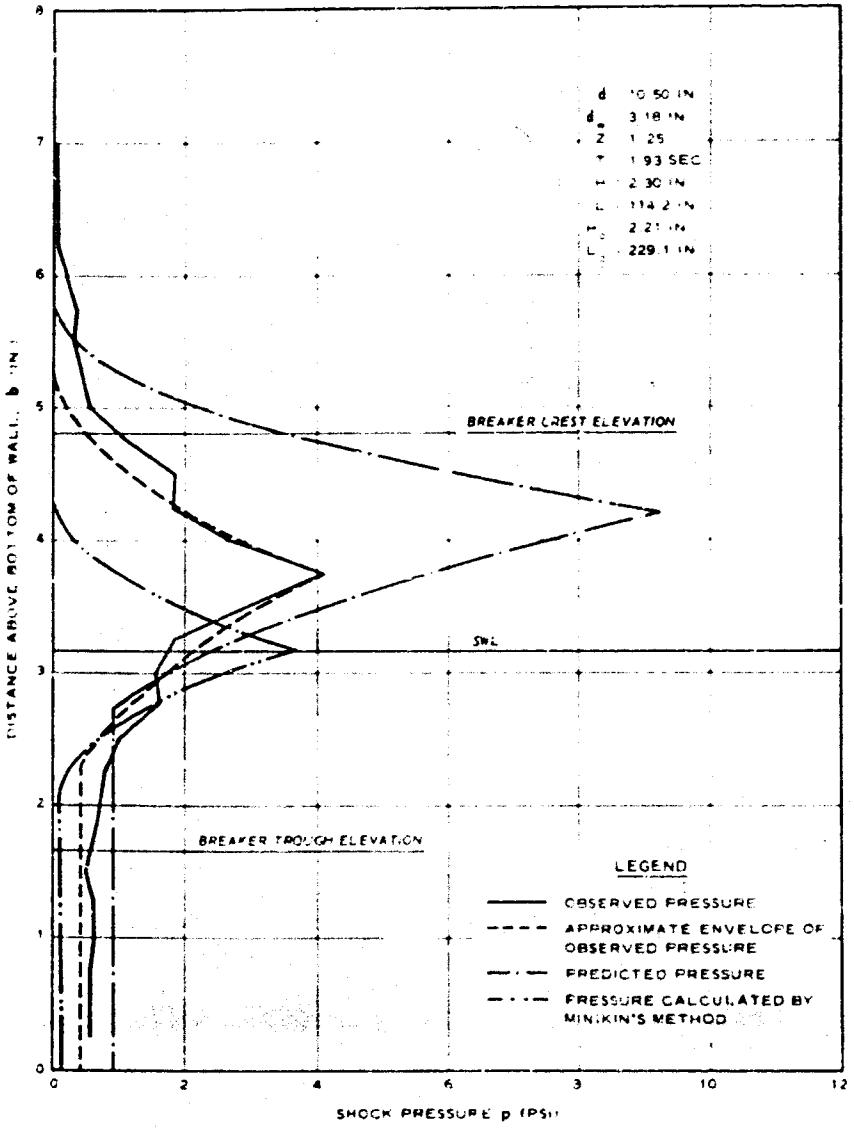

Fig. 15. Maximum shock pressure distribution on wall; test series 1

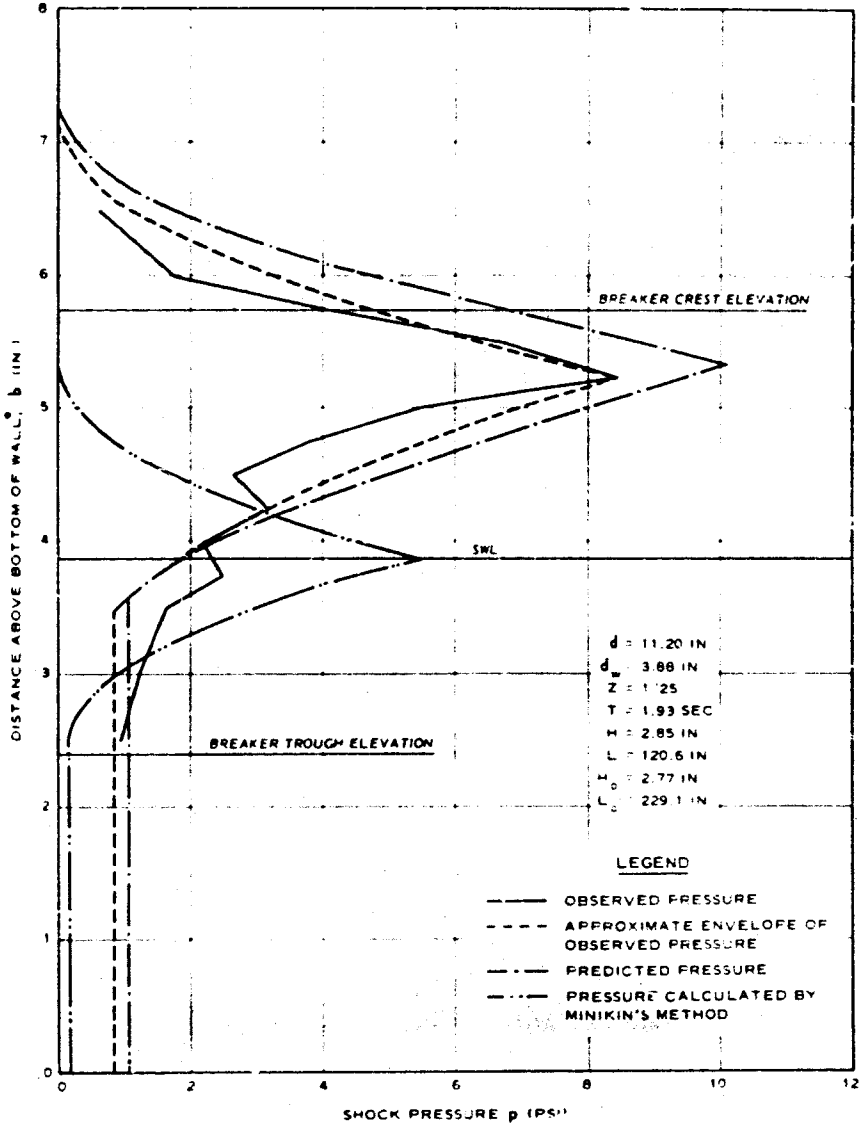

Fig. 16. Maximum shock pressure distribution on wall; test series 2

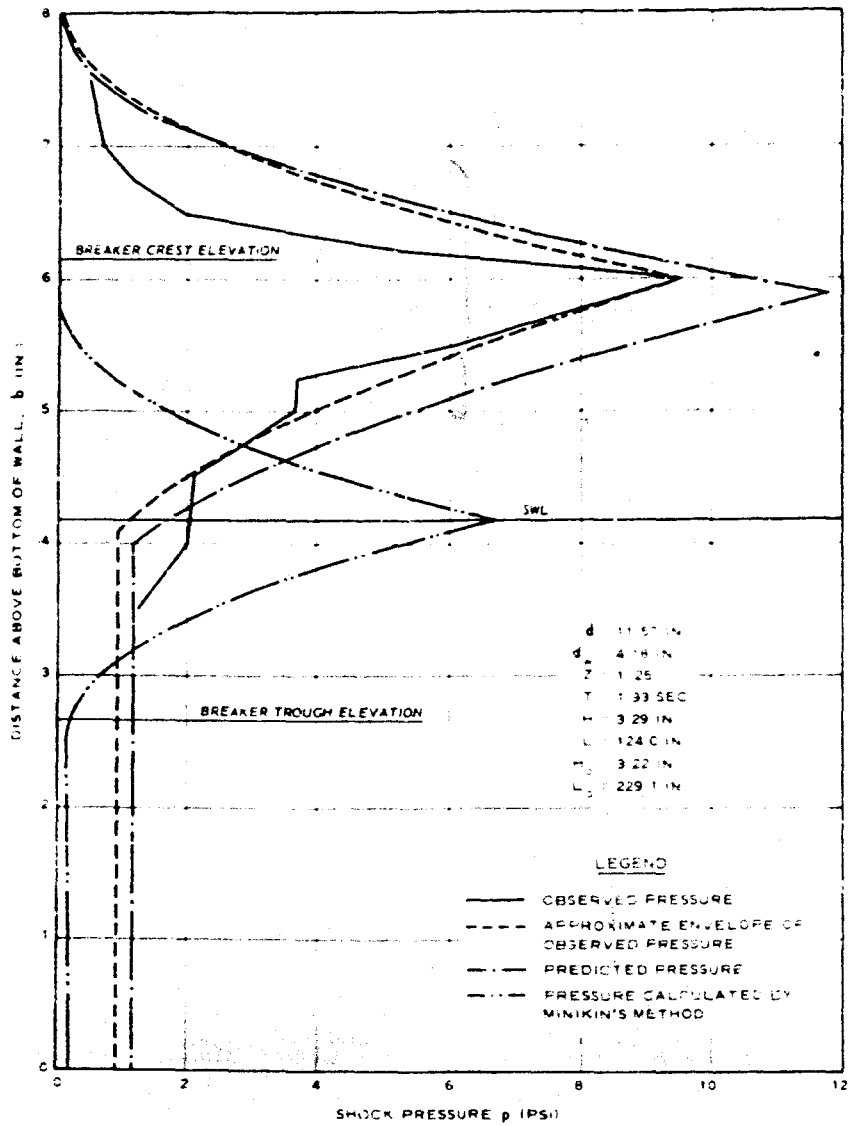

Fig. 17. Maximum shock pressure distribution on wall; test series 3

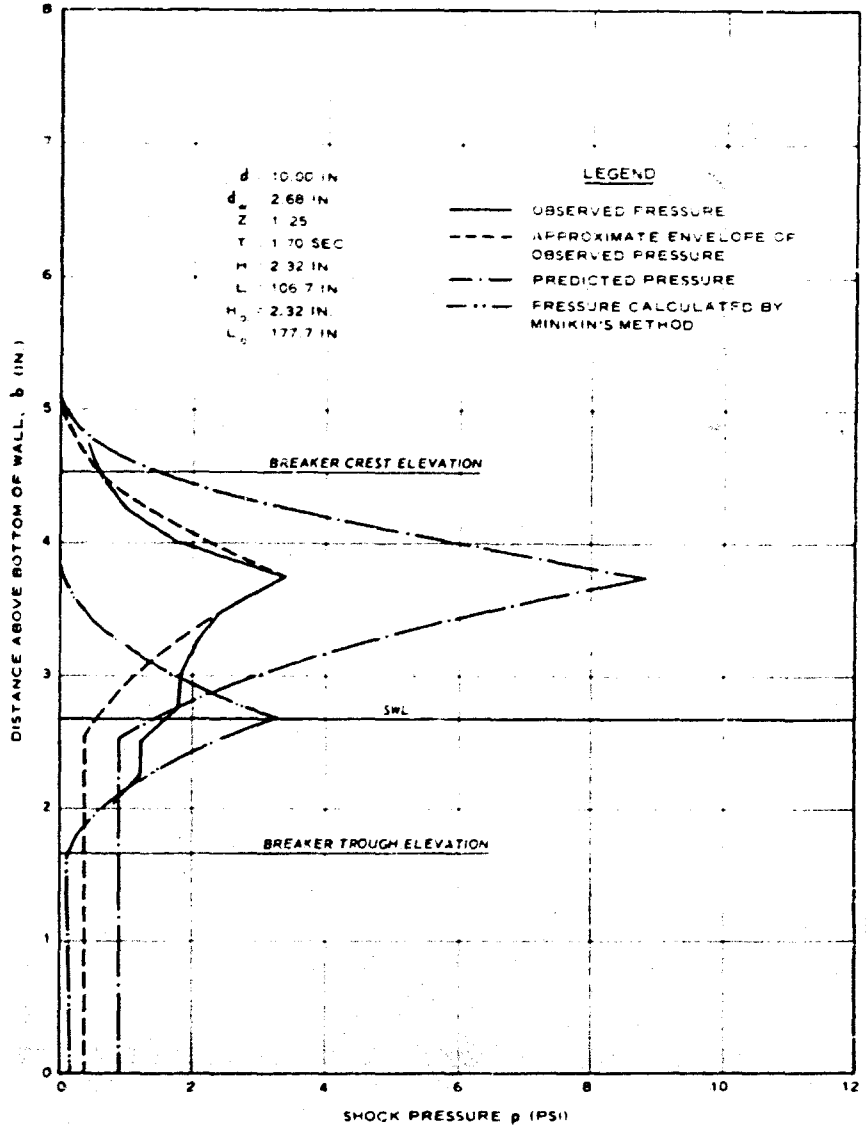

Fig. 18. Maximum shock pressure distribution on wall; test series 4

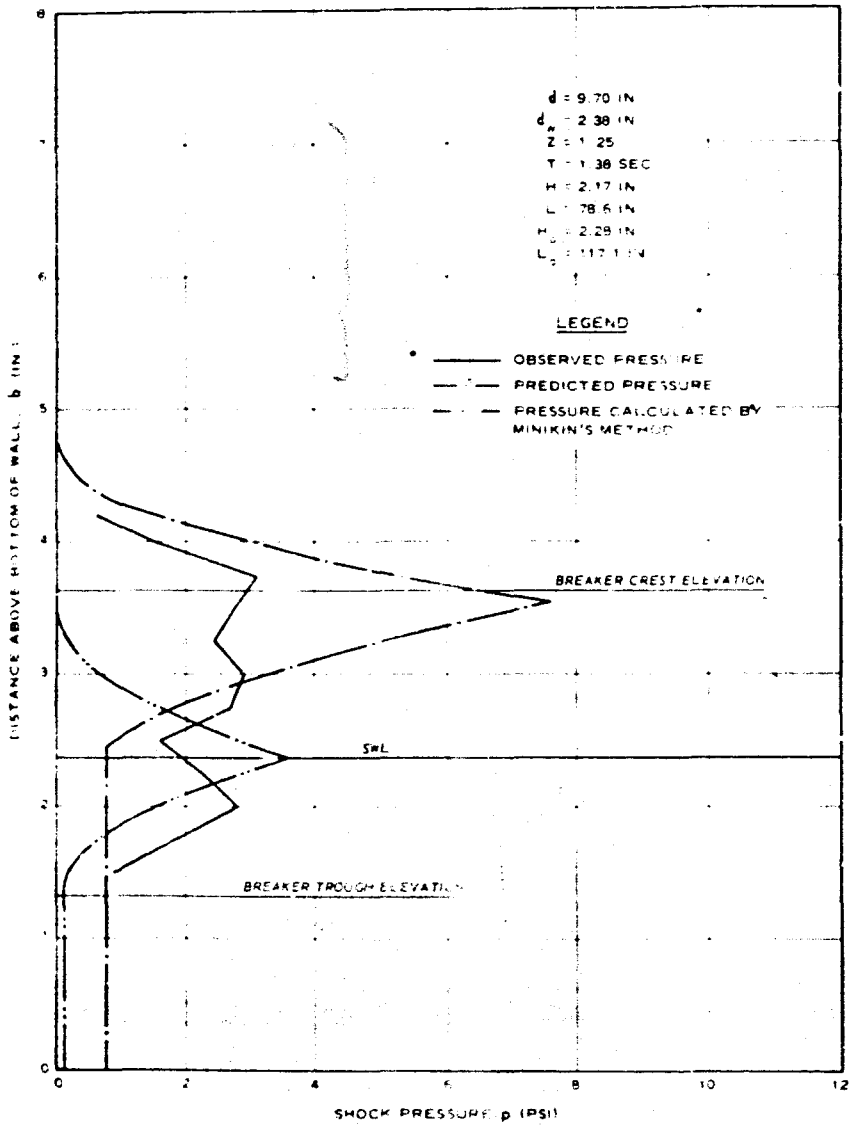

Fig. 19. Maximum shock pressure distribution on wall; test series 5

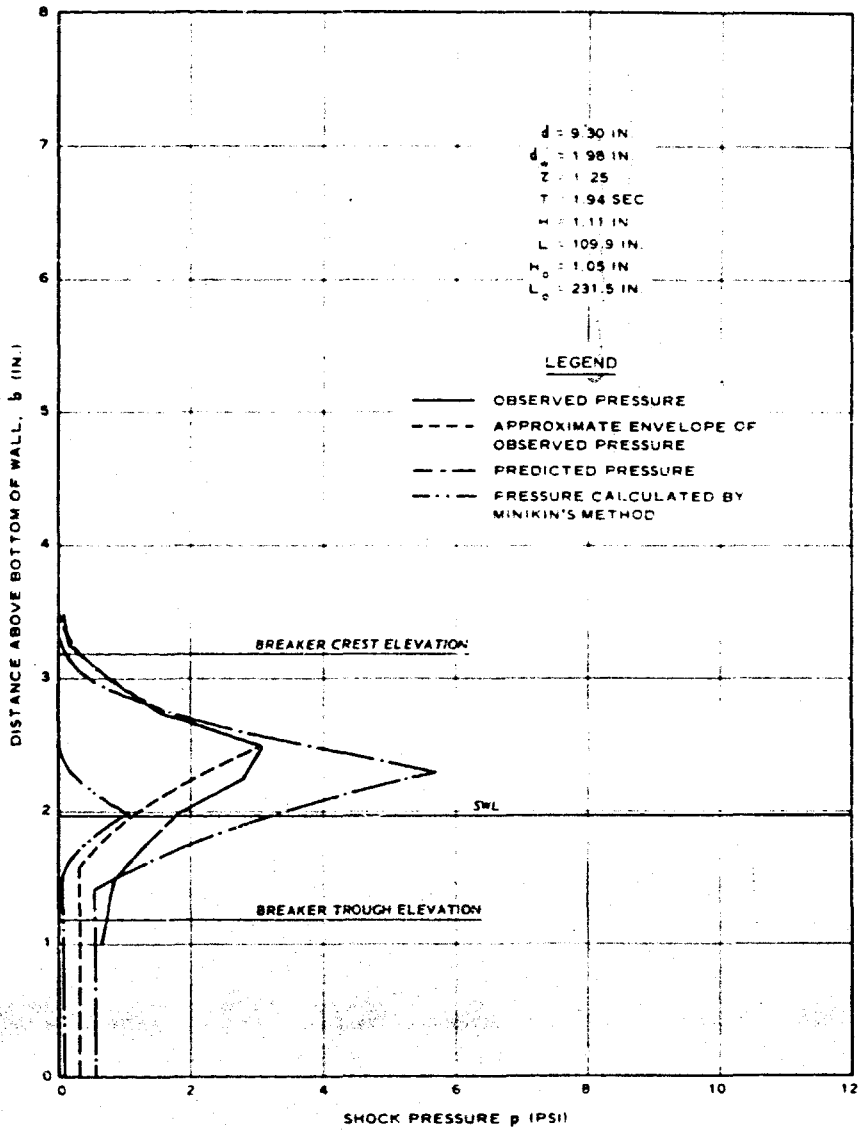

Fig. 20. Maximum shock pressure distribution on wall; test series 6

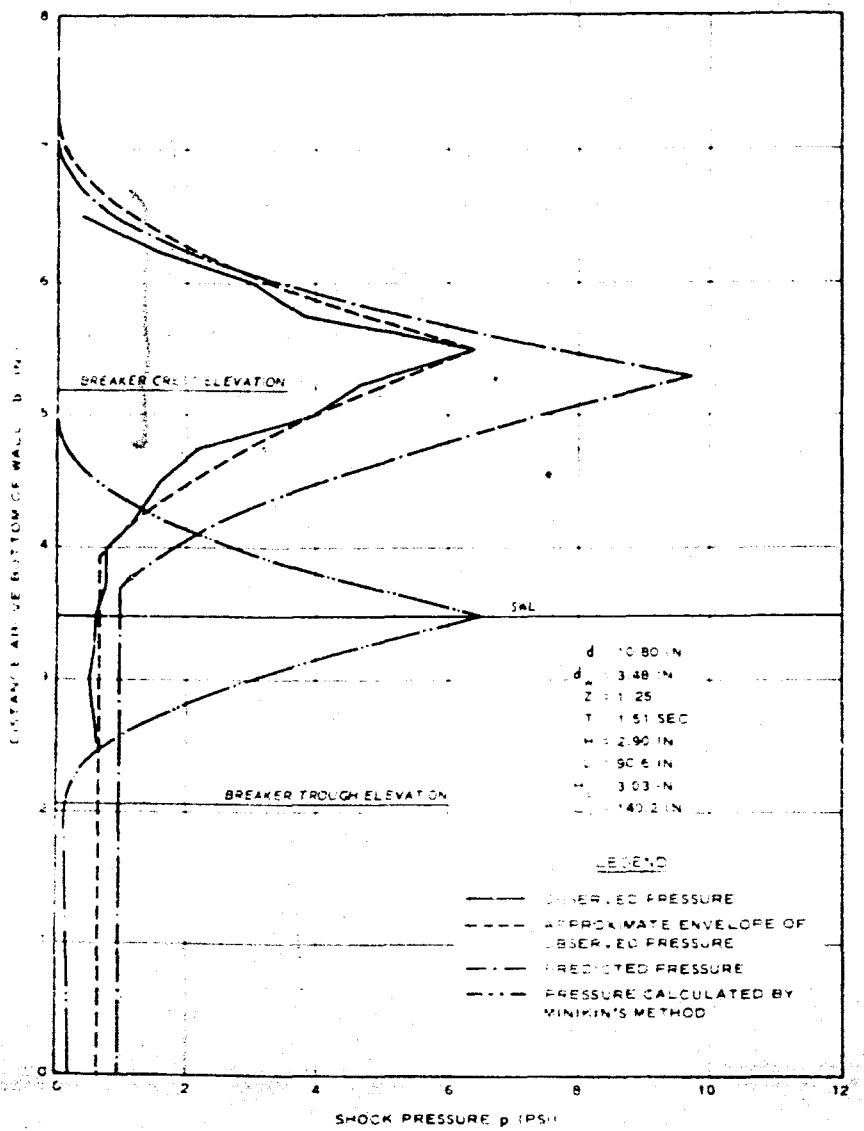

Fig. 21. Maximum shock pressure distribution on wall; test series 7

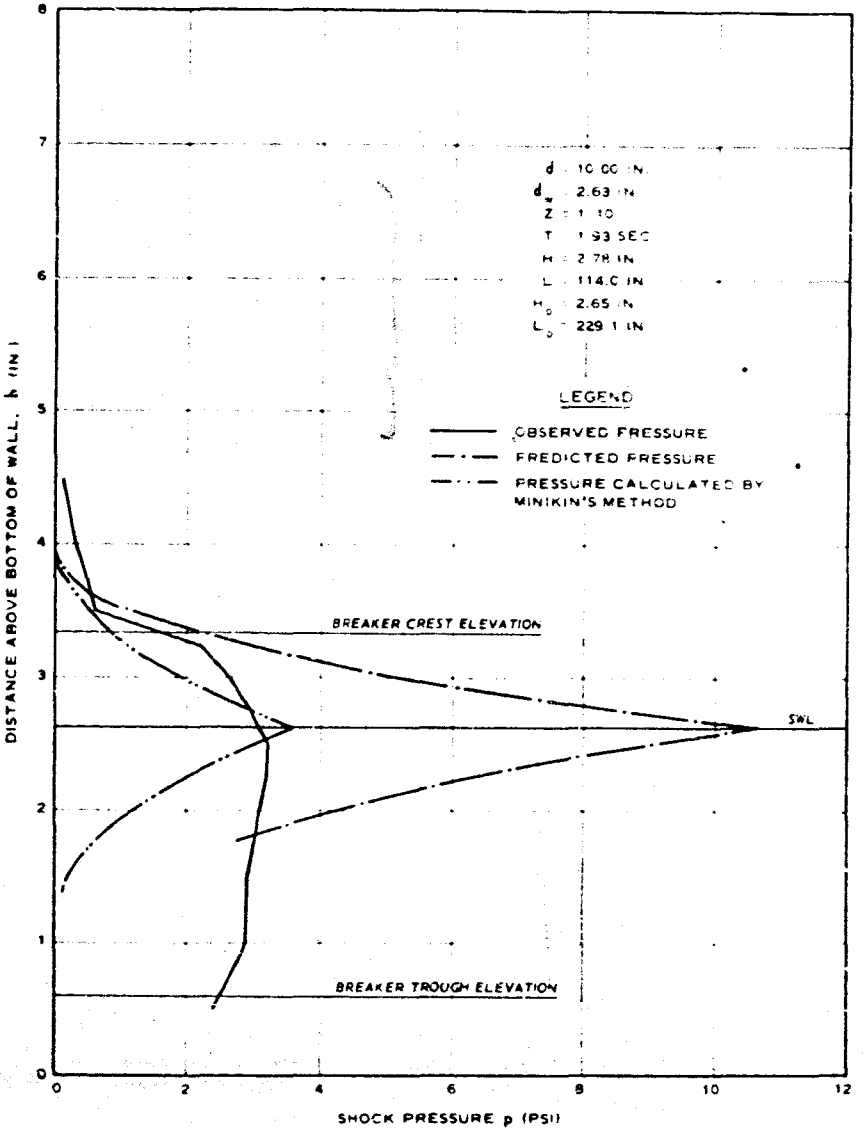

Fig. 22. Maximum shock pressure distribution on wall; test series 8

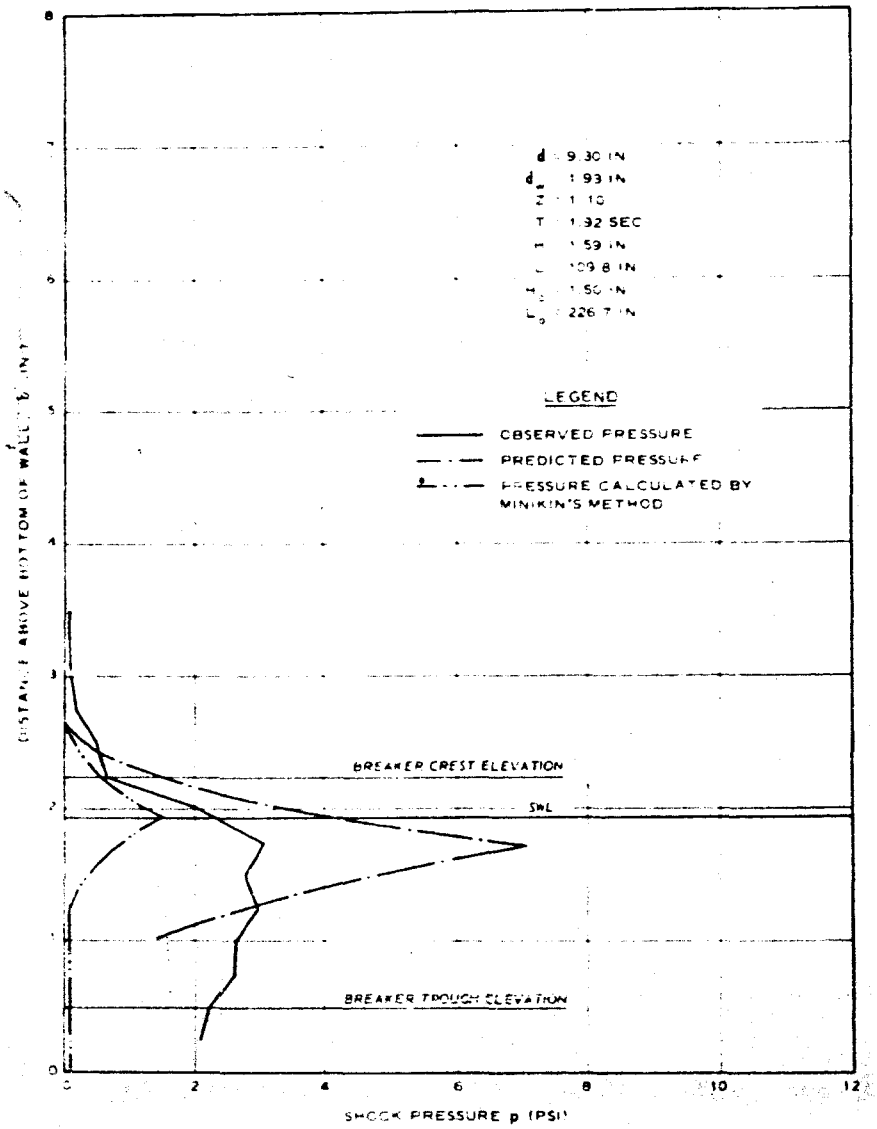

Fig. 23. Maximum shock pressure distribution on wall; test series 9

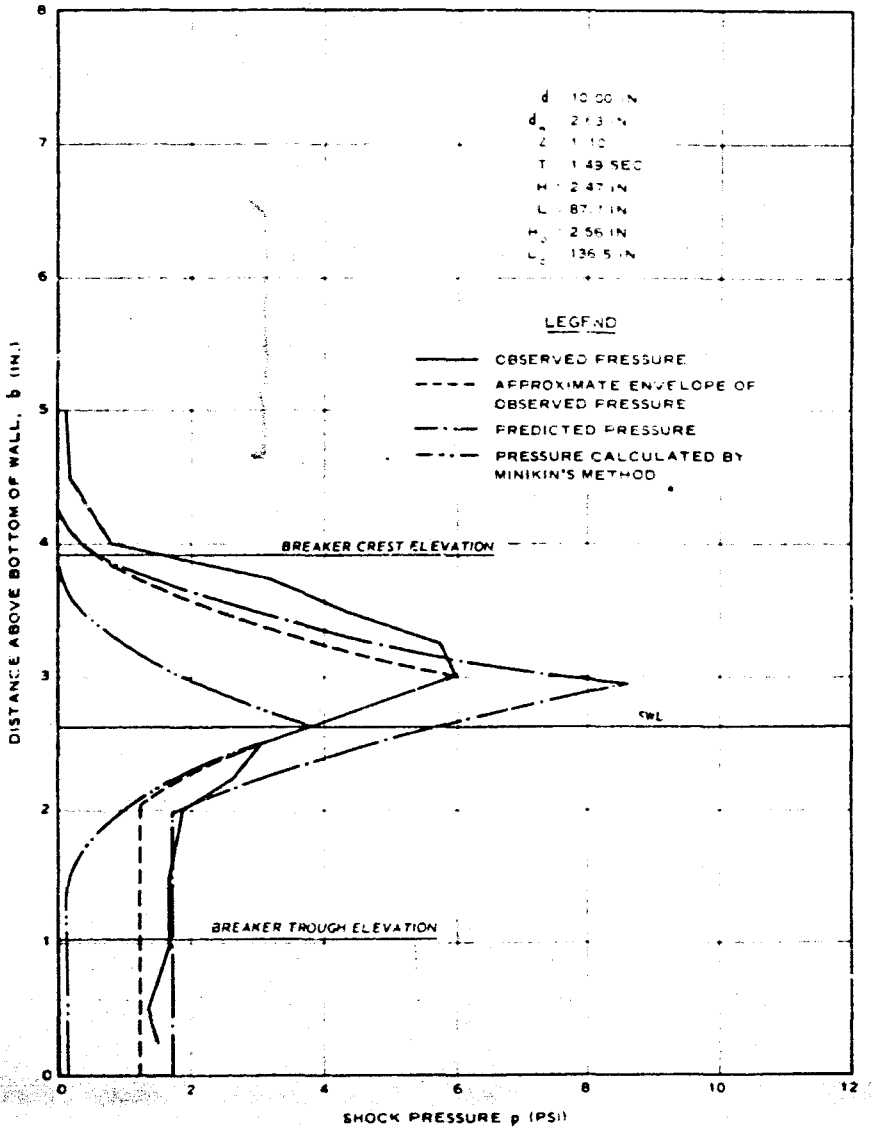

Fig. 24. Maximum shock pressure distribution on wall; test series 10

at breaking is a function of both wave and beach characteristics. McCowan[18] found that the breaking height of a solitary wave is proportional to the breaking depth. Since the breaking depth or depth of water at the wall is more easily measured than the breaking height, Minikin's pressure distribution was modified to the following:

$$p = p_{max}\left(1 - \frac{2y}{d_w}\right)^2$$

This relation fits the portion of the pressure distribution above the point of maximum shock pressure very well. However, below the point of maximum shock pressure, it was found that the expression

$$p = p_{max}\left(1 - \frac{1.5y}{d_w}\right)^2$$

more closely approximated the observed shape. The symbol y in the above equations represents the distance above or below the point of maximum pressure at which pressure p will occur. It was also observed that below the point where $p \approx 0.1p_{max}$, the magnitude of the shock pressure was approximately constant. Therefore, below $p = 0.1p_{max}$ the shock pressure p was assumed to be constant and equal to $0.1p_{max}$. In order to more clearly see how this empirical approximation of the shape of the shock pressure distribution compares with the observed pressure distribution, the approximate distribution has been plotted in figs. 15 through 18, 20, 21, and 24 and is shown by the dashed line marked "approximate envelope of observed pressure."

89. A beach slope of 1/10 was used in test series 8, 9, and 10. The variations in the shock pressure in these three series of tests between individual tests of a series and between the individual waves proved to be similar to the scatter observed in the first seven series of tests with the 1/25 beach slope. The change in beach slope had little or no effect on the scatter of the pressure data. The marked difference between the 1/10 and 1/25 beach slope tests was the shape of the maximum pressure distribution on the wall, especially in test series 8 and 9. In both of these series, the shock pressure increased to a maximum at a point slightly below the elevation of the crest of the breaking wave and then remained

approximately constant at that value to the bottom of the wall. These maximum shock pressure distributions were plotted just like those presented for the previous series of tests and are shown in figs. 22 and 23. The shock pressure distribution recorded for test series 10 on the other hand was very similar to those measured for the tests with the 1/25 beach slope. Here the pressure increased to a maximum below the crest of the breaking wave and then decreased sharply to a lesser value which remained constant to the bottom of the wall. In order to compare the shape of the series 10 pressure distribution with the distribution measured in the first seven series of tests, an approximate envelope was also plotted in fig. 24. This envelope is the same as that found previously but with one exception--rather than assuming the shock pressure to be constant at $0.1p_{max}$, the shock pressure was assumed to be constant at $0.2p_{max}$. The parabolic distribution above and below the maximum pressure shown by the dashed line is the same as before. The magnitudes of the maximum shock pressures for test series 8, 9, and 10 were approximately the same as that observed in test series 1 through 7 considering the size of the waves. Based on this limited comparison, the effect of changing the beach slope on the magnitude of the maximum shock pressure was not evident.

Discussion and Analysis of the Maximum Shock Pressure

90. Now that the individual results of each test series have been examined in detail, let us consider the testing program as a whole. We are interested in analyzing the data with the aim of finding a method of predicting the maximum shock pressure. An approximate relation has been established for the shape of the shock pressure distribution on the wall in terms of the maximum shock pressure. Therefore, with a relation for the value of the maximum shock pressure, one would then be able to calculate the pressure at any point on the wall. Since only the ideal case has been considered here (the wall was rigid, smooth, impervious, and high enough so that no overtopping occurred, and the beach slope was smooth and flat), the maximum shock pressure can be assumed to be a function of the wave characteristics alone. From the data already presented, it was seen

that the slope of the beach had no observable effect on the shock pressure for the two slopes considered. Therefore, the shock pressure was assumed to be independent of the slope of the beach in front of the wall. Since the water depth was chosen so that a wave of a given size broke on the wall so as to cause the highest shock pressure, the water depth at the wall can also be eliminated as a pertinent variable. The primary characteristics of the wave are its deepwater wavelength and its deepwater wave height. The deepwater wavelength and period can be used interchangeably since they are functions of each other and of gravity. All of the other characteristics of the wave such as celerity, energy, and the wave height and wavelength in any other depth of water can be expressed in terms of the deepwater wave height and wavelength. The other pertinent variables are the acceleration of gravity, g , and the density of the water, ρ . In this study the product ρg , which is the specific weight, will be used instead of the two separate parameters.

91. In the past, most investigators have said that the wave height has the greatest influence on the shock pressure. They have attempted to show that the maximum shock pressure is directly proportional to the wave height. This conclusion seems reasonable, and all data thus far collected have shown that waves with greater amplitude generally cause higher shock pressures. Upon examination of the maximum shock pressure values recorded in this study and the maximum shock pressure data of other investigators, it can be seen that the variation between pressure and wave height is generally linear. In order to show this more clearly, the maximum shock pressure is plotted versus wave height in fig. 25. Both oscillatory- and solitary-wave data are included in this figure. The line labeled $p_{max} = kH$ is the relation between shock pressure and wave height which most authors propose. In general, the shock pressures conform closely to the relation $p_{max} = kH$ in the region of model data, i.e. for relatively small wave heights. However, the prototype data available fall well below the line. Although those prototype data plotted may not be the maximum shock pressures possible, neither are any of the other values since there is no method now known of calculating the absolute maximum shock pressure. Therefore, in determining a relation for the maximum

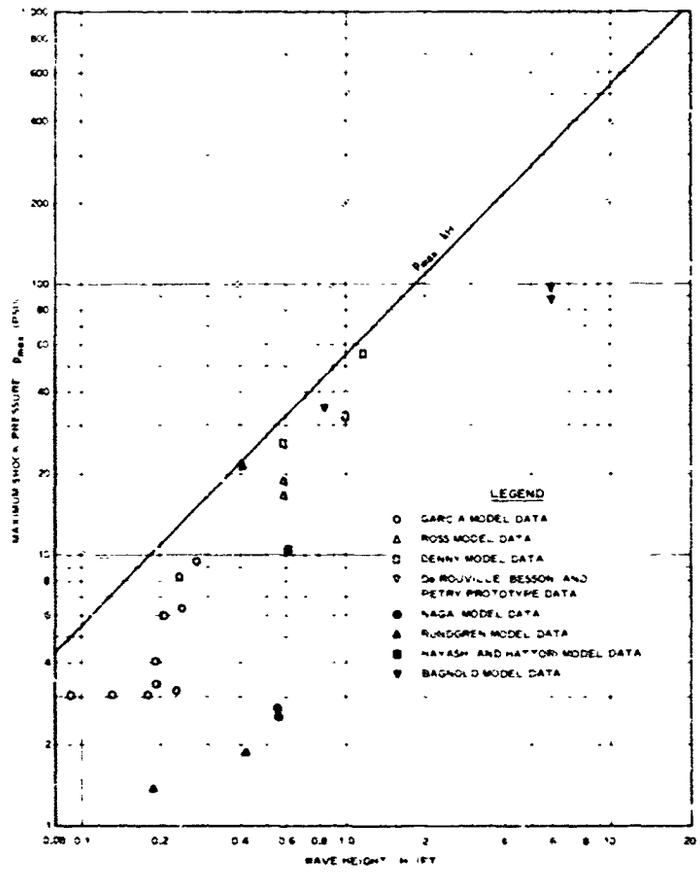

Fig. 25. Maximum shock pressure versus wave height

shock pressure it must be based solely on the data which have been recorded thus far. Since these data cover many thousands of tests made over the past 25 years, it is believed that the maximum pressure possible is not very much greater than those pressures which have been recorded.

92. Upon comparison of the data recorded in this study and those by Ross, it was determined that wave height was not the only wave characteristic which is important in the determination of the shock pressure value. Upon careful study of these data it was evident that the wavelength or period may also play an important role in determining the magnitude of the shock pressure. Therefore, a plot was made of shock pressure versus wave period. In order to eliminate the effects of wave height the maximum shock pressure was divided by the product of the specific weight

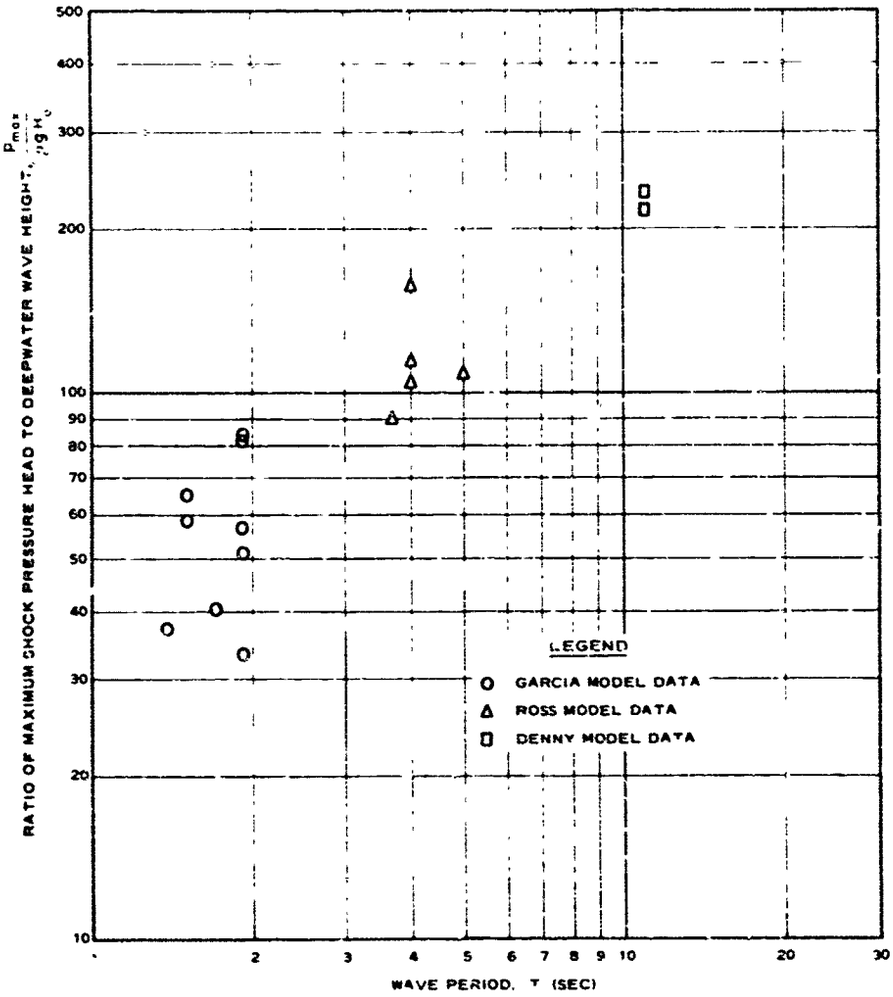

Fig. 26. Ratio of maximum shock pressure to deep-water wave height versus wave period

and the deepwater wave height. This ratio of maximum shock pressure head to deepwater wave height was then plotted versus the wave period (fig. 26). It can be seen that the shock pressure increases with wave period. On the basis of fig. 26, it was determined that the maximum shock pressure is also a function of some positive power of the wave period, or deepwater wavelength. Therefore, those relations that include a negative power of the wavelength do not truly represent the shock pressure phenomenon. The wave steepness is an expression which includes a negative power of the wavelength.

93. In this analysis, therefore, a relation will be sought that gives the maximum shock pressure as a function of positive powers of both the wave height and the wavelength. A general function for the maximum shock pressure can be written in the following form in terms of the parameters already discussed:

$$P_{max} = f_1(H_o, L_o, \rho g)$$

The subscript "o" denotes deepwater characteristics. The deepwater characteristics of the wave will be used here since the wave height and wavelength vary with water depth. Therefore, the deepwater characteristics are the only sound basis of comparison. The wave characteristics for any other depth of water can be easily found in terms of the deepwater characteristics. Due to the limitations of the experimental apparatus, it was impossible to generate deepwater waves for this study. Waves in the cnoidal region were used; the deepwater characteristics of these waves were computed using their measured characteristics in water of finite depth and the first-order approximation of the oscillatory-wave theory as discussed in Appendix B.

94. By performing a dimensional analysis on the above function for maximum shock pressure, one can write

$$\frac{P_{max}}{\rho g H_o} = f_2\left(\frac{L_o}{H_o}\right)$$

The function $f_2(L_o/H_o)$ can be assumed to have the form $(L_o/H_o)^n$, where n is a constant exponent.

95. Let us now include another relation which is made up of both the wave height and the wavelength--namely, the wave energy. The wave energy E_o is given by the expression

$$E_o = \frac{1}{8} \rho g H_o^2 L_o$$

This is the total deepwater wave energy per wavelength. It is composed of half kinetic energy due to the motion of the water particles and half

potential energy due to the elevation of the water particles above the still-water level. Solving for the wavelength in terms of wave energy, one obtains

$$L_o = \frac{8E_o}{\rho g H_o^2}$$

Substituting the above expression into the relation for maximum shock pressure, one has

$$\frac{p_{max}}{\rho g H_o} = f_2\left(\frac{E_o}{\rho g H_o^3}\right)$$

Now by using the previous assumption that

$$f_2\left(\frac{L_o}{H_o}\right) = k_1\left(\frac{L_o}{H_o}\right)^n$$

the relation

$$\frac{p_{max}}{\rho g H_o} = k_2\left(\frac{E_o}{\rho g H_o^3}\right)^n$$

can be obtained, where k_1 and k_2 are constants of proportionality. Solving for p_{max} alone, one then has

$$p_{max} = k_2(\rho g)^{1-n} H_o^{1-3n} E_o^n$$

Since the wave energy E_o is a function of both wave height and wavelength, let us assign a value to the constant n by setting the exponent of the wave height H_o equal to zero. The wave height H_o is a redundant variable since it is included in the expression for the wave energy. Therefore, since $(1-3n) = 0$, $n = 1/3$, which when substituted in the above equation yields

$$p_{max} = k_2(\rho g)^{2/3} E_o^{1/3}$$

Now if ρg is assumed constant since there is only two percent difference

between the specific weight of sea water and that of fresh water, one can write

$$P_{max} = k_3 \left(H_o^2 L_o\right)^{1/3}$$

This relation satisfies the requirement stated earlier that the pressure must be a function of positive powers of both the wave height and the wavelength. To show how this relation compares with observed data, the data from this study as well as the data collected by other investigators are plotted in fig. 27. The line in fig. 27 labeled

$$P_{max} = 50(\rho g)^{2/3} E_o^{1/3}$$

is the curve enveloping all of the data available. The constant k_2 which is equal to 50 here was found empirically from the plotted data in fig. 27. The wave energy for each of the points in this figure was calculated from the equation

$$E_o = \frac{1}{8} \rho g H_o^2 L_o$$

96. The data included in fig. 27 are the values of maximum shock pressure for each of the ten series of tests of this study and the higher shock pressure values published by the other investigators listed on the figure. In examining this figure, one must realize that due to the scatter of the data and the perfect conditions which must exist in order to generate high shock pressures, there are many other data points for which the shock pressures are much less. These points have not been included since the purpose of this study was to examine only the highest pressures and to attempt to devise a method of predicting the maximum shock pressure. The data in fig. 27 include only oscillatory-wave data. On the plot of maximum shock pressure versus wave height in fig. 25, both oscillatory- and solitary-wave data were included. The solitary-wave data were not included in fig. 27 because there is no satisfactory method of comparing the energy of an oscillatory wave in deep water with the energy of a solitary wave.

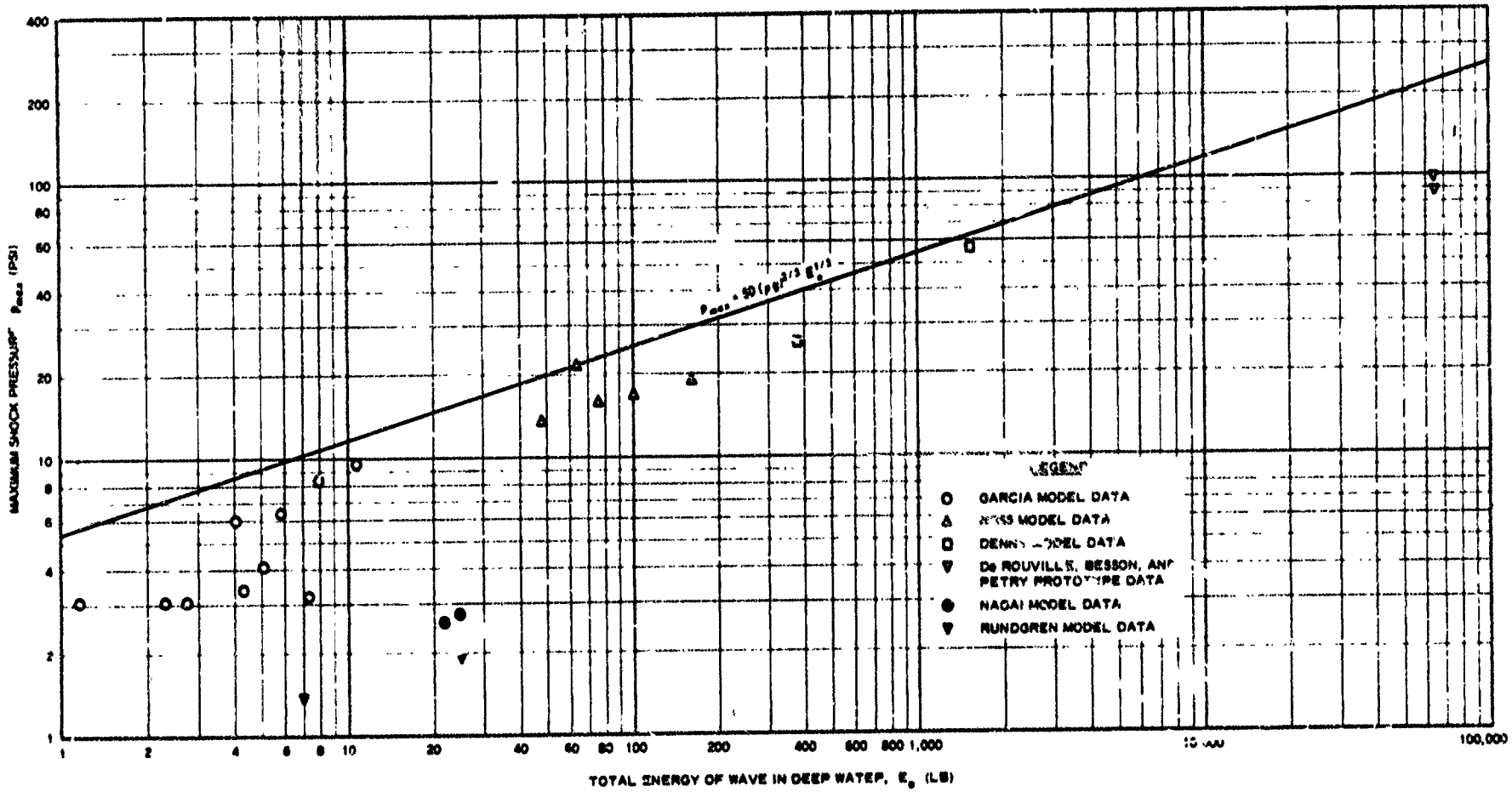

Fig. 27. Maximum shock pressure versus total energy of wave in deep water

97. Thus far, both the general shape of the shock pressure distribution and the magnitude of the maximum shock pressure have been discussed. The maximum shock pressure has been found to obey the relation

$$p_{max} = 50(\rho g)^{2/3} E_o^{1/3}$$

The shape of the pressure distribution has been found to follow the relation

$$p = p_{max}\left(1 - \frac{2y}{d_w}\right)^2$$

above the point of maximum pressure and

$$p = p_{max}\left(1 - \frac{1.5y}{d_w}\right)^2$$

below the point of maximum pressure. Below the point where $p = 0.1p_{max}$ with the 1/25 beach slope or $p = 0.2p_{max}$ with the 1/10 slope, the pressure was generally constant. However, nothing has been said yet concerning the location of the maximum shock pressure, other than that it generally occurs between the still-water level and the elevation of the breaker crest. In order to predict the elevation of the shock pressure for given wave conditions, the ratio between the elevation of the maximum shock pressure above the bottom of the wall, $b_{p_{max}}$, and the still-water depth at the wall, d_w, was examined. This ratio was then compared with the wave steepness, H_o/L_o. The comparison was made with the wave steepness since all previous studies of breaking-wave characteristics point out that the breaking depth and breaking height of a wave are functions of the wave steepness. The resulting plot of the ratio $b_{p_{max}}/d_w$ versus the deepwater wave steepness H_o/L_o is shown in fig. 28. The data for each of the ten series of tests are displayed in this figure. It can be seen that there is a definite relation between the elevation of the point of maximum shock pressure, the still-water depth at the wall, and the deepwater wave steepness. In addition, it is seen that the slope of the beach in front of the wall is also an important factor in determining the location

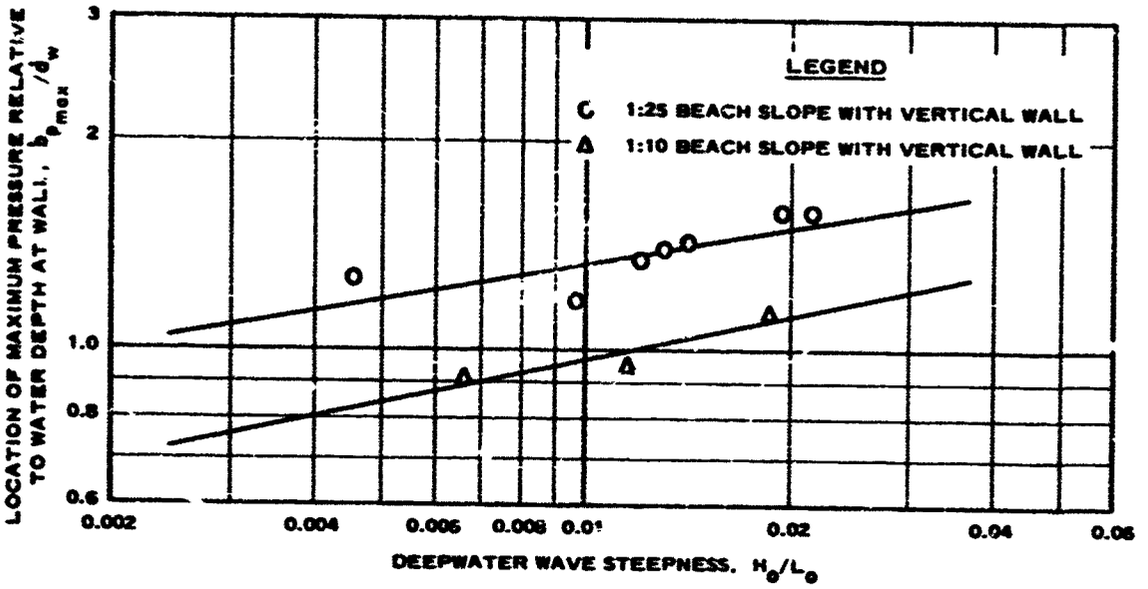

Fig. 23. Location of maximum shock pressure relative to the water depth at the wall versus deepwater wave steepness

of the maximum shock pressure. Due to the lack of extensive data, it was assumed that the ratio $b_{p_{max}}/d_w$ could be represented as a power of the deepwater wave steepness H_o/L_o. Therefore, this relation could be represented with a straight line on a log-log plot as shown in fig. 28. The upper line is for the 1/25 beach slope, and the lower line is for the 1/10 beach slope. These lines were calculated by the method of least squares.

98. In order to compare the proposed method of calculating the shock pressure on a wall caused by breaking waves, the predicted pressure distribution has been depicted in figs. 15 through 24 by the curves labeled "predicted pressure." For each wave condition the maximum shock pressure was calculated from the equation

$$p_{max} = 50(\rho g)^{2/3} E_o^{1/3}$$

The location of the point of maximum shock pressure was taken from the curves in fig. 28. The shock pressure at other points on the wall was calculated using the pressure distribution discussed previously. Based

on the data available, it is believed that this method of calculating the maximum shock pressure is more valid and accurate than any method thus far proposed by other investigators.

99. However, one must realize that there are only limited data and virtually no theoretical knowledge concerning this phenomenon. Therefore, by necessity, only a first approximation to the solution of the problem is proposed here.

100. Thus far, this discussion has been concerned with only the magnitude of the shock pressure, but it must be remembered that both the magnitude and time characteristics of the load determine the response of any given structure subjected to the loading. Depending upon the dynamic characteristics of the structure, a given pressure pulse may either have very little effect or be very detrimental.

101. Generally speaking, heavy massive structures such as monolithic concrete breakwaters would be affected very little, if any, when subjected to a very short-duration pressure pulse. On the other hand, a light flexible structure such as a sheet steel pile wall might suffer greater damage from a short-duration pressure pulse than it would from a static load of the same magnitude. Therefore, an attempt was made to measure the duration of the shock pressure from the oscillograph record of pressure. It was found that the duration of the shock pressure varied as greatly as its magnitude. It was also noted that the higher pressures are generally associated with shorter durations; and conversely, the lower shock pressures are associated with longer durations. This causes the shock impulse to be fairly constant for a given wave size. The shock impulse is defined to be the integral of the shock pressure with respect to time from immediately before the start of the shock pressure pulse to the time when the pressure has decreased to the magnitude of the secondary pressure. Due to the small range of wave periods tested in this study it was impossible to draw any conclusions concerning the variation of the shock pressure duration with the wave period. The shock pressure durations measured in this study varied from approximately 0.002 to 0.02 sec. This variation exhibited no pattern with respect to wave period.

102. The data of two other studies containing shock impulse records

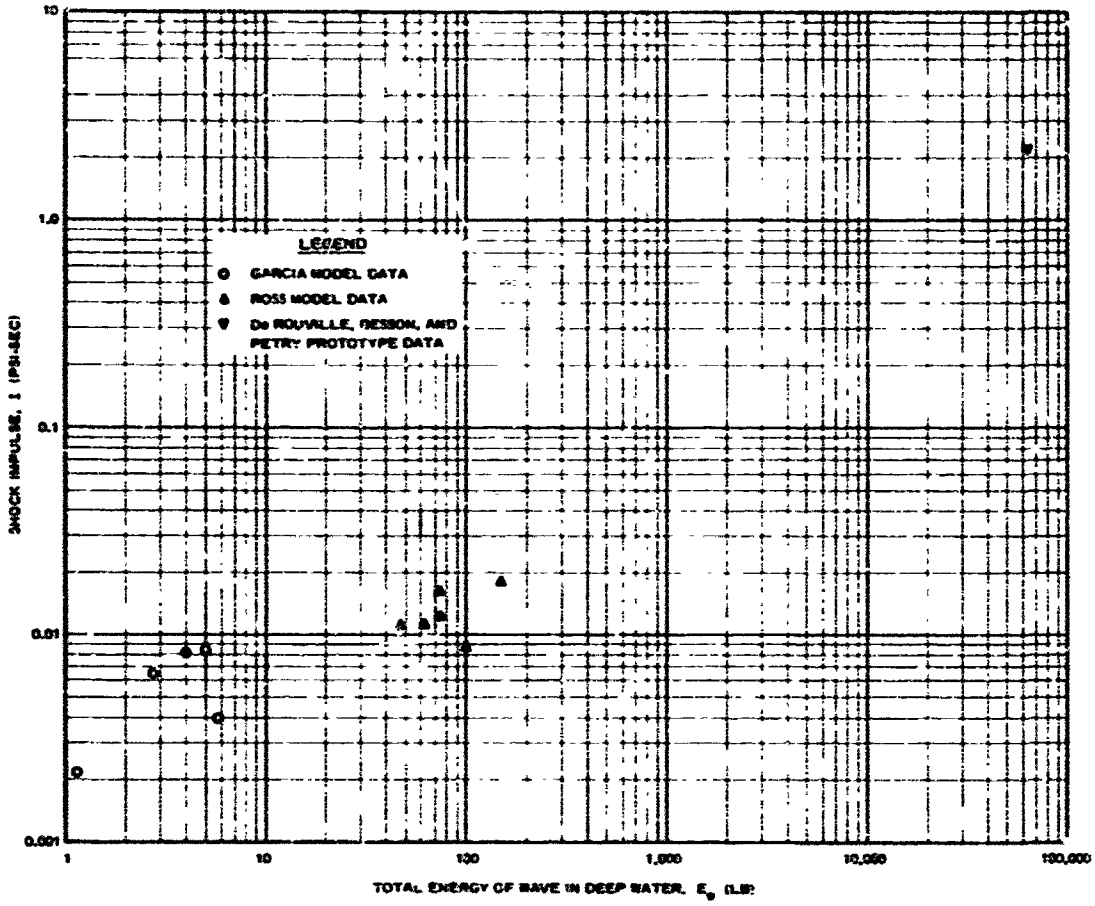

Fig. 29. Shock impulse per unit area versus total energy of wave in deep water

were compared with the impulse data gathered in this study in order to obtain a large range of data. These data are shown in fig. 29. The shock impulse, I , was plotted versus the deepwater wave energy since it is believed that the wave energy more faithfully represents the wave size than any other parameter. A general increasing trend can be seen between shock impulse and wave energy in fig. 29. However, due to the small amount of data, no definite conclusions will be made concerning the shock impulse. Fig. 29 shows the impulse of the maximum shock pressure. It can be assumed in the first approximation that the distribution of shock impulse on the wall is similar to the distribution of shock pressure and that the point of maximum shock impulse coincides with the point of maximum shock pressure.

A Comparison of the Results of Other Investigators

103. The results of other investigators have been briefly discussed wherever their data have been included to supplement the data from this study. In this section the data and theories of the other investigators will be treated more thoroughly with primary emphasis on the comparison of their results. It is emphasized, however, that one must use caution in comparing the data of other investigators since each uses different equipment and each presents his data and results in a different manner. In addition, a detailed analysis of the work of some authors is exceedingly difficult, if not impossible, since the data presented are far from complete and often only those which support their theory or conclusion are included.

104. Bagnold was one of the first to make a careful and detailed study of shock pressures caused by breaking waves. Based on the results of his experiments, Bagnold concluded that such pressures are caused by compression of a layer of air trapped between the face of the wave and the wall. Bagnold states that this layer of air is compressed at a faster rate than it can escape, causing a rapid increase in pressure in the air layer. In order for the highest shock pressure to occur, the layer of air must be thin. If the wave breaks some distance in front of the wall, or if the water surface is disturbed, a comparatively thick layer of air will be trapped. A thick layer of air acts like a cushion, and no shock pressure or a lesser shock pressure is observed. Bagnold used solitary waves in still water to eliminate disturbances from previous waves. Bagnold's theory appears reasonable; however, there are a few contradictions which are evident. First, the observation was made that shock pressures occur in disturbed water after a few waves have broken on the wall just as readily as they occur in still water. This observation was also made by Ross who measured pressures for long trains of oscillatory waves. Secondly, shock pressures have been observed at the base of the wall below the point of maximum drawdown. Shock pressures at the very base of the wall were observed in the present study. This means that either the compressed air is forced down to the bottom of the wall or some other

phenomenon causes the shock pressure. Motion pictures were taken during this study at a film speed of 64 frames per second in order to see if air pockets could be detected. In these pictures it was impossible to see any trapped pocket of air. Although these motion pictures do not preclude the existence of air pockets, they do point out that the observation of such a layer of air, if in existence, is nearly impossible. A sequence of eight consecutive frames of these motion pictures is shown in fig. 4.

105. The other investigators who used solitary waves were Hayashi and Hattori, and Denny. Hayashi and Hattori were primarily interested in the secondary pressure. They recorded the shock pressures but did not discuss them. The greatest shock pressure recorded by Hayashi and Hattori has been included in the plot of shock pressure versus wave height in fig. 25.

106. Denny's work was a continuation of Bagnold's. He studied both solitary waves and oscillatory waves. The highest pressures recorded for his three wave heights are plotted in fig. 25. These points include both the solitary- and oscillatory-wave data. The points of Denny's data plotted in fig. 27 for shock pressure versus wave energy are for oscillatory waves. The period of the oscillatory waves studied by Denny was the same as the natural period of his wave flume, which on the basis of the data given can be calculated to be approximately 11 sec. The waves used by Denny are the largest which have been used in any model study. Therefore, by including Denny's data the range of wave sizes can be extended almost into the region of prototype size waves.

107. The other model study of note which was included in the data presented is the one conducted by Ross in which oscillatory waves were used. The range of wave sizes was intermediate between the small waves studied in this experimental program and the large waves which Denny used in his experiments. Ross conducted a large number of tests which included the measurement of both shock pressure and shock impulse along with complete information of wave parameters. It can be seen from fig. 27 that the results of Ross' study closely fit the indicated relation between shock pressure and deepwater wave energy. The five Ross data points included in fig. 27 are the highest shock pressures recorded by him. As in

the case of all of the studies which have been conducted, there was great scatter in his data and many records were made of lesser pressures. A few of the shock impulse measurements of Ross are also included in fig. 29. Ross also noted that the shock impulse remained fairly constant even though there was great scatter in the magnitude of the shock pressure.

108. Based on their results, both Denny and Ross concluded that there was a definite relation between shock pressure and wave height, and that the shock pressure is directly proportional to the wave height.

109. Results of two other model studies are also included in figs. 25 and 27. They are the studies conducted by Hagai and the one conducted by Rundgren. The shock pressures observed in both of these studies were much lower than those observed by other investigators.

110. De Rouville, Besson, and Pétry conducted the only prototype study in which shock pressures were measured. The highest shock pressure data recorded by them have been plotted in fig. 27. These data are significant since they show that shock pressures are not solely a laboratory phenomenon and that they occur on full-scale breakwaters. It was assumed that the pressures measured by de Rouville, Besson, and Pétry were close to the maximum. They used three pressure cells set at fixed elevations and thus did not record a complete pressure distribution. This assumption is considered valid since their data fit in well with the model data of other studies, including this one. They also fit reasonably well the proposed relation between shock pressure and wave energy. As was the case with all other studies, there were many measurements of less intense shock pressures than those presented due to the fact that almost ideal conditions must exist in order for high shock pressures to occur.

A Discussion of the Secondary Pressure

111. In the beginning of this Part the secondary pressure was discussed briefly. It was pointed out that there was little variation in the secondary pressure for any one set of conditions. Due to the pressure scale used on the oscillograph in order to record the shock pressures, the variations in the secondary pressure were less than the errors

introduced in reading the oscillograph record.

112. The pressure following the initial shock pressure is caused by a condition of the motion of the water at the wall during runup and by the static head of water on the wall during runup. The secondary pressure is the second maximum observed on the pressure-time diagram, and it occurs at the point of maximum runup. At the time of maximum runup the static head is the greatest on the wall and the water particles have zero velocity. During descent of the runup, the pressure decreases to zero as the water level falls to below the level of the pressure cell. Essentially, this phenomenon is the same as the clapotis. The clapotis is caused by a nonbreaking wave that is reflected from a wall. The clapotis pressure is also caused by a combination of static head and velocity of the water particles. Since there is a great similarity between the clapotis and the motion of the breaking wave on the wall after impact, a comparison between the measured secondary pressure and the theoretical clapotis pressure was made. The clapotis pressure was calculated by Sainflou's[1] method. In making the clapotis pressure calculations it was assumed that there was no beach slope in the flume. Therefore, the water depth and wave dimensions at the wall were assumed to be the same as those in the section of the flume with the horizontal bottom. Once the calculation was made, the clapotis pressure was assumed to act only as far down as the top of the beach slope. In other words, the bottom of the clapotis pressure diagram was cut off at the top of the beach slope or actual bottom of the test wall. Upon comparing the secondary pressure with the clapotis pressure it was found that they nearly coincide in most cases. The diagrams showing this comparison for each of the test series are figs. 30 through 39. There is a large amount of scatter in the secondary pressures from test series 1 shown in fig. 30. This scatter is due to the fact that a 50-psia pressure cell was used in this series of tests and the magnitude of the secondary pressure was outside the accuracy limits of the pressure cell. The other nine series of tests were conducted with a 15-psia pressure cell, and more consistent data were recorded. On the basis of this comparison it is believed that present methods for calculating clapotis

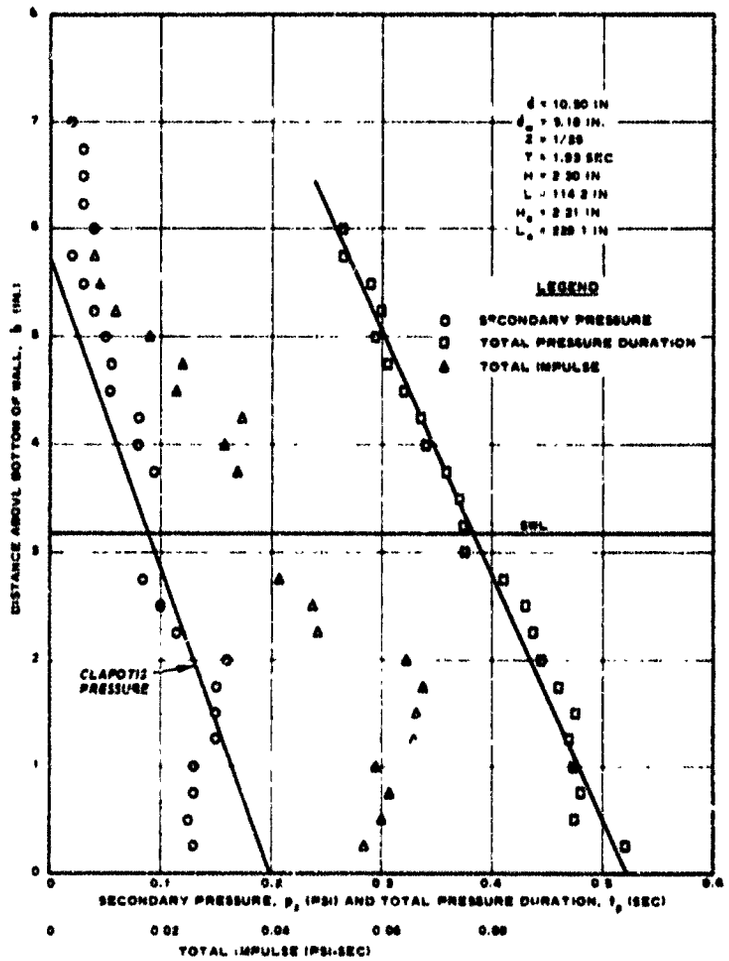

Fig. 30. Distribution of secondary pressure, total impulse, and total pressure duration on wall; test series 1

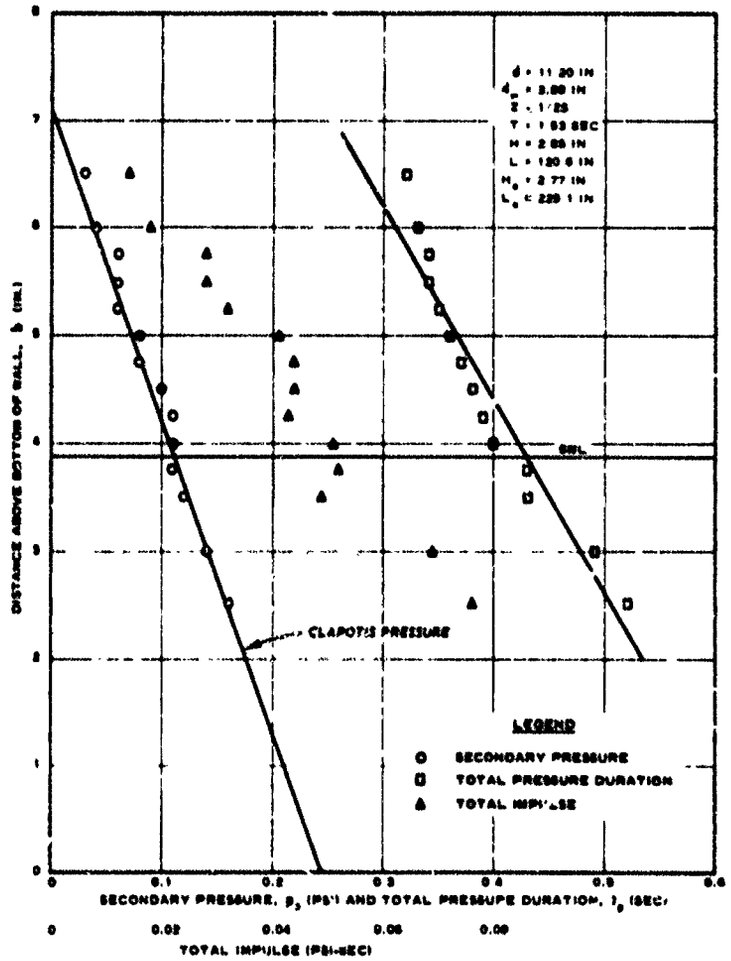

Fig. 31. Distribution of secondary pressure, total impulse, and total pressure duration on wall; test series 2

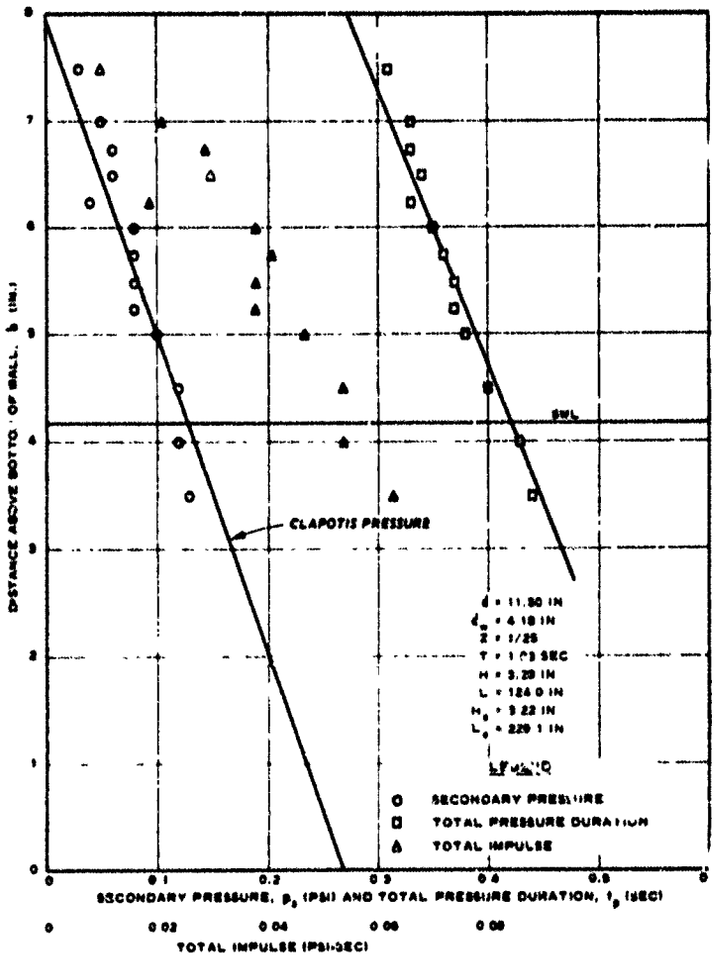

Fig. 32. Distribution of secondary pressure, total impulse, and total pressure duration on wall; test series 3

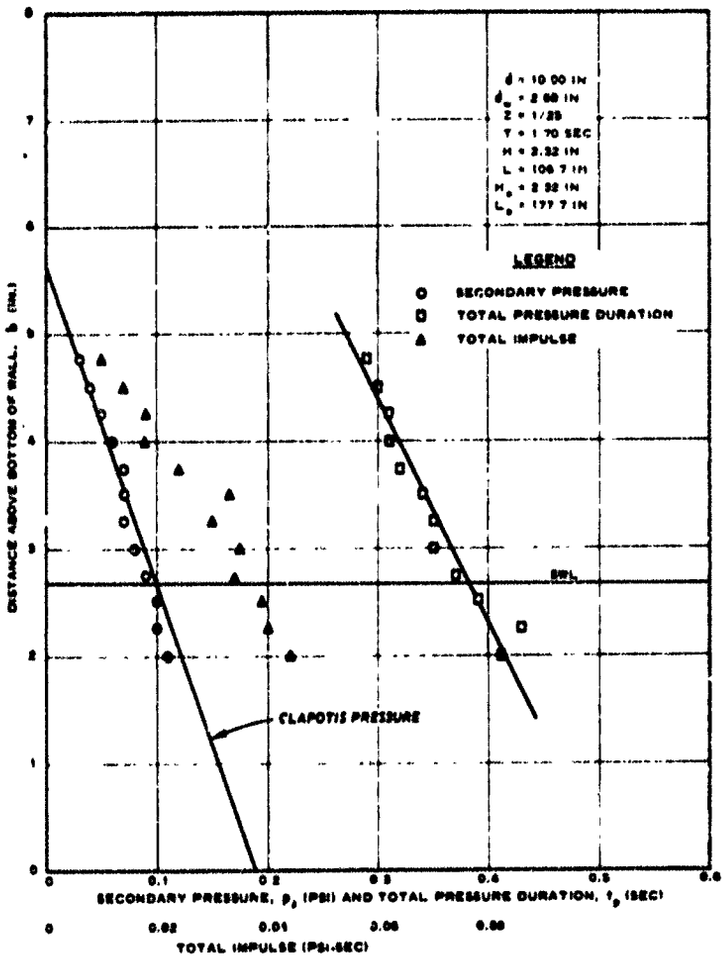

Fig. 33. Distribution of secondary pressure, total impulse, and total pressure duration on wall; test series 4

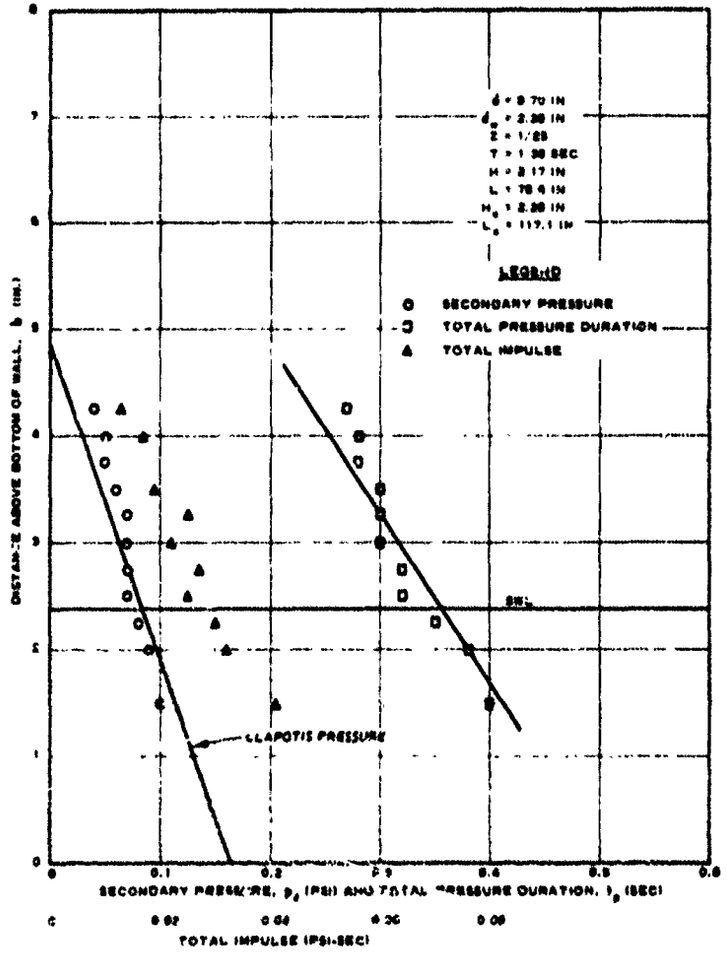

Fig. 34. Distribution of secondary pressure, total impulse, and total pressure duration on wall; test series 5

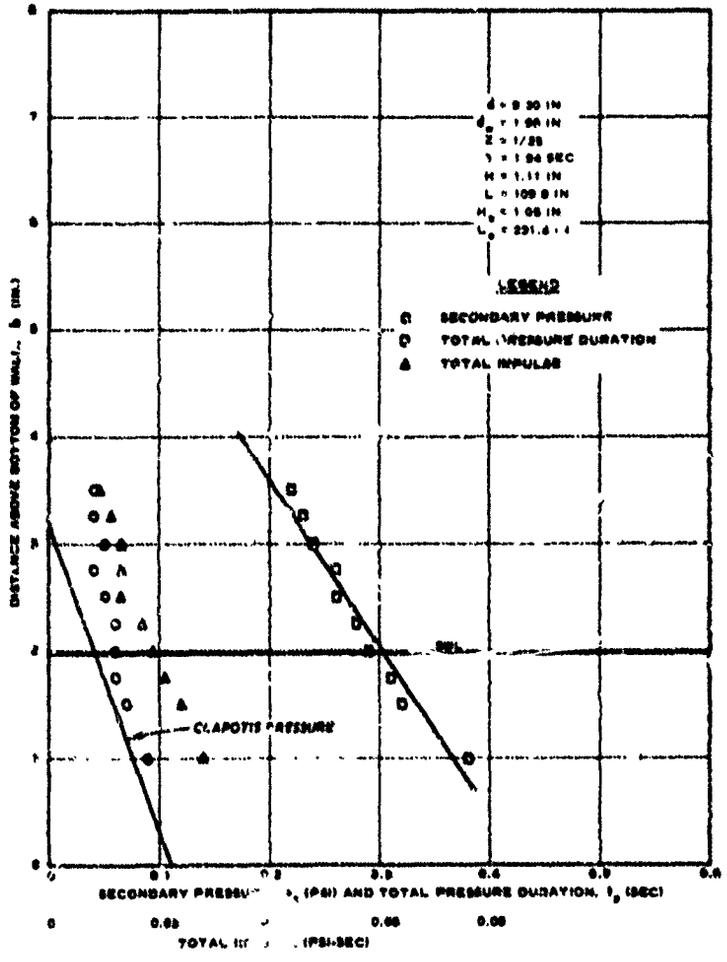

Fig. 35. Distribution of secondary pressure, total impulse, and total pressure duration on wall; test series 6

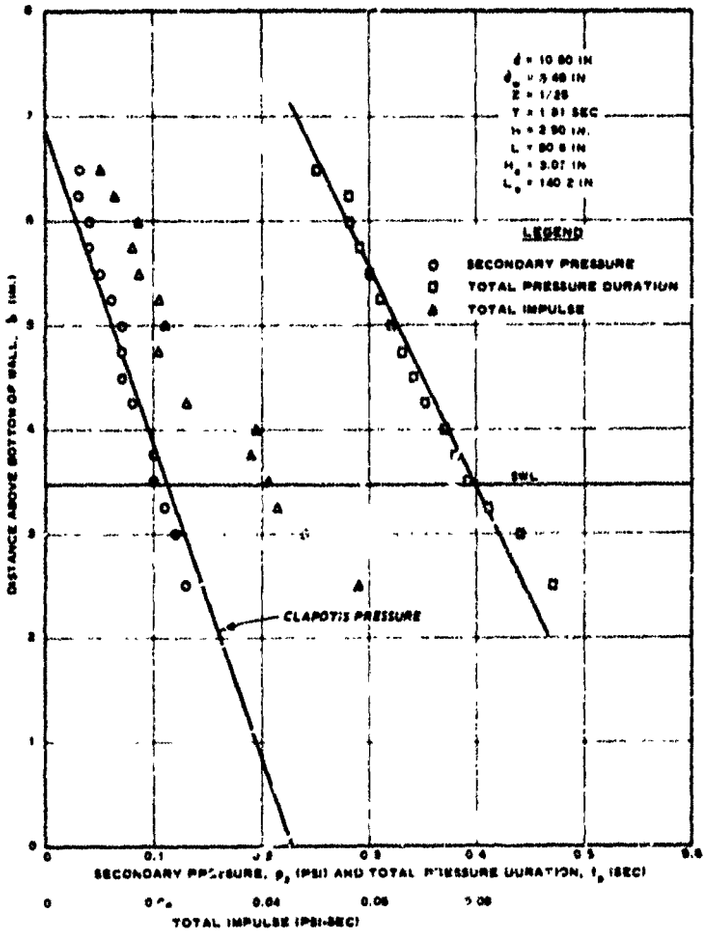

Fig. 36. Distribution of secondary pressure, total impulse, and total pressure duration on wall; test series 7

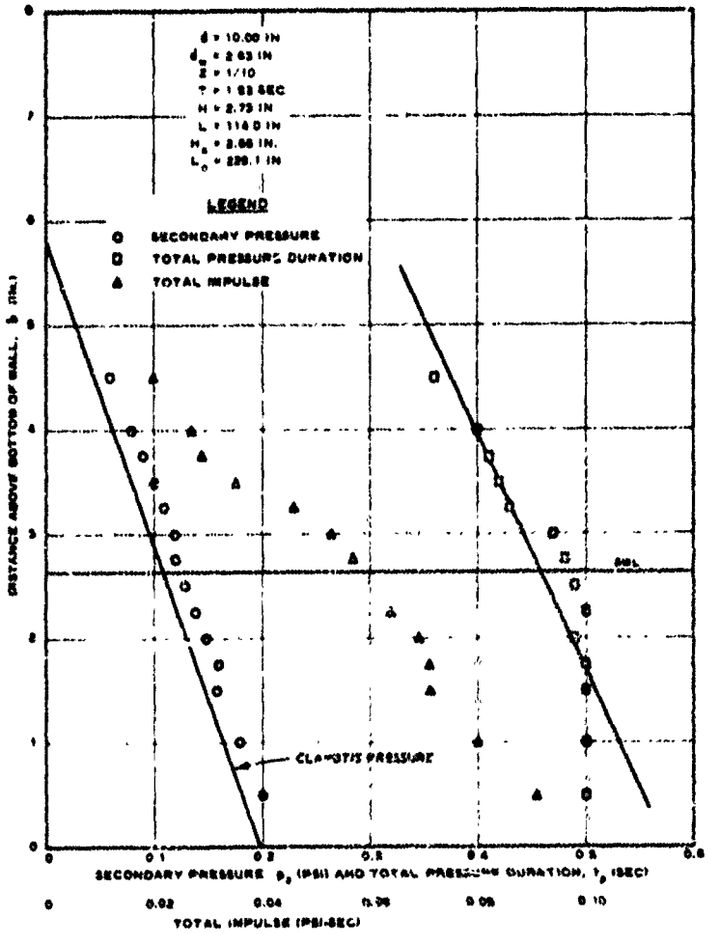

Fig. 37. Distribution of secondary pressure, total impulse, and total pressure duration on wall; test series 8

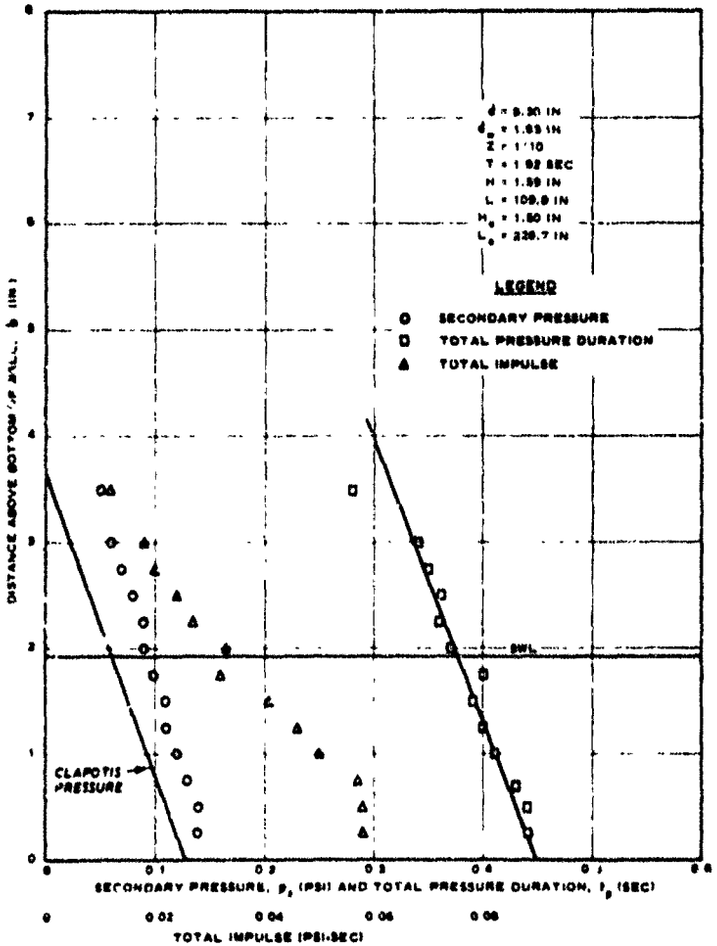

Fig. 38. Distribution of secondary pressure, total impulse, and total pressure duration on wall; test series 9

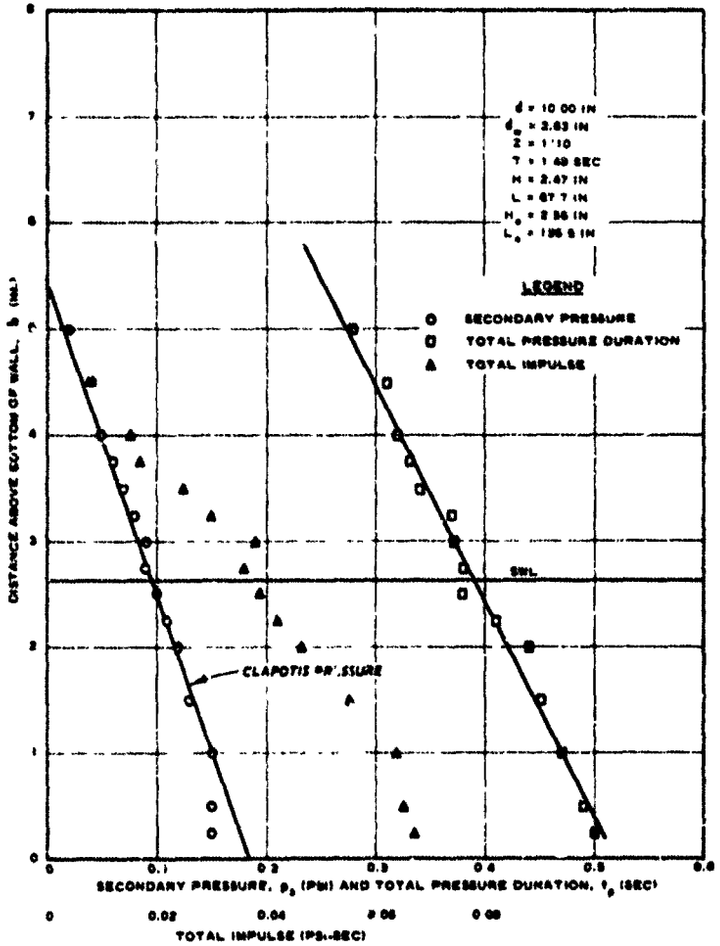

Fig. 39. Distribution of secondary pressure, total impulse, and total pressure duration on wall; test series 10

pressure can be used with good accuracy in calculating the secondary pressure due to breaking waves.

113. The total pressure duration, which is measured from the time of impact to the time when the pressure returns to zero, and the total impulse, which is the integral of the pressure over the total duration of the pressure, have also been included for each test series in figs. 30 through 39. Essentially, the total pressure duration is a measure of the time during which the wave is in contact with the wall at each point on the wall.

114. In order to show how the total duration varies with the wave period, a plot of the ratio of pressure duration at the still-water level and wave period versus wave steepness is shown in fig. 40. It can be seen

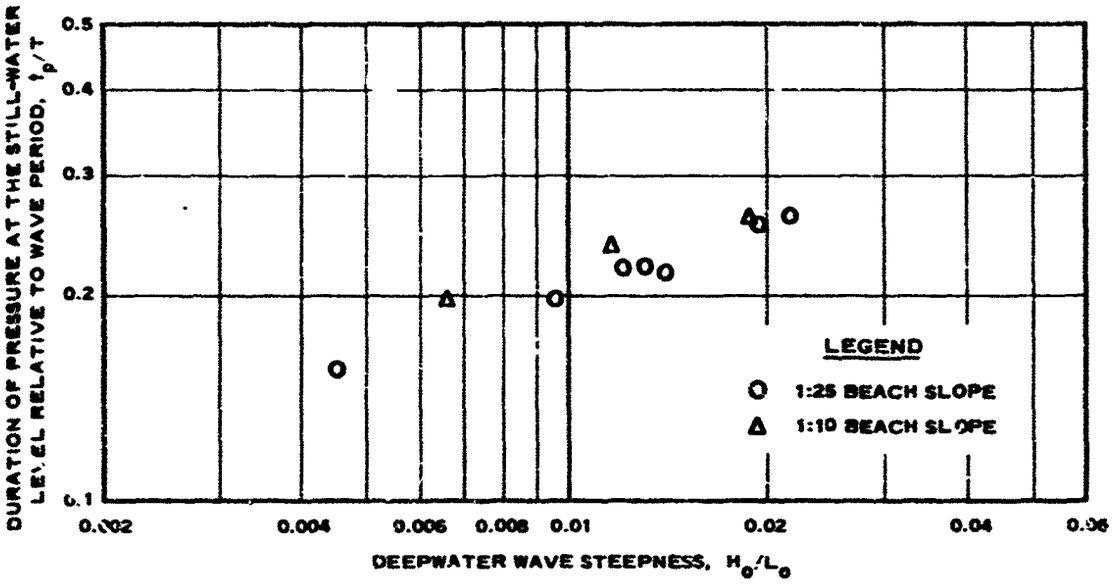

Fig. 40. Duration of pressure on wall at the still-water level relative to the wave period versus deepwater wave steepness

from this diagram that the duration of the pressure with respect to wave period increases with increasing wave steepness. The wavelength and period are functions of each other. Therefore, this plot shows that the total duration of the pressure on the wall increases with increasing wave height.

115. The impulse shown in figs. 30 through 39 for each of the test series is the total impulse and includes the shock impulse. However,

since the shock impulse is only about 10 percent of the total impulse, the data shown in these figures are nearly equal to the product of the secondary pressure and total pressure duration.

116. The total duration and impulse data were included primarily to show that the total impulse and pressure duration are not the same at all points on the wall and to show that the total impulse is more dependent upon the secondary pressure and its duration than on the shock pressure.

The Effect of a Wall on the Breaking Characteristics of the Wave

117. Studies have been conducted, both theoretical and experimental, on the breaking characteristics of waves on beaches. However, no previous studies have considered the presence of a barrier on the beach such as the test wall in this study. An analysis of the characteristics of the waves breaking against the test wall was made to determine if the data and methods now available to predict breaking characteristics of waves on unobstructed beaches could also be applied to waves on obstructed beaches. If relations between waves causing maximum shock pressure and waves breaking on unobstructed beaches could be derived, one would then be able to predict when shock pressures would occur using data now available.

118. There have been relatively few prototype studies concerning breaking waves; however, the studies conducted have contributed considerably to the knowledge of breaking-wave pressures. Most of the experimental and theoretical works involving full-scale tests were conducted as a result of the need for useful surf forecasts for amphibious operations during World War II. The U. S. Navy Hydrographic Office[17] published a volume in 1944 dealing with the methods of forecasting breakers and surf. That study was mostly empirical and combined the data from the breaking-wave studies, both model and prototype, which had been conducted up to that time. From these data, curves were plotted that relate the wave heights at breaking and the water depths at breaking to the deepwater wave steepness. Also as part of the effort to produce accurate methods of forecasting breakers and surf, Munk[18] investigated the application of solitary-wave theory to breaking-wave problems.

119. The results of both of these studies are reproduced in figs. 41 and 42 to compare them with the data from the present study. Fig. 41 is a plot of the ratio of wave height at breaking to wave height in deep water, H_B/H_o, versus the deepwater wave steepness, H_o/L_o. The ratio H_B/H_o is called the relative height of the breaking wave. On fig. 41 it can be seen that the results of Munk's study and those of the U. S. Navy Hydrographic Office agree closely. Also shown in fig. 41 are the data recorded in this study. Considering the fact that there are only ten data points from this study, hardly enough to form strong conclusions, there is very little difference between the breaking height of a wave on an obstructed beach and the breaking height on an unobstructed beach. This observation leads one to the conclusion that, when an obstruction such as a vertical wall is present on the beach, the wave reflected from the wall has very little, if any, effect on the incident wave. On an unobstructed beach there is little or no reflected wave due to the long runup on the beach; thus, each breaker is essentially independent of previous waves. It is noted that there is considerable scatter in the data from which the curve of the Navy Hydrographic Office and the curve of Munk were drawn. The spread of those data would include all of the data points from the present study.

120. Information concerning the breaking depth is also important in breakwater design. Although the present study is primarily concerned with shock pressures, if the depth at which a given wave will break to produce maximum shock pressure can be predicted, then the possibility of a breakwater's being subjected to such pressure will be known. The diagram shown in fig. 42 is similar to fig. 41; however, the water depth at breaking rather than the breaker height is plotted. Two of the curves shown in fig. 42 are from studies by the U. S. Navy Hydrographic Office and the work of Munk, as marked. These curves are plots of the breaking depth relative to the deepwater wave height, d_B/H_o, versus the deepwater wave steepness, H_o/L_o, and are plotted from data of waves breaking on unobstructed beaches of various slopes and have been derived in a manner similar to the methods used for the breaking height shown in fig. 41. The data from the present study, which are also plotted in fig. 42, are not

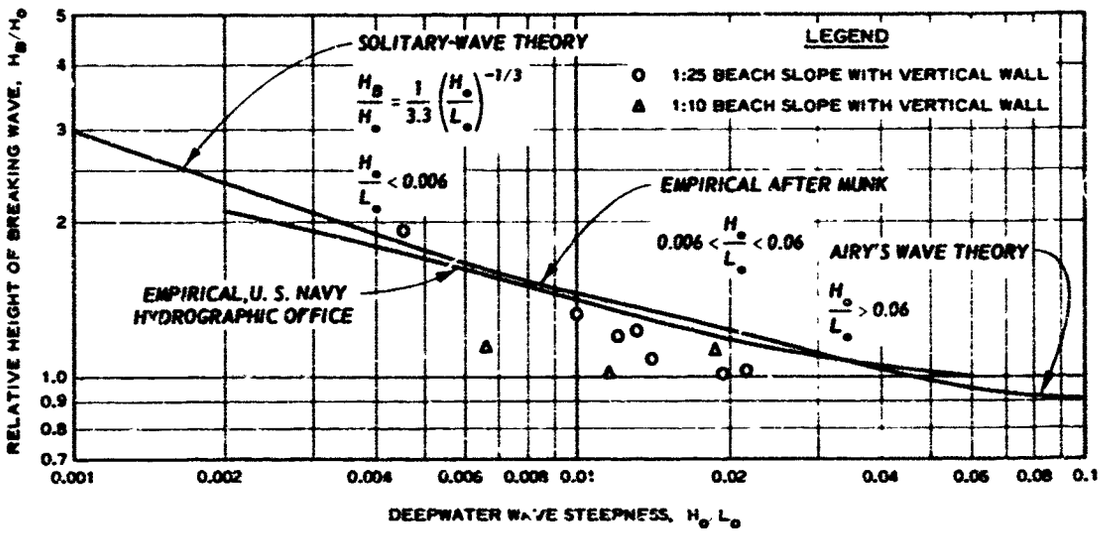

Fig. 41. Relative height of breaking wave versus deepwater wave steepness

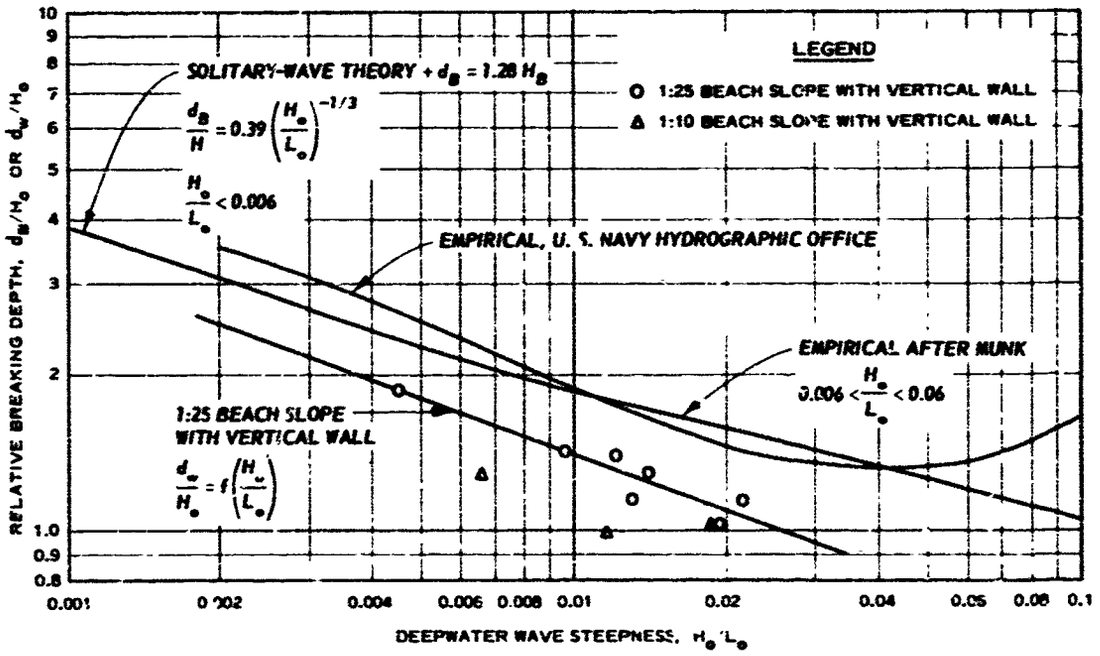

Fig. 42. Relative breaking depth versus deepwater wave steepness

plotted against the same ordinate variable as the two curves mentioned above. The data points from the present study represent the still-water depth at the wall relative to the deepwater wave height, d_w/H_o, versus the deepwater wave steepness, H_o/L_o. The water depth at the wall, d_w, was used to plot the data from this study rather than the breaking depth, d_B, since the depth at the wall is the more significant variable when speaking of shock pressures on the wall; also, d_B can be more easily measured.

121. The water depth at the wall is different and is less than the actual breaking depth since the wave must break a small distance in front of the wall in order to impact on the wall and cause maximum shock pressures. The point of breaking is down the beach slope from the wall and therefore in deeper water. The line through the 1/25 beach slope data points in fig. 42 was drawn to show the trend of data more clearly. The line was calculated by the method of least squares.

122. In fig. 42, as in fig. 41, the curve of the U. S. Navy Hydrographic Office was drawn from data which exhibited much scatter. The curve after Munk on fig. 42 was drawn using his breaking-height curve (fig. 41) and the relation $d_B = 1.28H_B$ which Munk proposed. This relation between the breaking depth and breaking height of a wave is based on the solitary-wave theory, and is discussed in Appendix B.

123. It is also of interest to look at other parameters of the breaking wave such as the elevation of the crest above the bottom. The breaking height is the vertical distance from the breaker crest to the preceding trough. The elevation of the crest of the breaker in this case is measured vertically from breaker crest to the base of the test wall. Figs. 43 and 44 are plots of the data from this study relating the breaker crest elevation to the deepwater wave height and the still-water depth at the wall. Fig. 43 shows the relation between the relative elevation of the breaker crest, y_B/H_o, versus the deepwater wave steepness, H_o/L_o. It can be seen that the crest elevation of the breaker behaves in a manner similar to the breaker height. The flatter waves tend to peak up more noticeably when they break, whereas the steeper waves increase very little in wave height over the deepwater waves and their crest elevation is much

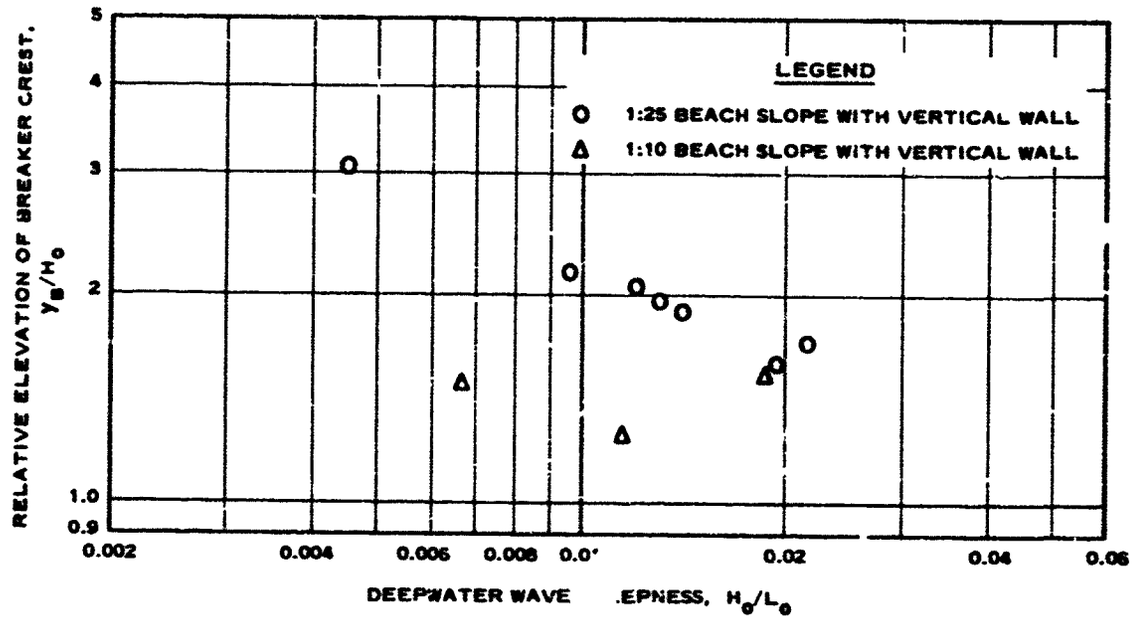

Fig. 43. Relative elevation of breaker crest versus deepwater wave steepness

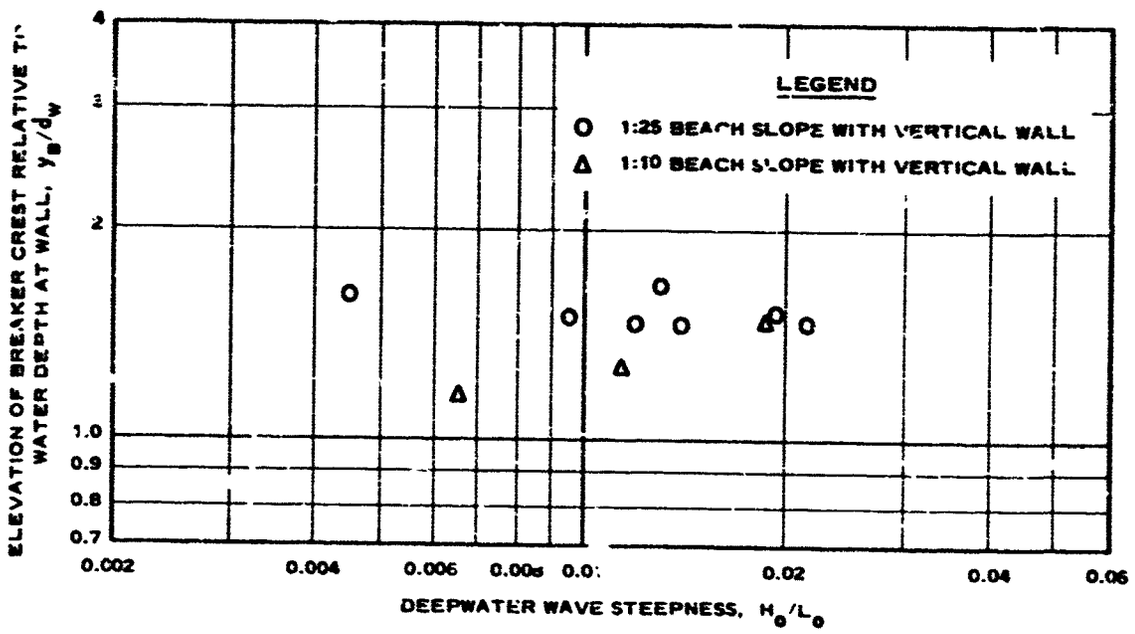

Fig. 44. Elevation of breaker crest relative to depth of water at wall versus deepwater wave steepness

less than that of a flatter wave of the same deepwater height. On fig. 43 there are two points for the 1/10 beach slope which fall considerably below the other data points. In examining these waves closely it was observed that their wavelength was considerably longer than the horizontal length of the beach slope. On the basis of these two tests, it appears that the short beach slope acts somewhat like a berm. By the time the wave begins to be affected by the more shallow water on the slope, it has reached the wall. It is believed that this causes the crest of the wave at breaking to be lower and the breaker height to be smaller since the wave does not build up gradually as it would on a longer slope. The wave is still in the state of transformation when it breaks. In both of these tests the wavelength in the flume was approximately 50 percent greater than the length of the beach slope.

124. Fig. 44 is a combination of fig. 42, which shows the water depth at the wall necessary to cause shock pressures, and fig. 43 which shows the breaker crest elevation. Fig. 44 is also based on the data from the present study, and it shows that the ratio between the breaker crest elevation and the water depth at the wall, y_B/d_w, is constant for all deepwater wave steepnesses when conditions are such that the wave breaks on the wall and causes maximum shock pressures.

125. In conclusion, it is emphasized that all the breaking-wave data which are based on the experimental portion of this study pertain only to conditions which produce maximum shock pressures. No attempt was made to make any comparison with waves breaking against a wall which do not cause shock pressures, and no data are presented for such cases. The only comparison of breaking characteristics is with data which have been gathered by other investigators who studied breaking waves on unobstructed beaches. It is believed, however, that much more information is needed concerning the characteristics of waves breaking on walls. More conclusive information concerning the effect of the wall on the breaking characteristics of the waves, as compared to the breaking characteristics on an unobstructed beach, would also be of great value.

PART V: SUMMARY AND CONCLUSIONS

126. The purpose of this study was to aid in the development of a more reliable and sound method for designing breakwaters which will be subjected to the action of breaking waves. This aim was accomplished by the use of an experimental investigation and by consolidating the data of other investigators. The other studies have heretofore been generally unrelated, and very little attempt was made by any of the investigators to make use of work which had been done previously.

127. In addition to information concerning shock pressures due to breaking waves, the secondary pressure and the breaking-wave characteristics were also considered in the analysis. This study considered only the ideal case of a smooth, rigid vertical wall which was high enough to preclude overtopping, whereas in reality, very few breakwaters are built with exactly this configuration. However, increased knowledge of the simple case will lead to more accurate methods of analyzing the more complex structures.

128. It is believed that the most important finding of this study is that the maximum shock pressure has been shown to be proportional to the one-third power of the deepwater wave energy, in the first approximation, over the entire range of data now available from laboratory and prototype tests. However, the shock pressure exhibits wide scatter for seemingly identical conditions. In addition, relations were developed for the distribution of the shock pressure on the test wall. These relations were derived from the data generated in the laboratory during this study, but other investigators have observed similar distributions of shock pressures on walls. Although the shock impulse is an important parameter in breakwater design, insufficient data are available to make any conclusions other than that the shock impulse also tends to increase with increasing wave energy and is about 10 percent of the total impulse transferred to the wall. The shock impulse was also found to be fairly constant for given conditions; the higher pressures are associated with the shorter durations and vice versa.

129. The secondary pressure was also studied, and it was found that

the secondary pressure is nearly equal to the clapotis pressure. The secondary pressure was fairly constant for similar wave conditions and did not exhibit the degree of scatter that was observed for shock pressures.

130. The final major consideration of this study was the effect of the wall on the breaking characteristics of the wave. The breaking characteristics of a wave breaking against a wall so as to cause maximum pressure were compared with the characteristics of a wave which is allowed to break on an unobstructed beach. It was found, for the limited range of data available, that there was little difference between a wave breaking on a beach obstructed by a wall and a wave breaking on an unobstructed beach. Thus the information now available concerning breaking waves on unobstructed beaches can be used to analyze waves which break against vertical walls.

131. This study provides a start for the development of more accurate methods of designing breakwaters which must withstand the action of breaking waves. However, there is much to be done to obtain a complete understanding of the effects of breaking waves. More laboratory and theoretical investigations are needed to determine the effects of other variables which were neglected in this investigation. Prototype tests are also needed to confirm the validity of laboratory results and to investigate those variables which cannot be reproduced in the laboratory.

LITERATURE CITED

1. Sainflou, G., "Essai sur les digues maritimes verticales" (Essay on Vertical Breakwaters), Annales des Ponts et Chaussées, Vol 98, No. 2, July-Aug 1928, pp 5-48; translated by Clarence C. Hatch, Western Reserve University, Cleveland, Ohio.

2. Gaillard, D. D., "Wave Action in Relation to Engineering Structures," 1904, The Engineer School, U. S. Army Corps of Engineers, Ft. Belvoir, Va.

3. Hirai, I., "The Force and Power of Waves," The Engineer, 20 Aug 1920, pp 184-185.

4. Larras, J., "Le déferlement des lames sur les jeteés verticales," Annales des Ponts et Chaussées, Vol 107, No. 5, 1937, pp 643-680.

5. De Rouville, A., Besson, P., and Pétry, P., "Etat actual des études internationales sur les efforts dus aux lames" (Development of International Studies on Wave Force), Annales des Ponts et Chaussées, Vol 108, No. 7, July 1938, pp 5-113; translated by U. S. Army Engineer Waterways Experiment Station Research Center, Vicksburg, Miss., TR No. 40-13, May 1940.

6. Bagnold, R. A., "Interim Report on Wave-Pressure Research," Journal, Institution of Civil Engineers, Vol 12, No. 7, June 1939, pp 202-226.

7. Minikin, R. R., "Pressure of Breaking Waves," The Dock and Harbour Authority, Vol 26, Mar 1946, pp 262-266.

8. _____, Winds, Waves and Maritime Structures, Griffin & Co. Ltd, London, 1950.

9. Denny, D. F., "Further Experiments on Wave Pressures," Journal, Institution of Civil Engineers, Vol 35, No. 4, Paper No. 5804, Feb 1951, pp 330-345.

10. Ross, C. W., "Shock Pressure of Breaking Waves," Proceedings, Fourth Conference on Coastal Engineering, Chicago, 1953, Council on Wave Research, The Engineering Foundation, University of California, 1954, pp 323-332.

11. _____, "Laboratory Study of Shock Pressures of Breaking Waves," Technical Memorandum No. 59, Feb 1955, U. S. Army Beach Erosion Board, Washington, D. C.

12. Nagai, S., "Shock Pressures Exerted by Breaking Waves on Breakwaters," ASCE, Waterways and Harbors Division, Journal, Vol 86, WW2, June 1960, pp 1-38.

13. Rundgren, L., "Water Wave Forces; A Theoretical and Laboratory Study," Transactions, Royal Institute of Technology, Institution of Hydraulics, Stockholm, Bulletin 54, 1958.

14. Hayashi, T. and Hattori, M., "Pressure of the Breaker Against a Vertical Wall," Coastal Engineering in Japan, Committee on Coastal

Engineering, Japan Society of Civil Engineers, Tokyo, Japan, Vol 1, 1958, pp 25-37.

15. Carr, J. H., "Breaking Wave Forces on Plane Barriers," Report E-11.3, Nov 1954, Hydrodynamics Laboratory, California Institute of Technology, Pasadena, Calif.

16. Leendertse, J. J., "Forces Induced by Breaking Water Waves on a Vertical Wall," Technical Report R-092, 9 Mar 1961, U. S. Naval Civil Engineering Laboratory, Port Hueneme, Calif.

17. U. S. Navy Hydrographic Office, "Breakers and Surf; Principles in Forecasting," H. O. No. 234, Nov 1944, Washington, D. C.

18. Munk, W. H., "The Solitary Wave Theory and Its Application to Surf Problems," Annals of the New York Academy of Sciences, Vol 51, Article 3, May 1949, pp 376-424.

SELECTED BIBLIOGRAPHY

Aartsen. M. A., "Model Study on the Impact of Waves,' Proceedings, Sixth Conference on Coastal Engineering, Florida, 1957, Chapter 45, pp 743-748.

Aartsen, M. A. et al., "Wave Impacts on the Steel Gates of a Discharge Sluice," Publication No. 16, Apr 1959, Delft Hydraulics Laboratory, Delft, Netherlands.

Aartsen, M. A. and Venis, W. A., "Model Investigations on Wave Attack on Structures," Publication No. 17, Apr 1959, Delft Hydraulics Laboratory, Delft, Netherlands.

Abraham, G., "Some Aspects of Surface Water Wave Scale Effects," Transactions, American Society of Civil Engineers, Vol 127, Part I, Paper No. 3285, 1962, pp 60-74.

Benezit, V., "Essai sur les digues maritimes verticales," (Treatise on Vertical Ocean Breakwaters), Annales des Ponts et Chaussées, Sept-Oct 1923, pp 125-159.

Biesel, F., "Study of Wave Propagation in Water of Gradually Varying Depths," Gravity Waves, U. S. National Bureau of Standards Circular 521, U. S. Department of Commerce, 1952, pp 243-253.

Bigelow, H. B. and Edmondson, W. T., "Wind Waves at Sea, Breakers and Surf," Publication No. 602, 1947, Hydrographic Office, U. S. Naval Department, Washington, D. C.

Borgman, L. E. and Chappelear, J. E., "The Use of the Stokes-Struik Approximation for Waves of Finite Height," Proceedings, Sixth Conference on Coastal Engineering, Florida, 1957, Chapter 16, pp 252-280.

Carr, J. H., "Wave Forces on Plane Barriers," Report No. E-11.1, Oct 1953, Hydrodynamics Laboratory, California Institute of Technology, Pasadena, Calif.

Carr, J. H., "Wave Forces on Curved and Stepped Barriers," Report No. E-11.2, June 1954, Hydrodynamics Laboratory, California Institute of Technology, Pasadena, Calif.

Carrier, G. F. and Greenspan, H. P., "Water Waves of Finite Amplitude on a Sloping Beach," Journal of Fluid Mechanics, Cambridge University Press, Vol 4, Part 1, May 1958, pp 97-109.

Chappelear, J. E., "On the Theory of the Highest Waves," Technical Memorandum No. 116, July 1959, U. S. Army Beach Erosion Board, Washington, D. C.

Coen-Cagli, E., "L'action des lames de tempete sur les digues maritimes a paroi verticale," Le Génie Civil, Vol 109, No. 9, Aug 1936, pp 177-182; translated by U. S. Army Engineer Waterways Experiment Station Research Center, Vicksburg, Miss., TR No. 43-36, 1940.

d'Auria, L., "On the Force of Impact of Waves and the Stability of the Superstructure of Breakwaters," Journal of the Franklin Institute, Nov 1890, pp 373-376.

Defant, A., Physical Oceanography, Vol 2, Pergamon Press, New York, 1961.

Diephuis, J. G. H. R., "Scale Effects Involving the Breaking of Waves," Proceedings, Sixth Conference on Coastal Engineering, Florida, 1957, Chapter 11, pp 194-201.

El Ghamry, O. A., "Wave Forces on a Dock," Technical Report No. HEL-9-1, Oct 1963, Hydraulic Engineering Laboratory, University of California, Berkeley.

"Engineering Aspects of Water Waves, a Symposium," Transactions, American Society of Civil Engineers, Vol 118, Paper No. 2556, 1953, pp 545-685.

a. Mason, M. A., "Surface Water Wave Theories," pp 546-574.

b. Daily, J. W. and Stephan, S. C., Jr., "Characteristics of the Solitary Wave," pp 575-587.

c. Carr, J. H., "Long-Period Waves or Surges in Harbors," pp 588-616.

d. Johnson, J. W., "Engineering Aspects of Diffraction and Refraction," pp 617-652.

e. Hudson, R. Y., "Wave Forces on Breakwaters," pp 653-685.

Ertel, H., "Determinación teórica del empuje de las olas," Beiträge zur Geophysik, Vol 68, No. 4, 1959, pp 250-253.

Gerstner, F. V., "Theorie der Wellen" (Theory of Waves), Abhandlungen der Königlichen Böhmischen Gesellschaft der Wissenschaften, Prague, 1802; translated by Ronald M. Kay, Institute of Engineering Research, University of California, Berkeley, Report Series 3, No. 339, Sept 1952.

Gouda, M. A., "Hydrodynamic Wave Pressure on Breakwaters," Transactions, American Society of Civil Engineers, Vol 126, Part IV, Paper No. 3150, 1961, pp 87-99.

Gourret, "Sur un movement approaché de clapotis, application au calcul des digues maritimes verticales," Annales des Ponts et Chaussées, Mar 1935, pp 337-451.

Greenspan, H. P., "On the Breaking of Water Waves of Finite Amplitude on a Sloping Beach," Journal of Fluid Mechanics, Cambridge University Press, Vol 4, Part 3, July 1958, pp 330-334.

Hamilton, W. S., "Forces Exerted by Waves on a Sloping Board," Transactions, American Geophysical Union, Vol 31, No. 6, Dec 1950, pp 849-855.

Hanes, F. P., "Development of Wave-Height Measuring Device," Miscellaneous Paper No. 5-231, June 1957, U. S. Army Engineer Waterways Experiment Station, CE, Vicksburg, Miss.

Haurwitz, B. et al., "Ocean Surface Waves," Annals of the New York Academy of Sciences, Vol 51, Article 3, pp 343-572.

Hayashi, T. and Hattori, M., "Effect of the Wave Pressures and the Impulses of Breaking Waves on the Stability of Breakwaters," International Association of Hydraulic Research Congress, London, Vol 1, Paper 1.5, 1963, pp 33-40.

Hudson, R. Y., "Wave Force on Breakwaters, Engineering Aspects of Water Waves," Transactions, American Society of Civil Engineers, Vol 118, 1953, pp 653-685.

Inman, D. L. and Nasu, N., "Orbital Velocity Associated with Wave Action near the Breaker Zone," Technical Memorandum No. 79, Mar 1956, U. S. Army Beach Erosion Board, Washington, D. C.

Ippen, A. T. and Kulin, G., "The Shoaling and Breaking Characteristics of the Solitary Wave," Proceedings, Fifth Conference on Coastal Engineering, Grenoble, France, 1954, Chapter 4, pp 27-49; also published as Technical Report No. 15, Apr 1955, Department of Civil and Sanitary Engineering, Massachusetts Institute of Technology, Cambridge, Mass.

Iversen, H. W., "Laboratory Study of Breakers," Gravity Waves, U. S. National Bureau of Standards Circular 521, U. S. Department of Commerce, 1952, pp 9-32.

Jacobsen, L. S. and Ayre, R. S., Engineering Vibrations, with Applications to Structures and Machinery, McGraw-Hill, New York, 1958.

Johnson, J. W., "Scale Effects in Hydraulic Models Involving Wave Motion," Transactions, American Geophysical Union, Vol 30, No. 4, Aug 1949, pp 517-525.

Keulegan, G. H. and Patterson, G. W., "Mathematical Theory of Irrotational Translation Waves," Journal of Research, U. S. National Bureau of Standards, Vol 24, Jan 1940, pp 47-101.

Kuribayashi, T., Muraki, Y., and Udai, G., "Field Investigation of Wave Forces on Breakwaters," Coastal Engineering in Japan, Japan Society of Civil Engineers, Tokyo, Japan, Vol 2, 1959, pp 17-27.

Lamb, H., Hydrodynamics, 6th ed., Dover, New York, 1945.

Langhaar, H. L., Dimensional Analysis and Theory of Models, Wiley, New York, 1951.

Larras, J., "Recherches experimentales sur le déferlement des lames" (Experimental Investigations on the Breaking of the Waves), Annales Ponts et Chaussées, Vol 122, Series 8, Sept-Oct 1952, pp 525-542; also Special Libraries Association Translation No. 62-16474.

_____, "Nouvelles Recherches sur le Déferlément des lames" (New Research on the Breaking of Waves), La Houille Blanche, No. 10, May-June 1955, pp 340-344; also Special Libraries Association Translation No. 62-16757.

LeMehauté, B. and Brebner, A., "An Introduction to the Mathematical Theories of Two-Dimensional Periodic Progressive Gravity Waves," CE Research Report No. 11, July 1960, Civil Engineering Department, Queen's University, Kingston, Ontario.

Mason, M. A., "A Study of Progressive Oscillatory Waves in Water," Technical Report No. 1, 1948, U. S. Army Beach Erosion Board, Washington, D. C.

_____, "Some Observations of Breaking Waves," Gravity Waves, U. S. National Bureau of Standards Circular 521, U. S. Department of Commerce, 1952, pp 215-220.

Milne-Thomson, L. M., Theoretical Hydrodynamics, 4th ed., Macmillan, New York, 1960.

Mitsuyasu, H., "Experimental Study of Wave Force Against a Wall," Coastal Engineering in Japan, Japan Society of Civil Engineers, Tokyo, Japan, Vol 5, 1962, pp 33-47.

Molitor, D. A., "Wave Pressures on Sea-Walls and Breakwaters," Transactions, American Society of Civil Engineers, Vol 100, Paper No. 1913, 1935, pp 904-1017.

Morison, J. R., "Wave Pressure on a Vertical Wall," Technical Report HE-116-298, Dec 1948, Institute of Engineering Research, University of California, Berkeley, Calif.

Morison, J. R. and Crooke, R. C., "The Mechanics of Deep Water, Shallow Water, and Breaking Waves," Technical Memorandum No. 40, Mar 1953, U. S. Army Beach Erosion Board, Washington, D. C.; also published as Technical Report Ser 3, Issue 344, Feb 1953, Institute of Engineering Research, University of California, Berkeley, Calif.

Mueller, L. A., Knutson, H. A., and Koch, A. A., "Some Dynamic Aspects in the Design of Marine Structures on the Great Lakes," Proceedings, Fourth Conference on Coastal Engineering, Chicago, 1953, Chapter 24, pp 333-339.

Nagai, S., "Sliding of Composite-Type Breakwaters by Breaking Waves," ASCE, Waterways and Harbors Division, Journal, Vol 89, WW1, Paper 3428, Feb 1963, pp 1-20.

O'Brien, M. P., "A Summary of the Theory at Oscillatory Waves," Technical Report No. 2, 1942, U. S. Army Beach Erosion Board, Washington, D. C.

Prins, J. E., "Model Investigations of Wind Wave Forces," Publication No. 24, Sept 1960, Delft Hydraulic Laboratory, Delft, Netherlands.

Putnam, J. A., Munk, W. H., and Traylor, M. A., "The Prediction of Longshore Currents," Transactions, American Geophysical Union, Vol 30, No. 3, June 1949.

Quinn, A. DeF., Design and Construction of Ports and Marine Structures, McGraw, New York, 1961.

Rouse, H., ed., Engineering Hydraulics, Wiley, New York, 1950.

Sainflou, M., "La resistance aux tempetes des brise-lames a parements verticaux" (Resistance to Storms of Breakwaters with Vertical Sides), Le Génie Civil, 26 Jan 1929, pp 81-84.

_____, "Note sur le calcul des digues maritimes verticales," Annales des Ponts et Chaussées, Vol 105, No. 2, Nov 1935, pp 735-753.

Stevenson, T., "Account of Experiments upon the Force of the Waves of the Atlantic and German Oceans," Transactions of the Royal Society of Edinburgh, Vol 16, 1849, pp 23-32.

Stoker, J. J., Water Waves; The Mathematical Theory with Applications, Interscience Publishers, Inc., New York, 1957.

Stokes, G. G., "On the Theory of Oscillatory Waves," Transactions of the Cambridge Philosophical Society, Vol 8, 1947, pp 441-455.

U. S. Army, Office, Chief of Engineers, "Design of Breakwaters and Jetties," EM 1110-2-2904, 30 Apr 1963, U. S. Government Printing Office, Washington, D. C.

U. S. Army Corps of Engineers, "Shore Protection Planning and Design," Technical Report No. 4, 1961, Beach Erosion Board, Washington, D. C.

U. S. National Bureau of Standards, Gravity Waves, Circular 521, U. S. Department of Commerce, Washington, D. C., Nov 1952.

Wiegel, R. L., "Experimental Study of Surface Waves in Shoaling Water," Transactions, American Geophysical Union, Vol 31, No. 3, June 1950, pp 377-385.

Wiegel, R. L. and Beebe, K. E., "The Design Wave in Shallow Water," ASCE, Waterways and Harbors Division, Journal, Vol 82, Paper 910, WW1, Mar 1956, pp 910-1 - 910-21.

Wiegel, R. L. and Johnson, J. W., "Elements of Wave Theory," Proceedings of First Conference on Coastal Engineering, Long Beach, Calif., 1951, Chapter 2, pp 5-21.

Table 1

Summary of Data

Test Series	T sec	H in.	L in.	d in.	H_o in.	L_o in.	H_o/L_o	H_B in.	d_w in.	z	p_{max} psi	E_o lb
1	1.93	2.30	114.2	10.50	2.21	229.1	0.00965	3.15	3.18	1/25	4.08	5.05
2	1.93	2.85	120.6	11.20	2.77	229.1	0.0121	3.34	3.88	1/25	8.40	7.93
3	1.93	3.29	124.0	11.50	3.22	229.1	0.0141	3.50	4.18	1/25	9.56	10.72
4	1.70	2.32	106.7	10.00	2.32	177.7	0.0131	2.87	2.68	1/25	3.37	4.31
5	1.38	2.17	78.6	9.70	2.28	117.1	0.0195	2.32	2.38	1/25	3.07	2.75
6	1.94	1.11	109.9	9.30	1.05	231.5	0.00454	2.02	1.98	1/25	3.08	1.15
7	1.51	2.90	90.6	10.80	3.03	140.2	0.0216	3.14	3.48	1/25	6.40	5.81
8	1.93	2.78	114.0	10.00	2.65	229.1	0.0116	2.73	2.63	1/10	3.20	7.26
9	1.92	1.59	109.8	9.30	1.50	226.7	0.00662	1.74	1.93	1/10	3.08	2.30
10	1.49	2.47	87.7	10.00	2.56	136.5	0.0188	2.89	2.63	1/10	6.00	4.04

Table 2

Shock Pressure Data, Test Series 1

H = 2.·0 in.
L = 115 2 in.
T = 1.9· sec

H_o = 2.21 in.
L_o = 229.1 in.

d = 10.50 in.
d_w = 3.18 in.
z = 1/2·

Distance Above Bottom of Wall b, in.	Shock Pressure (in psi) for the Successive Breaking Waves Indicated			
	First	Second	Third	Fourth
0.25	0.36	0.45	0.31	0.29
	0.3·	0.53	0.30	0.23
0.50	0.32	0.45	0.32	0.35
	0.3·	0.42	0.32	0.34
	0.32	0.50	0.32	0.31
	0.36	0.30	0.3·	0.34
	0.37	0.52	0.28	0.30
	0.39	0.54	0.3·	0.33
0.75	0.37	0.40	0.33	0.34
	0.35	0.48	0.29	0.37
	0.36	0.51	0.3·	0.30
	0.40	0.55	0.3·	0.33
1.00	0.35	0.50	0.37	0.34
	0.37	0.52	0.37	0.32
	0.38	0.61	0.34	0.30
	0.37	0.55	0.30	0.28
1.25	0.36	0.48	0.40	0.34
	0.38	0.59	0.41	0.42
	0.36	0.53	0.36	0.37
	0.37	0.50	0.37	0.35
1.50	0.36	0.50	0.39	0.37
	0.35	--	0.37	0.32
	0.37	0.48	0.39	0.40
	0.3·	0.50	0.35	0.34
1.75	0.37	0.59	0.51	0.36
	0.38	0.51	0.3·	0.32
	0.35	0.62	0.38	0.43
	0.39	0.48	0.36	0.33
2.00	0.37	0.51	0.44	0.68
	0.39	0.43	0.32	0.50
	0.39	0.58	0.33	0.42
	--	0.67	0.39	0.59
2.25	0.50	0.72	0.42	0.47
	0.42	0.39	0.49	0.40
	0.40	0.77	0.40	0.56
	0.49	0.41	0.34	0.48
	0.49	0.51	0.40	0.50
2.50	0.47	0.60	0.50	0.35
	0.41	0.61	0.35	0.33
	0.48	0.54	0.97	0.33
	0.44	0.58	0.32	0.40
	0.53	0.74	0.35	0.48
2.75	0.54	0.93	0.85	0.69
	0.44	0.59	0.67	0.40
	0.50	0.43	0.57	1.62
	0.46	0.87	0.30	0.88
	0.53	0.77	0.60	1.10
3.00	0.78	0.50	1.57	--
	0.54	0.77	1.05	0.73
	0.55	0.84	1.07	0.61
	0.60	1.11	0.72	0.42
3.25	0.61	0.61	0.83	0.66
	--	1.86	0.31	0.71
	1.12	1.37	1.50	0.81
	0.75	1.06	--	1.00
	1.30	1.24	1.10	0.80
	0.66	1.28	1.21	0.56
3.50	1.17	0.52	0.75	--
	0.84	0.71	0.65	0.52
	1.05	0.76	0.52	0.78
	0.85	1.12	1.08	1.00
	0.84	0.70	1.50	0.83
	0.89	0.80	0.93	0.70
	0.87	0.50	1.31	0.56
	1.84	1.18	0.67	0.46
	2.28	0.78	1.53	0.72
	1.98	0.57	[illegible]	0.66
	3.00	1.03	[illegible]	1.44
	1.41	0.67	[illegible]	0.91
	0.84	1.03	0.51	0.75
	0.98	0.97	0.45	1.15

Distance Above Bottom of Wall b, in.	Shock Pressure (in psi) for the Successive Breaking Waves Indicated			
	First	Second	Third	Fourth
3.75	1.18	0.70	0.91	--
	1.10	1.71	0.76	0.71
	1.12	2.47	0.40	0.36
	1.08	4.08	2.15	1.20
	1.36	1.81	0.46	0.85
	1.08	2.51	0.72	0.55
	1.03	2.06	0.92	0.82
	1.58	0.80	0.79	0.83
	1.37	1.58	0.54	0.48
	1.40	0.71	0.61	0.60
4.00	1.61	1.59	0.41	1.00
	1.67	2.68	0.41	0.38
	1.37	2.59	0.73	0.43
	2.16	2.54	0.70	0.56
	1.82	1.15	0.58	0.73
	1.05	2.04	0.97	0.72
4.25	1.55	1.35	0.42	0.46
	1.83	1.49	0.56	0.71
	1.77	1.59	0.48	0.90
	1.40	1.50	0.60	0.52
4.50	1.04	1.87	0.28	0.70
	1.12	1.07	0.49	0.62
	1.23	0.83	0.31	0.57
	1.20	0.96	0.20	0.37
4.75	0.75	0.78	0.23	0.45
	0.77	0.86	0.28	0.39
	0.73	1.05	0.27	0.56
	0.65	0.68	0.3·	0.3·
5.00	0.46	0.47	0.20	0.32
	0.37	0.48	0.13	0.40
	0.44	0.48	0.19	0.36
	0.50	0.54	0.22	0.31
5.25	0.33	0.29	0.14	0.20
	0.32	0.32	0.15	0.18
	0.30	0.32	0.13	0.42
	0.27	0.25	0.15	0.21
5.50	0.20	0.27	0.15	0.11
	0.21	0.18	0.10	0.14
	0.19	0.21	0.08	0.12
	0.19	0.20	0.13	0.14
5.75	0.26	0.13	0.09	0.09
	0.32	0.06	0.11	0.08
	0.13	0.12	0.06	0.09
	0.13	0.22	0.08	0.11
6.00	0.10	0.11	0.06	0.12
	0.13	0.14	0.09	0.07
	0.11	0.11	0.07	0.05
	0.10	0.17	0.07	0.06
6.25	0.08	0.15	0.05	0.04
	0.09	0.08	0.05	0.04
	0.08	0.32	0.05	0.05
6.50	0.06	0.04	0.04	0.02
	0.05	0.04	0.03	0.03
6.75	0.06	0.05	0.03	0.03
	0.05	0.04	0.04	0.03
7.00	0.04	0.03	0.04	0.03
	0.04	0.04	0.03	0.03

Table 3

Shock Pressure Data, Test Series 2

H = 2.85 in.
L = 120.6 in.
T = 1.93 sec

H_o = 2.77 in.
L_o = 229.1 in.

d = 11.20 in.
d_w = 3.88 in.
z = 1/25

Distance Above Bottom of Wall b, in.	Shock Pressure (in psi) for the Successive Breaking Waves Indicated			
	First	Second	Third	Fourth
2.50	0.42	0.61	0.56	0.90
	0.43	0.78	0.51	0.96
	0.43	0.77	0.51	0.63
	0.42	0.75	0.53	0.78
3.00	0.42	0.76	0.88	1.06
	0.44	0.90	0.72	0.85
	0.45	0.88	0.63	0.85
	0.46	0.86	0.61	1.25
3.50	0.46	0.73	0.62	1.33
	0.48	0.94	0.63	1.13
	0.43	1.16	0.62	0.97
	0.46	0.88	0.62	1.65
3.75	0.48	1.02	0.74	1.06
	0.49	--	0.62	0.71
	0.49	1.31	0.70	2.50
	0.50	1.32	0.81	2.06
4.00	0.52	1.55	0.80	1.18
	0.55	1.06	0.85	0.99
	0.53	1.06	0.77	1.19
	0.52	1.29	0.85	2.21
	0.55	1.37	1.01	1.40
4.25	0.52	1.66	0.88	1.73
	0.52	1.17	1.03	1.21
	0.59	1.51	1.18	1.50
	0.56	1.32	1.30	1.16
	0.53	1.85	1.06	3.17
	0.55	1.24	1.12	1.22
4.50	0.54	1.14	1.06	1.68
	0.51	1.61	0.60	1.71
	0.50	1.92	2.37	2.67
	0.55	2.35	1.12	1.22
	0.55	1.79	1.03	1.37
	0.64	1.54	1.52	2.11
4.75	0.64	2.10	1.42	3.52
	0.66	2.14	1.14	1.96
	0.66	2.06	1.76	2.42
	0.68	2.16	1.02	1.28
	0.72	1.62	1.56	1.40
	0.62	2.94	1.60	3.00
	0.58	1.78	1.00	1.26
	0.59	2.48	2.03	1.85
	0.65	2.20	1.24	3.82
5.00	0.68	5.37	3.45	1.96
	0.76	2.20	2.80	2.54
	0.92	3.02	1.66	2.62
	0.84	2.56	1.80	1.68
	1.20	2.48	2.46	0.72
	0.62	5.16	1.22	1.86
	0.76	2.20	1.70	2.00
5.25	0.86	8.30	2.46	1.04
	0.86	8.40	1.74	2.36
	0.84	5.22	1.66	1.82
	0.84	3.92	1.20	1.56
	1.02	2.60	2.52	0.84
	0.94	3.56	2.08	1.60
	0.92	2.82	2.96	1.20
	1.75	2.34	1.10	0.87
	2.00	1.21	1.22	0.60
	2.28	3.28	0.97	0.97
5.50	1.06	3.74	2.42	1.54
	1.46	1.50	2.22	0.90
	1.40	3.92	1.58	1.44
	1.36	6.74	0.74	1.52
	1.34	3.84	0.96	0.96
	1.16	3.16	0.76	1.02
5.75	1.24	3.52	0.80	0.66
	1.20	3.70	1.08	0.60
	1.20	--	0.66	1.10
	1.00	4.06	0.80	0.70
	0.94	2.08	0.94	0.98
6.00	1.02	1.76	0.50	0.62
	0.98	1.12	0.37	0.35
	1.08	1.39	0.42	0.48
6.50	0.57	0.39	0.20	0.18
	0.57	0.31	0.18	0.32
	0.57	0.35	0.19	0.45
	0.51	0.32	0.16	0.25

Table 4

Shock Pressure Data, Test Series 3

H = 3.29 in.
L = 124.0 in.
T = 1.93 sec

H_o = 3.22 in.
L_o = 229.1 in.

d = 11.50 in.
d_w = 4.18 in.
z = 1/25

Distance Above Bottom of Wall b, in.	Shock Pressure (in psi) for the Successive Breaking Waves Indicated			
	First	Second	Third	Fourth
3.50	0.52	0.69	1.26	0.69
	0.52	0.98	0.84	0.49
	0.56	0.64	0.98	0.70
4.00	0.59	0.80	0.97	0.57
	0.59	0.97	1.07	0.60
	0.59	0.95	2.01	0.49
4.50	1.17	1.41	1.66	1.39
	0.73	1.19	2.11	0.94
	0.84	1.00	1.43	1.07
	0.85	0.65	1.33	1.33
5.00	0.90	1.32	3.68	1.08
	0.94	1.78	2.46	1.17
	0.96	1.40	1.74	1.55
	1.27	1.34	2.26	2.22
5.25	1.06	1.46	3.72	1.24
	2.58	1.02	3.20	1.22
	3.32	1.18	2.12	0.84
	2.52	1.44	1.86	1.30
	1.56	1.26	1.70	0.86
5.50	2.52	0.92	4.40	1.57
	2.00	1.23	4.20	1.53
	2.19	1.92	1.90	1.06
	2.25	1.12	2.95	0.80
	1.42	1.32	3.24	1.16
	1.48	0.68	3.36	1.18
	1.48	1.28	1.62	1.02
	1.30	1.60	4.74	0.98
	1.32	1.32	1.94	1.20
	3.50	1.32	6.10	0.88
	5.50	0.92	4.08	1.38
5.75	2.64	0.98	4.08	1.48
	4.00	1.52	1.72	1.36
	1.88	0.98	2.72	1.58
	3.60	1.42	2.14	1.40
	1.60	1.36	3.74	1.14
	1.38	0.72	2.96	0.98
	7.72	0.82	4.38	1.34
	1.46	0.78	2.46	1.00
	5.42	0.72	2.06	1.16

Distance Above Bottom of Wall b, in.	Shock Pressure (in psi) for the Successive Breaking Waves Indicated			
	First	Second	Third	Fourth
6.00	3.72	1.38	6.36	0.96
	2.30	0.90	2.12	0.78
	1.82	1.60	3.00	0.86
	9.56	0.51	3.86	0.70
	7.22	1.60	2.92	0.94
	1.72	2.32	1.88	0.66
	2.20	0.66	2.84	0.80
	8.40	--	1.80	1.02
	7.96	1.18	1.14	0.70
	7.12	1.00	1.70	0.92
	4.02	1.26	1.64	0.73
	5.18	1.36	1.20	0.60
	7.43	1.43	2.23	0.62
6.25	2.48	1.66	0.92	0.90
	4.02	1.24	1.76	0.78
	4.90	0.88	1.58	0.60
	3.88	--	1.32	0.60
	4.56	0.98	1.36	--
6.50	1.95	0.91	0.76	0.47
	1.86	0.88	0.56	0.63
	1.55	1.17	0.89	0.65
	1.69	1.35	0.59	0.65
6.75	1.09	0.80	0.35	0.47
	1.06	0.73	0.36	0.40
	1.01	0.56	0.52	0.40
	1.17	0.67	0.40	0.40
7.00	0.67	0.38	0.22	0.29
	0.53	0.66	0.28	0.35
	0.66	0.35	0.26	0.29
7.50	0.27	0.26	0.18	0.44
	0.29	0.29	0.16	0.22

Table 5

Shock Pressure Data, Test Series 4

H = 2.32 in.
L = 106.7 in.
T = 1.70 sec

H_o = 2.32 in.
L_o = 177.7 in.

d = 10.00 in.
d_w = 2.68 in.
z = 1/25

Distance Above Bottom of Wall b, in.	Shock Pressure (in psi) for the Successive Breaking Waves Indicated			
	First	Second	Third	Fourth
2.00	0.28	0.30	0.51	0.51
	0.36	0.50	0.60	0.38
	0.72	0.41	0.38	0.44
	0.55	0.38	0.61	0.50
2.25	0.60	0.43	0.44	0.40
	0.52	1.19	0.53	0.80
	0.73	0.65	0.62	0.48
	0.66	0.68	0.54	0.47
2.50	0.31	0.66	0.66	0.64
	0.59	0.72	0.59	1.19
	0.40	0.59	0.56	0.45
	0.70	0.76	0.53	0.76
	0.86	0.72	0.71	0.60
2.75	0.58	0.88	0.39	0.76
	1.01	0.71	0.72	1.19
	1.06	0.61	0.76	0.51
	0.73	0.81	0.66	0.60
	0.90	0.72	1.77	0.62
	0.72	0.92	1.27	1.12
3.00	0.34	0.65	1.44	0.87
	1.21	0.87	1.81	0.83
	0.49	0.63	1.19	0.52
	1.36	0.88	0.81	0.66
	1.34	0.71	0.89	0.68
3.25	0.53	0.66	0.68	0.33
	0.93	0.98	0.93	0.58
	0.82	0.76	0.56	0.49
	2.01	0.66	1.05	0.68
	2.04	0.69	0.81	0.56
3.50	0.81	0.79	0.73	0.68
	1.08	0.78	0.47	0.66
	0.69	0.93	0.96	2.08
	0.68	0.58	0.89	0.72
	0.54	0.83	.39	2.09
	0.69	0.76	1.59	0.44
	0.73	0.61	0.93	0.49
	0.99	0.68	1.46	0.79
	0.99	0.74	0.75	0.82
	1.51	0.81	1.19	1.84
	2.44	0.57	0.97	1.56
	0.63	.59	1.62	0.49
	0.60	0.38	0.96	0.45
3.75	0.69	0.66	0.70	0.31
	2.64	0.37	0.83	0.50
	0.90	0.63	1.42	0.80
	2.84	0.68	1.33	0.92
	3.37	0.67	0.89	0.48
	3.32	0.70	0.82	0.63
	1.12	0.50	0.48	0.47
	1.63	0.58	0.52	0.48
	1.36	0.65	0.73	0.47
4.00	1.78	0.50	0.77	0.37
	1.18	0.59	0.50	0.31
	0.72	0.57	0.33	0.89
	1.66	0.49	0.54	--
	1.35	0.50	0.37	0.30
4.25	0.57	0.37	0.40	0.29
	0.94	0.30	0.46	0.31
	1.02	0.27	0.39	0.23
	1.02	0.35	0.43	0.20
	0.90	0.34	0.28	0.34
4.50	0.51	0.28	0.30	0.16
	0.62	0.27	0.38	0.14
	0.58	0.35	0.41	--
	0.45	0.26	0.27	0.19
4.75	0.31	0.22	0.31	0.10
	0.28	0.26	0.27	0.10
	0.25	--	0.24	0.10
	0.30	0.28	0.39	0.10

Table 6

Shock Pressure Data, Test Series 5

H = 2.17 in.
L = 78.6 in.
T = 1.38 sec

H_o = 2.28 in.
L_o = 117.1 in.

d = 9.70 in.
d_w = 2.38 in.
z = 1/35

Distance Above Bottom of Wall b, in.	Shock Pressure (in psi) for the Successive Breaking Waves Indicated			
	First	Second	Third	Fourth
1.50	0.60	0.83	0.20	0.31
	0.60	0.79	0.31	0.31
	0.47	0.66	0.20	0.86
2.00	1.14	0.85	0.44	0.68
	0.96	0.86	0.89	2.80
	0.87	0.63	0.91	0.47
	0.95	0.80	0.62	0.65
2.25	1.13	0.50	0.39	0.64
	1.00	0.40	0.40	2.23
	1.41	1.16	0.55	1.05
	0.99	0.77	0.72	0.32
2.50	1.59	0.87	1.00	0.73
	1.18	0.47	0.98	0.97
	1.22	0.56	0.33	0.18
	1.37	0.57	0.62	1.00
2.75	2.03	0.95	2.70	0.70
	1.90	0.46	1.04	1.10
	2.09	0.77	1.59	1.34
	1.37	0.93	2.09	0.47
	1.60	0.73	0.70	0.72
3.00	1.77	0.76	0.68	0.88
	1.77	0.57	0.69	2.00
	2.13	0.97	1.21	1.00
	2.07	1.29	1.65	1.22
	2.27	0.76	0.83	1.00
	2.06	2.89	1.48	0.60
	1.51	0.98	0.34	0.71
	1.37	0.64	0.19	0.52
	1.35	0.20	0.19	0.30
3.25	1.97	0.64	0.77	0.91
	2.09	0.78	1.02	0.41
	2.43	0.59	0.59	0.95
	1.86	0.83	0.83	0.52
	2.14	1.04	1.04	0.86
3.50	2.31	0.91	0.18	0.35
	1.93	0.69	0.42	0.44
	1.89	0.55	0.39	0.61
	2.39	0.61	0.47	0.56
	2.72	0.79	0.24	0.86
3.75	2.83	0.54	0.16	0.37
	2.63	--	0.26	0.35
	2.60	--	0.15	0.71
	2.49	--	0.21	0.39
	3.07	0.37	0.28	0.22
	2.65	--	0.19	0.54
4.00	1.53	0.33	0.23	0.34
	0.85	0.25	0.23	0.27
	1.02	0.31	0.32	0.25
	1.04	0.27	0.29	0.22
	1.28	0.33	0.23	0.30
4.25	0.66	0.23	0.19	0.21
	0.50	0.19	0.18	0.09
	0.68	0.21	0.13	0.20

Table 7

Shock Pressure Data, Test Series 6

H = 1.11 in.
L = 109.9 in.
T = 1.94 sec

H_o = 1.05 in.
L_o = 231.4 in.

d = 9.30 in.
d_w = 1.98 in.
z = 1/25

Distance Above Bottom of Wall b, in.	Shock Pressure (in psi) for the Successive Breaking Waves Indicated			
	First	Second	Third	Fourth
1.00	0.17	0.40	0.62	0.42
	0.16	0.34	0.50	0.54
	0.16	0.27	0.27	0.33
1.50	0.23	0.26	0.31	0.27
	0.18	0.51	0.51	0.60
	0.20	0.40	0.50	0.47
	0.17	0.58	0.87	0.40
1.75	0.21	0.54	0.43	0.45
	0.32	0.40	0.30	0.46
	0.20	1.18	0.38	0.54
	0.28	0.69	1.29	0.45
	0.18	0.59	0.61	0.72
2.00	0.35	1.37	1.12	0.75
	0.37	0.42	0.83	1.65
	0.32	0.69	1.03	1.03
	0.29	0.72	0.94	0.56
	0.35	1.53	0.58	0.71
2.25	0.45	2.47	1.52	2.00
	1.88	0.90	1.09	1.40
	0.55	0.80	2.34	1.18
	0.42	0.95	1.20	1.67
	0.31	1.06	1.23	1.02
	0.30	1.40	1.17	2.79
	0.27	0.90	2.06	1.50
	0.29	2.26	2.23	1.94
2.50	0.30	1.30	1.63	2.18
	0.34	1.33	2.61	1.58
	0.32	1.58	2.35	1.55
	0.31	1.34	1.11	1.63
	0.32	1.08	1.73	1.79
	0.37	1.00	2.10	3.08
	0.30	0.71	0.87	0.67
	0.35	0.70	2.10	2.01
	0.30	0.86	1.63	1.97
	0.32	1.10	0.85	1.85

Distance Above Bottom of Wall b, in.	Shock Pressure (in psi) for the Successive Breaking Waves Indicated			
	First	Second	Third	Fourth
2.75	0.28	0.60	0.85	0.90
	0.30	0.80	0.72	1.36
	0.28	0.55	1.14	1.53
	0.28	0.64	0.78	0.71
	0.27	0.70	0.56	0.59
	0.33	0.78	0.82	0.83
	0.28	0.44	0.51	0.64
3.00	0.18	--	0.26	0.50
	0.20	0.72	0.42	0.23
	0.19	0.43	0.22	0.20
	0.18	0.26	0.20	0.25
	0.19	0.23	0.35	0.40
	0.18	0.22	0.24	0.31
3.25	0.11	0.15	0.11	0.15
	0.11	0.11	0.11	0.11
	0.12	0.10	0.10	0.11
3.50	0.08	0.07	0.07	0.06
	0.07	0.06	0.06	0.06
	0.07	0.07	0.07	0.05

Table 8

Shock Pressure Data, Te t Series 7

H = 2.90 in.
L = 90.6 in.
T = 1.51 sec

H_o = 3.03 in.
L_o = 140.2 in.

d = 10.80 in.
d_w = 3.4[illegible] in.
z = 1/25

Distance Above Bottom of Wall b, in.	Shock Pressure (in psi) for the Successive Breaking Waves Indicated			
	First	Second	Third	Fourth
2.50	0.23	0.62	0.37	0.21
	0.23	0.50	0.32	0.20
	0.22	0.41	0.37	0.20
3.00	0.21	0.50	0.34	0.20
	0.21	0.40	0.47	0.19
	0.21	0.46	0.41	0.17
3.25	0.22	0.47	0.45	0.18
	0.21	0.45	0.56	0.17
	0.21	0.55	0.50	0.20
3.50	0.21	0.51	0.46	0.17
	0.21	0.50	0.52	0.17
	0.20	0.51	0.43	0.17
	0.21	0.60	0.51	0.18
3.75	0.21	0.76	0.60	0.17
	0.21	0.75	0.46	0.17
	0.20	0.66	0.51	0.18
	0.21	0.70	0.57	0.16
4.00	0.20	0.62	0.62	0.17
	0.20	0.75	0.68	0.18
	0.20	0.53	0.56	0.18
	0.20	0.61	0.70	0.17
4.25	0.22	0.97	1.06	0.18
	0.22	1.26	1.11	0.20
	0.22	0.97	0.80	0.18
	0.21	1.06	1.07	0.20
	0.21	0.97	0.83	0.19
	0.21	1.00	1.16	0.16
	0.20	0.93	0.72	0.17
4.50	0.21	1.05	1.47	0.18
	0.22	1.41	1.40	0.18
	0.22	1.11	1.58	0.19
	0.22	0.98	1.20	0.18
4.75	0.22	1.29	2.02	0.16
	0.22	1.27	1.17	0.18
	0.22	2.20	1.56	0.18
	0.21	1.15	1.61	0.27
5.00	--	1.08	0.14	0.18
	0.20	1.64	0.83	0.14
	0.22	1.71	3.29	0.21
	0.22	0.95	3.95	0.21
	0.21	2.33	3.87	0.18
	0.21	1.59	1.90	0.21

Distance Above Bottom of Wall b, in.	Shock Pressure (in psi) for the Successive Breaking Waves Indicated			
	First	Second	Third	Fourth
5.25	--	2.24	0.16	0.16
	0.20	2.60	1.70	0.16
	0.22	1.72	4.66	0.14
	0.20	2.60	1.58	0.14
	0.20	3.16	2.18	0.12
	0.21	3.31	2.97	0.16
	0.20	2.71	2.30	0.19
	0.21	2.92	2.74	0.15
	0.20	2.34	3.03	0.17
5.50	0.20	4.09	2.89	0.19
	0.20	5.41	2.64	0.16
	0.20	6.40	3.90	0.18
	0.20	3.80	1.98	0.26
	0.20	1.50	2.14	0.20
	0.20	4.26	1.58	0.34
	0.20	1.82	1.62	0.18
	0.20	1.82	4.20	0.12
5.75	0.16	1.80	1.46	0.12
	0.17	3.85	1.38	0.20
	0.20	3.79	1.00	0.21
	0.18	1.74	0.99	0.20
	0.19	3.60	1.09	0.29
	0.18	1.89	1.50	0.20
	0.20	3.48	0.98	0.30
	0.19	2.16	0.73	0.18
6.00	0.17	3.03	0.39	0.20
	0.16	1.63	0.66	0.12
	0.16	1.77	0.77	0.14
	0.17	1.13	0.65	0.18
	0.18	2.10	0.70	0.14
6.25	0.15	1.52	0.23	--
	0.15	0.90	0.40	0.17
	0.13	0.50	0.26	0.16
	0.13	0.49	0.26	0.17
6.50	0.12	0.24	0.12	0.17
	0.11	0.21	0.16	0.19
	0.11	0.33	0.18	0.12

Table 9

Shock Pressure Data, Test Series 8

H = 2.78 in.
L = 114.0 in.
T = 1.03 sec

H_c = 2.65 in.
L_o = 229.1 in.

d = 10.00 in.
d_w = 2.63 in.
z = 1/10

Distance Above Bottom of Wall b, in.	Shock Pressure (in psi) for the Successive Breaking Waves Indicated			
	First	Second	Third	Fourth
0.50	2.42	1.3[illegible]	2.13	0.90
	2.41	1.30	1.53	0.60
	2.38	1.4[illegible]	2.08	1.22
	2.43	1.34	2.13	1.19
1.00	2.75	1.47	2.16	1.29
	2.69	1.49	1.98	0.97
	2.90	1.[illegible]2	1.84	1.13
	2.70	1.47	2.43	0.89
1.50	2.[illegible]2	1.43	1.60	0.88
	--	1.36	1.21	1.27
	2.72	1.21	1.57	1.13
	2.80	1.22	1.44	0.96
	2.83	1.33	1.28	1.10
	3.00	2.24	1.92	0.75
	2.42	1.52	1.49	1.11
	2.63	2.43	1.07	2.23
2.00	2.61	1.43	1.74	1.23
	2.65	1.40	1.84	1.22
	2.40	1.35	1.65	1.13
	2.66	1.48	2.10	--
	3.08	1.47	1.90	1.76
	2.78	1.32	2.[illegible]9	1.07
	2.84	1.39	2.23	1.34
2.25	2.[illegible]7	1.64	1.79	0.97
	2.77	1.66	1.95	1.96
	2.[illegible]5	1.[illegible]0	2.00	1.14
	2.[illegible]7	1.62	1.51	1.32
	3.00	1.[illegible]7	1.82	0.91
	3.10	1.72	2.21	1.30
	3.05	1.71	2.17	1.61
	3.18	1.72	2.[illegible]5	1.23
	3.10	2.01	1.91	1.26
	2.91	1.69	2.12	0.[illegible]
	2.97	1.8[illegible]	2.82	1.[illegible]4
	2.89	1.4[illegible]	1.31	1.[illegible]
	3.20	1.46	2.14	0.[illegible]
	2.88	1.[illegible]8	1.95	1.35
	3.[illegible]	1.3[illegible]	1.5[illegible]	1.[illegible]

Distance Above Bottom of Wall b, in.	Shock Pressure (in psi) for the Successive Breaking Waves Indicated			
	First	Second	Third	Fourth
2.75	2.44	1.16	2.07	1.11
	2.5[illegible]	1.07	1.68	0.8[illegible]
	2.68	1.12	1.67	0.75
	2.95	1.20	2.14	1.47
3.00	2.67	0.98	1.23	0.76
	2.50	0.87	1.42	0.88
	2.09	0.87	1.10	0.83
	2.41	0.86	2.00	0.70
3.[illegible]5	1.66	0.47	0.72	0.5[illegible]
	2.20	0.53	0.67	0.50
	1.31	0.43	0.69	0.53
	1.60	0.41	0.92	0.55
3.50	0.60	0.25	0.52	0.41
	0.47	0.23	0.27	0.28
	0.58	0.44	0.26	0.30
	0.49	0.33	0.35	0.25
	0.52	0.32	0.19	--
3.75	0.37	0.24	0.17	0.21
	0.3[illegible]	0.22	0.21	0.31
	0.47	0.24	0.24	0.35
4.00	0.10	0.11	0.12	0.20
	0.16	0.13	0.31	0.15
	0.20	0.12	0.13	0.16
4.50	0.08	0.07	0.05	0.08
	0.07	0.05	0.05	0.08
	0.09	0.07	0.05	0.08

Table 10

Shock Pressure Data, Test Series 9

H = 1.59 in.
L = 100.8 in.
T = 1.92 sec

H_o = 1.50 in.
L_o = 226.7 in.

d = 9.30 in.
d_w = 1.93 in.
z = 1/10

Distance Above Bottom of Wall b, in.	Shock Pressure (in psi) for the Successive Breaking Waves Indicated			
	First	Second	Third	Fourth
0.25	2.10	1.82	1.22	1.38
	1.97	1.90	0.55	1.23
	2.01	1.61	1.10	1.46
	1.91	1.82	0.93	1.52
0.50	2.10	1.76	0.70	1.40
	2.23	1.89	1.43	1.27
	2.13	1.77	1.50	1.26
	2.02	1.79	0.82	1.35
0.75	2.60	1.82	0.75	1.23
	2.48	1.64	1.54	1.23
	2.49	1.72	1.64	1.42
	2.63	1.83	1.01	1.33
	2.25	1.86	1.24	1.52
1.00	2.65	1.50	1.23	1.48
	2.45	1.34	1.63	1.54
	2.39	1.72	1.62	1.32
	2.26	1.70	1.72	1.29
	2.35	1.67	1.43	1.00
1.25	2.43	1.80	2.43	1.44
	2.41	1.91	2.70	1.27
	2.30	1.91	1.22	1.20
	2.68	1.58	2.20	1.07
	2.54	1.64	2.99	1.30
1.50	2.80	1.50	1.87	1.30
	2.80	1.75	1.96	1.40
	2.77	1.82	1.56	1.53
	2.68	1.83	1.80	1.15
	2.64	1.78	1.94	1.34
1.75	3.08	1.77	1.20	0.78
	2.58	1.97	1.63	1.29
	2.60	1.80	0.86	0.90
	2.73	1.68	1.31	0.58
	2.61	1.90	1.31	1.07
	2.76	1.65	1.79	0.99

Distance Above Bottom of Wall b, in.	Shock Pressure (in psi) for the Successive Breaking Waves Indicated			
	First	Second	Third	Fourth
2.00	1.80	1.07	0.48	0.31
	2.10	1.29	0.55	0.35
	1.89	1.40	0.42	0.30
	1.75	1.52	0.38	0.48
	1.68	1.55	0.63	0.40
2.25	0.59	0.65	0.20	0.20
	0.38	0.56	0.20	0.16
	0.65	0.41	0.16	0.20
	0.52	0.45	0.32	0.38
	0.57	0.46	0.20	0.10
2.50	0.34	0.51	0.10	0.10
	0.27	0.21	0.09	0.08
	0.27	0.30	0.10	0.12
	0.25	0.33	0.09	0.10
2.75	0.13	0.10	0.05	0.07
	0.11	0.12	0.05	0.10
	0.08	0.08	0.06	0.06
	0.05	0.08	0.06	0.06
3.00	0.05	0.07	0.06	0.06
	0.05	0.05	0.05	0.05
	0.05	--	0.05	0.05
3.50	0.04	0.05	0.04	0.04
	0.05	0.05	0.05	0.05

Table 11

Shock Pressure Data, Test Series 10

H = 2.47 in.
L = 87.7 in.
T = 1.49 sec

H_c = 2.56 in.
L_o = 136.5 in.

d = 10.00 in.
d_w = 2.63 in.
z = 1/10

Distance Above Bottom of Wall b, in.	Shock Pressure (in psi) for the Successive Breaking Waves Indicated			
	First	Second	Third	Fourth
0.25	0.27	0.98	1.07	0.34
	0.28	1.03	1.48	0.36
0.50	0.28	0.88	1.00	0.34
	0.28	0.75	1.02	0.34
	0.27	0.81	1.34	0.35
	0.28	0.78	1.15	0.35
1.00	0.30	0.92	1.69	0.40
	0.29	0.84	0.99	0.35
	0.28	0.95	1.03	0.36
	0.29	0.75	0.81	0.36
1.50	0.29	1.08	1.05	0.34
	0.28	1.07	1.10	0.35
	0.28	1.03	1.65	0.37
	0.29	1.05	1.25	0.37
2.00	0.30	1.60	1.86	0.35
	0.29	1.39	1.58	0.39
	0.30	1.12	--	0.41
	0.30	1.18	1.27	0.38
2.25	0.28	2.11	2.34	0.35
	0.28	1.86	2.10	0.32
	0.29	2.21	1.67	0.39
	0.30	1.74	2.67	0.32
	0.30	2.35	2.66	0.33
2.50	0.50	2.78	1.88	0.75
	0.29	2.70	3.04	0.45
	0.27	2.56	2.40	0.37
	0.27	2.30	1.83	0.40
	0 26	2.01	2.01	0.38
2.75	0.28	2.37	2.60	0.34
	0.28	2.35	4.47	0.37
	0.30	2.13	3.41	0.46
	0.29	3.51	3.93	0.49
	0.29	3.75	2.66	0.41
3.00	0.29	4.85	3.52	0.40
	0.30	6.00	3.73	0.50
	0.30	4.91	4.53	0.40
	0.29	3.44	2.80	0.39
	0.30	4.19	2.60	0.43
	0.30	2.78	3.36	0.60
	0.32	3.18	2.76	0.54
	0.30	3.17	3.70	0.43
3.25	0.27	3.88	3.30	0.37
	0.28	4.37	3.97	0.49
	0.28	3.92	3.63	0.46
	0.29	5.76	2.78	0.38
	0.30	4.65	2.50	0.47
3.50	0.23	2.52	3.03	0.39
	0.24	2.50	4.00	0.38
	0.27	4.30	1.60	0.49
	0.25	3.10	1.15	0.41
	0.24	1.97	3.00	0.41
3.75	0.20	2.48	0.87	0.27
	0.18	1.90	1.09	0.30
	0.19	3.17	1.43	0.37
	0.18	2.84	0.61	0.31
	0.18	2.05	1.03	0.33
4.00	0.11	0.57	0.54	0.14
	0.13	0.49	0.38	0.22
	0.12	0.77	0.26	0.20
4.50	0.06	0.15	0.14	0.07
	0.06	0.14	0.13	0.10
5.00	0.02	0.09	0.04	0.04

APPENDIX A: DETAILED EXPLANATION OF EXPERIMENTAL PROCEDURE AND EQUIPMENT

1. The experimental portion of this study was conducted in a wave flume measuring 12 in. wide by 17 in. deep by 61 ft long from the wave generator to the test wall. The wave generator was of the flap type, hinged at the bottom. It was fitted with a variable-stroke mechanism and a variable-speed drive so that a variety of wave heights and wave periods could be generated. A diagram of the wave flume is shown in fig. 1 of the main text.

2. In order to cause the wave to break at the wall, a beach slope constructed of Plexiglas was fitted in the flume immediately in front of the test wall. The beach slope was weighted to eliminate any movement which might be caused by the different pressures above and below the slope due to the action of the waves. The top of the beach slope was taped to the sides of the flume and to the test wall to prevent any flow around the slope between its sides and the sides of the flume and the wall. The test wall was also taped to the sides of the flume to prevent any flow from going around it. A waterproof rubberized-cloth tape was used to accomplish the desired degree of sealing.

3. The test wall was built from 1/2-in. aluminum plate. It consisted of two plates fastened together with angle braces. Between the two plates there was a "T" slot so that a pressure cell could be fitted in and could be moved vertically along the wall. By using spacer blocks above and below the pressure cell mount, the pressure cell could be moved in the vertical direction in 0.25-in. increments. Thus, a distribution of the pressure on the test wall could be measured. The wall was clamped at the top to the top rails of the flume and braced at the bottom with braces which were also clamped to the top rails of the flume. Photographs of the test wall are shown in figs. 2a and 2b of the main text.

4. The pressure transducers were commercially available unbonded strain gages (Type 4-312) made by the Consolidated Electrodynamics Corporation. The sensing element of the pressure transducer consists of a full wheatstone bridge circuit of unbonded strain gages. The pressure-sensitive

face of the cell consists of a stainless steel diaphragm. Pressure against this diaphragm produces a displacement of the sensing element which changes the resistance of the active arms of the bridge circuit and causes an electrical output proportional to the applied pressure.

5. Two different pressure transducers were used, a 50-psia and a 15-psia. Absolute pressure cells were used in preference to gage pressure cells since the absolute cells are partially evacuated and hermetically sealed, and they could be completely immersed in water without fear of damage to the cell. The gage pressure cells, on the other hand, must be vented to the atmosphere. Since many of the pressure measurements were taken with the transducer completely underwater, the gage pressure cell would have been seriously damaged if water had accidentally gotten into the air vent.

6. The use of the 15-psia transducer involved loading it to approximately 62 percent beyond its rated capacity. The pressure limit for the transducer is twice the rated range. It was thought that the 15-psia pressure cell could reliably reproduce pressures up to approximately 75 percent of the rated range. This figure is based on the experience of the Measurements and Testing Section of the U. S. Army Engineer Waterways Experiment Station.

7. The cells were calibrated with a deadweight tester which is considered to be a second-degree standard. The 15-psia transducer was calibrated to approximately 65 percent over the rate range (10.00-psi gage pressure) and was found to be linear for the range calibrated, from 0- to 10.00-psi gage pressure.

8. The transducers have a compensated temperature range of from -65 F to +250 F according to the manufacturer's specifications.

9. For the first series of tests the pressure cell with a capacity of 50 psia was used. For the succeeding tests the 15-psia pressure cell was used in order to get higher sensitivity and accuracy for the measurement of the lower pressures. The natural frequency of the 50-psia cell was 11,000 cps, and that of the 15-psia cell was 5,000 cps. Linear response can be expected for frequencies up to approximately 10 percent of the natural frequency of the pressure cell.

10. The recording equipment for the pressure record consisted of a Carrier Amplifier, Type 1-118, and Recording Oscillograph, Type 5-124, both manufactured by the Consolidated Electrodynamics Corporation. The oscillograph was fitted with a Type 7-319 galvanometer, also made by the Consolidated Electrodynamics Corporation. The frequency characteristics of the galvanometer are such that it will give flat response with ±5 percent to frequencies up to 350 cps. The Type 1-118 Carrier amplification system consisted of a 3000-cps oscillator for power to the bridge circuit of the pressure transducer, and control and conditioning circuitry. The oscillograph used a light beam and light-sensitive paper to make the record. The light beam was focused on a mirror mounted on the movable pole piece of the galvanometer. From this mirror, the light beam was then reflected to the light-sensitive paper on which the record was made.

11. The large majority of the pressure records were run at a paper speed of 2 in. per sec. Selected records were run at 8 or 32 in. per sec in order to magnify the time scale so that more detailed examination could be made.

12. The wave characteristics were measured with resistance-type wave gages. These gages consisted of a strip of printed circuit board 1/4 in. wide by 1/16 in. thick by approximately 12 in. long, and plated on both sides with chrome in order to get better coupling between the rod and the water. The wave characteristics were recorded using universal amplifiers, Model BL-520, and a portable 6-channel oscillograph, Model BL-276, both manufactured by the Brush Electronics Company. The output of the wage gages was fed into the amplifiers through bridge circuits and Brush strain gage input boxes, Model BL-350.

13. The wave gages were fitted to Lory point gages with verniers which could be read to 0.01 in. With this arrangement the wave gages could be easily and accurately calibrated by raising them out of or lowering them into the water with the point gages. Due to drift in the gain of the amplifiers and the nonlinearity of the wave rod amplification system, the wave gages were calibrated every third or fourth test run, which was approximately every 45 min. Calibration curves were plotted for each calibration of the wave gages in order to assure accurate results.

The Brush oscillograph was run at a paper speed of 10 mm per sec in order to obtain the required definition for reading the wave record. A timing circuit provided a 1-sec timing pulse which was fed into both oscillographs recording the pressure and the wave records to tie the two records together and to provide a more accurate measure of the paper speed.

14. The two separate recording systems for the wave and pressure records were used for the first five of the ten test series. In the last five test series, both the pressure and wave records were recorded on the Consolidated Electrodynamics Corporation recording oscillograph. The change was made due to improved circuitry which had been developed and which enabled the wave records to be recorded on the same oscillograph as the pressure records. The problem involved was that the wave rods were grounded since the wave flume was in electrical contact with natural ground through the metal supports and water pipes. The wave rods were also grounded since they were submerged in the flume. The Carrier amplifier system providing the input to the oscillograph recording the pressure accepted only signals which were above ground.

15. The new system involved bypassing the amplifier and feeding the signal from the wave rods directly into the oscillograph. This was done with circuitry between the wave rods and oscillograph. This additional circuitry provided a power supply for the wave rods, balancing and sensitivity controls, a four-diode rectifier, and filtering elements.

16. This latter recording system was a great improvement over the earlier one which involved two separate records. The trace of the wave record was magnified approximately three times, and greater linearity could be achieved. The light-beam oscillograph records a straight trace rather than a curved trace as is recorded by the pen of the Brush oscillograph.

17. The greatest source of error involved in the wave measurements was due to the meniscus effects. This error was partially overcome in the calibration of the wave gages by calibrating the crest and trough portions of the wave rod in the same direction that the crest and trough draw the meniscus. A constant meniscus never forms due to the motion of the water. The crest of the wave tends to depress the meniscus since the water travels up the rod as the crest approaches. The trough tends to draw up the

meniscus since the water is t. .n travelling down the rod as the trough approaches.

18. Three wave rods were used in measuring the wave characteristics. Two were located in the constant-depth section of the wave flume, and the third was located 6 in. in front of the test wall. The distance between the two wave gages in the constant-depth portion of the flume was 89.8 in. The wave rod closest to the wall was positioned 6 in. from the wall as a compromise between being too close and thus being affected by the runup on the wall, and being too far away and thus not being able to accurately measure the elevations of the crest and trough of the wave as it broke.

19. The wave period and celerity were measured from the wave record. The wave period was calculated by measuring the period of the first three full-size waves and taking the average. The celerity measurement was made by taking the average travel time of the first three full-size waves of the train between the wave rod closest to the generator and the middle wave rod. Since the two wave rods were a known distance apart, the celerity was equal to this distance divided by the travel time between the two wave rods. The wavelength was calculated from the relation

$$L = cT$$

where L is the wavelength, c is the celerity, and T is the wave period. The wavelength calculated in the above manner agreed very closely with the first-approximation theoretical wavelength calculated from the formula

$$L = \frac{gT^2}{2\pi} \tanh \frac{2\pi d}{L}$$

where the symbols L and T are as defined above, g is the acceleration of gravity, and d is the depth of water corresponding to the wavelength. In this case d was the still-water level depth in the uniform-depth section of the wave flume. The value for the wavelength used in all succeeding calculations is the value from the wave records

calculated using the equation $L = cT$.

20. The wave height was measured in the constant-depth portion of the flume at the first wave rod from the generator. The height of the breaking wave was measured at the third wave rod, 6 in. from the test wall. The second wave rod was used only for the celerity measurements. The wave heights both at breaking and in the constant-depth section of the flume were determined from the average of the first four uniform waves of the train.

21. For use in the analysis of the data the overall average values for the wavelength, wave height, period, and celerity of each test series were used. The number of values averaged was approximately one-half of the number of test runs made in each series. Both wave and pressure records were taken for each test run, but measurements of the wave characteristics were made on only every other record. Measurements of all the pressure records were made.

22. Each test run consisted of recording the pressure on the wall and the wave characteristics of the first four breaking waves. These first four waves were always quite uniform in appearance and usually caused shock pressures of approximately the same intensity on the wall. The disturbance of the water due to the first four breaking waves and their reflections from the wall caused the breaking characteristics of the succeeding waves to change. Therefore, the shock pressures of the succeeding waves varied greatly and in some cases did not occur. In each of the test runs the wave generator paddle was started from the most forward position. It was found from experience that a more uniform train of waves could be generated if the train was preceded by a trough. Before each test run the water in the flume was allowed to calm completely, the water depth in the flume was checked, and the zero positions of the record traces were checked and adjusted, if necessary. Maximum effort was made to generate uniform trains of waves from one test run to the next.

23. In order to cause the maximum shock pressure on the wall, a system of trial and error was used. The still-water depth, both at the wall and in the section of the flume with a horizontal bottom, and the wave period were set. The wave height was adjusted so that the wave

appeared to break on the wall. The wave height was then adjusted further by checking the pressure record and determining the wave height which created the highest shock pressures. Once this wave height was established, the only change which was made from one run to the next within a series was the position of the pressure transducer on the wall.

24. It is believed that a discussion of the errors involved in the pressure and wave measurements is both desirable and necessary. The errors in the wave measurements arose from a number of factors in both the generating equipment and the recording equipment. Although the stroke and speed of the wave machine did not change once it was set, the wave height and wavelength tended to vary because of friction of the water on the bottom and sides of the flume and the small amount of play necessarily present in the wave generator. Considering the maximum variations of the individual waves in a single wave train from the average values of that train, it was found that the wave height varied approximately 8 percent, the wave period 2 percent, and the celerity of the wave 3 percent. The variation in the height of the wave at breaking was approximately 15 percent. The variation of the average values of wave height, wavelength, and period of single wave trains or test runs from the average of all the test runs of a series was generally less than the variations within a wave train. The maximum percentage differences between the average of all the test runs of a series and any single test run were as follows: wave heights, 4.3 percent; wave period, 1.0 percent; and wavelength, 3.7 percent.

25. These variations in the wave measurements combine the effects of nonuniformity produced by the bottom and side friction in the flume, the play and variations in the operation of the wave generator, the misalignment of the sides and bottom of the flume, and changes in the viscosity of the water due to temperature change. In addition, errors due to the recording system were also included; these generally included the meniscus effect on the wave rod, changes in the amplification of the signal from the wave rod, the pen friction, and the errors introduced in measuring the oscillograph records due to the finite width of the trace and grid lines.

26. The percentage differences between the measured wavelength

(calculated from the product of wave period and celerity) and the theoretical wavelength in the uniform-depth portion of the flume which was calculated from the relation

$$L = \frac{gT^2}{2\pi} \tanh \frac{2\pi d}{L}$$

were 6.7 percent for one of the ten series and below 2.5 percent for the other nine test series.

27. In measuring the pressure records, the calibration of the pressure cell was assumed to be linear. The actual variation from a straight line was a maximum of 1.5 percent for pressures above 0.50 psig. Below 0.50-psig pressure the maximum error was induced by the limitations of the record since the width of the record trace was approximately 0.02 in. This error due to the width of the trace could be as much as 10 percent in lower pressure ranges of the secondary pressure. A larger deflection to pressure ratio would reduce this error, but this was not possible in these experiments because of the much higher shock pressures.

APPENDIX B: DISCUSSION OF WAVE THEORIES

Theory of Small-Amplitude Waves

1. Many mathematical wave theories have been developed for the prediction of wave form and water particle motion. In the analysis of the data in this study, the first-order approximation or small-amplitude wave theory was used. In most coastal engineering problems such as this one, the small-amplitude wave theory yields sufficiently accurate results.

2. The basic assumptions of the small-amplitude theory are small wave height and small steepness; that is, the wave height is small compared to the wavelength. In addition, it is assumed that the velocity of the water particles is small. These assumptions are equivalent to neglecting all terms of the wave problem higher than the first degree, or to making the problem linear.

3. With the above assumptions in mind, one can formulate the problems of wave motion in two dimensions. Let x be the horizontal coordinate and y the vertical coordinate. Assuming an incompressible fluid, the velocity potential ϕ will satisfy the equation

$$\frac{\partial^2 \phi}{\partial x^2} + \frac{\partial^2 \phi}{\partial y^2} = 0$$

At the bottom, which is assumed to be horizontal, the velocity normal to the boundary is zero, thus giving rise to the boundary condition

$$\frac{\partial \phi}{\partial y} = 0 \qquad \text{at } y = -d$$

where d is the water depth from the free surface to the bottom. The boundary condition at the free surface, assuming zero pressure, can be derived from the Bernoulli equation. The free-surface condition, at $y = \eta \approx 0$, is

$$\eta = \frac{1}{g}\left(\frac{\partial \phi}{\partial t}\right)_{y=0}$$

Since it has been assumed that the wave steepness is small, it follows that the normal to the surface approximately coincides with the vertical; thus,

$$\frac{\partial \eta}{\partial t} = -\left(\frac{\partial \phi}{\partial y}\right)_{y=0}$$

Eliminating η from the two above relations, the free-surface condition becomes

$$\frac{\partial^2 \phi}{\partial t^2} + g\frac{\partial \phi}{\partial y} = 0$$

The Laplacian $\sigma^2\phi = 0$ can now be solved with the boundary condition for ϕ. It is found that

$$\phi = \frac{ga}{\sigma}\frac{\cosh m\,(y + d)}{\cosh md} \cdot \cos\,(mx - \sigma t)$$

satisfies the Laplacian. In the above equation $a = H/2$, half the wave height; $\sigma = 2\pi/T$, a function of the wave period; and $m = 2\pi/L$, a function of the wavelength. The surface elevation can be found to be of the form

$$\eta = a \sin\,(mx - \sigma t)$$

It can be shown that σ and m satisfy the relation $\sigma^2 = gm \tanh md$ or, in terms of wavelength and period,

$$T^2 = \frac{2\pi L}{g}\coth\frac{2\pi d}{L}$$

4. It is also useful to calculate the wave energy and energy flux.

The potential energy of the wave per unit width is

$$E_p = \rho \int_0^{\eta} \int_0^{L} gy \, dx \, dy$$

The potential energy, in terms of the wave height and wavelength, can be found, upon integration of the above equation, to be

$$E_p = \rho \frac{gH^2 L}{16}$$

The kinetic energy of a wave per unit width can be calculated from the relation

$$E_K = \rho/2 \int_0^{\eta=0} \int_0^{L} \left[\left(\frac{\partial \phi}{\partial x} \right)^2 + \left(\frac{\partial \phi}{\partial y} \right)^2 \right] dx \, dy$$

The kinetic energy is found to be equal to the potential energy; thus, the total wave energy is

$$E = \rho \frac{gH^2 L}{8}$$

5. The energy flux F per unit width across a surface perpendicular to a wave traveling in the x direction is given by

$$F = \rho \int_t^{t+T} \left(\int_{-d}^{\eta=0} \frac{\partial \phi}{\partial t} \cdot \frac{\partial \phi}{\partial x} \, dy \right) dt$$

The average flux F_{avg} per wave period T can be found to be

$$F_{avg} = \frac{\rho g H^2}{8} \cdot \frac{c}{2} \left(1 + \frac{2md}{\sinh 2md} \right)$$

or

$$F_{avg} = \frac{1}{2}\frac{E}{T}\left(1 + \frac{2md}{\sinh 2md}\right)$$

In the above equation $c = \sigma/m$, and it is the wave celerity. In water of infinite depth, $d \to \infty$,

$$F_{avg} = \frac{E_o}{2T}$$

6. Thus, one can obtain a relation between the wave energy in deep water, E_o, and the wave energy, E, in any depth of water, d, by equating the energy flux which remains constant.

$$\frac{\rho g H_o^2 L_o}{8} \cdot \frac{1}{2T} = \frac{\rho g H^2 L}{8} \cdot \frac{1}{2T}\left(1 + \frac{2md}{\sinh 2md}\right)$$

From this a relation between the wave characteristics in deep water and in water of depth d can be obtained:

$$H_o^2 L_o = H^2 L\left(1 + \frac{2md}{\sinh 2md}\right)$$

Now applying the relations between wave period, wavelength, and water depth

$$T^2 = \frac{2\pi L}{g}\coth\frac{2\pi d}{L}$$

and

$$T^2 = \frac{2\pi L_o}{g}$$

in deep water, the following useful equation can be obtained

$$\frac{H}{H_o} = \frac{\cosh\frac{2\pi d}{L}}{\left(\frac{2\pi d}{L} + \sinh\frac{2\pi d}{L}\cosh\frac{2\pi d}{L}\right)^{1/2}}$$

Thus, the deepwater wave characteristics can be calculated from the wave characteristics in water of depth d. The above formulas were used to calculate the deepwater wave characteristics in this study. Fig. B1 shows a plot of H/H_o versus d/L_o.

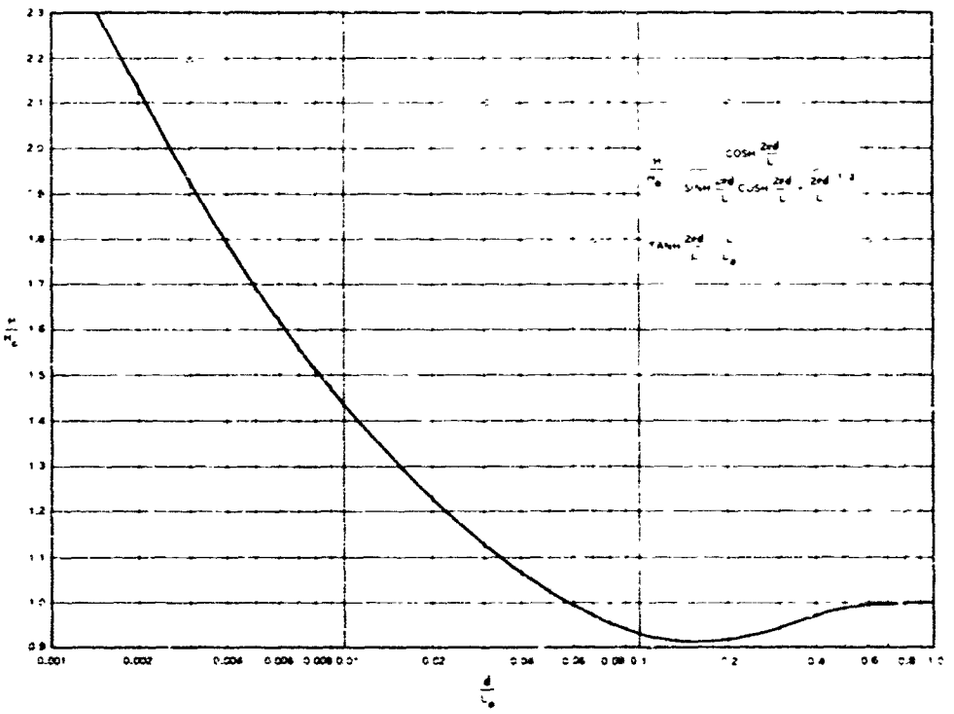

Fig. B1. Variation of wave height with water depth

Theory of Solitary Waves

7. The solitary-wave theory has often been used in predicting the characteristics of waves as they approach the breaking zone or surf zone on a sloping beach. Although this theory was not developed for this purpose, it has been found more effective than the oscillatory-wave theories. In the breaker zone, the assumptions of the first-order approximation of the oscillatory-wave solution do not hold, and Stokes' higher order theories become unmanageable.

8. The first approximation of the solitary wave is based upon the assumption that the velocity potential has a linear form. From the linear

velocity potential Boussinesq obtained a relation for the wave profile

$$\eta = H \operatorname{sech}^2\left(\frac{x}{2}\sqrt{\frac{3H}{d^3}}\right)$$

where x is measured from the center of the intumescence. Also in the first approximation, he found the celerity to be

$$c = \sqrt{g\,(d + H)}$$

The total energy of a solitary wave is given by the relation

$$E = \frac{8}{3}\rho g\sqrt{\frac{H^3 d^3}{3}}$$

The total energy of a solitary wave consisted of half potential and half kinetic energy as does that of the oscillatory wave.

9. McCowan, in higher approximation, found the relation between breaker height and the depth at breaking to be

$$\frac{H_B}{d_B} = \frac{1}{2}\tan(1 \text{ radian}) = 0.7813\ldots$$

for a solitary wave. This relation was based upon the assumption that the water particle velocity is equal to the wave celerity at the very crest of the wave.

10. Munk utilized Boussinesq's first approximation and McCowan's relation between depth and wave height at breaking, along with the energy flux deepwater oscillatory wave, in order to develop a relation for the breaking height of a wave. The energy flux of a wave at breaking is equal to its deepwater energy flux. The relation between the wave height at breaking and the wave height and wavelength in deep water is given as follows:

$$\frac{H_B}{H_o} = \frac{1}{3.3}\left(\frac{H_o}{L_o}\right)^{-1/3}$$

Munk recommended that this relation be used for waves with deepwater steepness of less than 0.006.

11. In the solitary-wave theory as in the oscillatory-wave theory, it is assumed that the first approximation gives sufficiently accurate results for coastal engineering problems which do not involve the orbital motion of the water particles (such as sediment transport problems).

Unclassified

Security Classification

DOCUMENT CONTROL DATA - R & D

(Security classification of title, body of abstract and indexing annotation must be entered when the overall report is classified)

1. ORIGINATING ACTIVITY (Corporate author)

U. S. Army Engineer Waterways Experiment Station
Vicksburg, Mississippi

2a. REPORT SECURITY CLASSIFICATION

Unclassified

2b. GROUP

3. REPORT TITLE

AN EXPERIMENTAL STUDY OF BREAKING-WAVE PRESSURES

4. DESCRIPTIVE NOTES (Type of report and inclusive dates)

Final report

5. AUTHOR(S) (First name, middle initial, last name)

William J. Garcia, Jr.

6. REPORT DATE	7a. TOTAL NO. OF PAGES	7b. NO. OF REFS
September 1968	113	83

8a. CONTRACT OR GRANT NO	9a. ORIGINATOR'S REPORT NUMBER(S)
b. PROJECT NO.	Research Report H-68-1
c.	9b. OTHER REPORT NO(S) (Any other numbers that may be assigned this report)
d.	

10. DISTRIBUTION STATEMENT

This document has been approved for public release and sale; its distribution is unlimited.

11. SUPPLEMENTARY NOTES	12. SPONSORING MILITARY ACTIVITY
	Office, Chief of Engineers, U. S. Army Washington, D. C.

13. ABSTRACT

Tests were conducted to gain more information concerning the shock pressures created by water waves breaking against vertical barriers. These wave pressures were studied using small-scale oscillatory waves in a flume fitted with a beach slope and test wall. The variation of pressure with both time and position on the wall was determined for several wave heights, wave periods, water depths, and beach slopes. Great scatter in the magnitude of the shock pressure was observed for each of the wave conditions tested. This variation in the value of the shock pressure is believed to be caused by slight variations in the shape of the incident breaking wave. Therefore, many tests were made using the same wave conditions in order to more accurately determine the magnitude of the shock pressure. The variation of pressure with time was found to be similar to that reported by previous investigators. The pressure-time variation can be divided into two parts; namely, initial shock pressure which occurs as the wave strikes the wall and a secondary pressure which is associated with the rumup. The shock pressure is characterized by a very intense pressure peak of short duration and is followed by the much less intense but longer duration secondary pressure. The maximum shock pressure that occurred for each wave condition was localized over a small region of the test wall between the still-water level at the wall and the elevation of the crest of the wave striking the wall. Above the region of maximum shock pressure, the magnitude of pressure decreases to zero. Below the region of maximum pressure, the shock pressure also decreases but to a value of approximately one-tenth the magnitude of the shock pressure and it then remains fairly constant to the bottom of the test wall. This type of distribution of shock pressures on the wall was observed for all

(Continued)

DD FORM 1 NOV 68 1473 REPLACES DD FORM 1473, 1 JAN 64, WHICH IS OBSOLETE FOR ARMY USE.

Unclassified

Security Classification

tests. Upon analysis of the maximum shock pressures observed for each of the wave conditions tested, it was found that the shock pressure increased with both wave height and wavelength. It was found through dimensional analysis that pressure is proportional to the cube root of the wave energy. Upon comparison of the data collected in this experimental program with the above relation between pressure and wave energy, only fair conformity was noted due to the small range of test data. Therefore, the range of data was expanded by the inclusion of the shock pressure data of other investigators from both model and prototype studies. Very good agreement was noted over this larger range of data. As opposed to the shock pressure, little scatter was noted in the magnitude of the secondary pressure. It was also noted that the secondary pressure varies regularly along the wall from a maximum at the bottom to zero at the point of maximum runup. This regular distribution is expected since the secondary pressure is caused by the runup of the wave rather than its impact on the wall. The secondary pressure was compared with the pressure caused by the same size wave forming a clapotis on the wall. The clapotis pressure was almost identical with the observed pressure. The characteristics of the wave at the point of breaking were also studied in order to make a comparison between waves breaking on an unobstructed beach and on a beach obstructed by a wall. Although it might be expected that a barrier on the beach would have a great effect on the breaking waves, the data showed the effect to be negligible. The depth of water in which the wave would break on an unobstructed beach is slightly greater than the depth of water at the wall which would cause the same wave to break and produce maximum shock pressures. The wave height at breaking for both the obstructed and the unobstructed beach was found to be the same.

14. KEY WORDS	LINK A		LINK B		LINK C	
	ROLE	WT	ROLE	WT	ROLE	WT
Barriers						
Shock pressures						
Water wave breaking						
Water wave forces						
Water wave experiments						